AD-699 132

THE ELECTRODE KINETICS OF THE CHROMOUS, CHROMIC COUPLE

SANDRA S. DONOVAN, ET AL

CASE WESTERN RESERVE UNIVERSITY
CLEVELAND, OHIO

OCTOBER 1969

ELECTROCHEMISTRY RESEARCH LABORATORY

DEPARTMENT OF CHEMISTRY
JOHN SCHOFF MILLIS SCIENCE CENTER
CASE WESTERN RESERVE UNIVERSITY
CLEVELAND, OHIO

TECHNICAL REPORT NO. 24

THE ELECTRODE KINETICS OF THE CHROMOUS-CHROMIC COUPLE

by

Sandra S. Donovan and Ernest Yeager

1 October 1969

Office of Naval Research
Contract N00014-67-C-0389
Project NR 359-277

OFFICE OF NAVAL RESEARCH

Contract N00014-67-C-0389

Project NR 359-277

TECHNICAL REPORT NO. 24

THE ELECTRODE KINETICS OF THE CHROMOUS-CHROMIC COUPLE

by

Sandra S. Donovan and Ernest Yeager

Department of Chemistry
CASE WESTERN RESERVE UNIVERSITY
Cleveland, Ohio 44106

1 October 1969

unclassified
Security Classification

DOCUMENT CONTROL DATA - R & D

(Security classification of title, body of abstract and indexing annotation must be entered when the overall report is classified)

1. ORIGINATING ACTIVITY (Corporate Author)	2a. REPORT SECURITY CLASSIFICATION
Case Western Reserve University Cleveland, Ohio 44106, USA	Unclassified
	2b. GROUP ---

3. REPORT TITLE

THE ELECTRODE KINETICS OF THE CHROMOUS-CHROMIC COUPLE

4. DESCRIPTIVE NOTES (Type of report and inclusive dates)

Technical Report No. 24

5. AUTHORS (Last name, first name, initial)

Donovan, Sandra S. and Yeager, Ernest

6. REPORT DATE	7a. TOTAL NO. OF PAGES	7b. NO. OF REFS
1 October 1969	205	82

8a. CONTRACT OR GRANT NO.	9a. ORIGINATOR'S REPORT NUMBER(S)
N00014-67-C-0389	Technical Report No. 24
8b. PROJECT NO. NR 359-277	9b. OTHER REPORT NO(S) (Any other numbers that may be assigned this report) ---

10. DISTRIBUTION STATEMENT

This document has been approved for public release and sale; its distribution is unlimited.

11. SUPPLEMENTARY NOTES	12. SPONSORING MILITARY ACTIVITY
---	Office of Naval Research Washington, D. C. 20360 Code 472, Chemistry Program

unclassified
Security Classification

DOCUMENT CONTROL DATA - R & D (Continued)

13. ABSTRACT

The $[Cr(H_2O)_6]^{2+}/[Cr(H_2O)_6]^{3+}$ couple has been studied with cyclic voltammetry on a hanging mercury electrode in acidic perchlorate, chloride-perchlorate, and bromide-perchlorate supporting electrolytes at controlled ionic strength and pH. In addition to the simple hexaaquochromium(II)/(III) couple, the $[Cr(H_2O)_6]Cl^{+}/[Cr(H_2O)_5Cl]^{2+}$ couple is involved in the mixed chloride-perchlorate supporting electrolytes and $[Cr(H_2O)_6]Br^{+}/[Cr(H_2O)_5Br]^{2+}$ couple is involved in the mixed bromide-perchlorate supporting electrolytes the rate constants for each of these couples were determined. Concentrations of the reacting species at the electrode surface were computer calculated from the diffusion coefficients using the experimental current-time data, with no a priori assumptions concerning the dependence of the kinetics on potential double layer corrections were applied.

DOCUMENT CONTROL DATA - R & D (Continued)

13. ABSTRACT (Continued)

The standard rate constants of the couples increase in the order $[Cr(H_2O)_6]^{2+}/[Cr(H_2O)_6]^{3+} < [Cr(H_2O)_6]Cl^{+}/[Cr(H_2O)_5Cl]^{2+} < [Cr(H_2O)_6]Br^{+}/[Cr(H_2O)_5Br]^{2+}$ with the $[Cr(H_2O)_6]^{2+}/[Cr(H_2O)_6]^{3+}$ couple having the same standard rate constant in all of the supporting electrolytes examined. For both of the halogen containing couples, the first order standard rate constants (not considering surface coverage with halogen ions) show a dependence on bulk halogen concentrations. In the case of the $[Cr(H_2O)_6]Cl^{+}/[Cr(H_2O)_5Cl]^{2+}$ couple, the second order rate constants, taking the surface chloride coverage into consideration, were shown to be virtually independent of bulk chloride concentration over the range studied.

The experimental free energies of activation for the hexaaquochromium(II)/(III) heterogeneous and homogeneous reactions were compared with the values predicted by weak interaction theory. (Marcus-Hush) For the homogeneous reaction the agreement between experiment and theory is good (theoretical: 22.4 kcal/mole; experimental: 24 ± 2 kcal/mole). For the electrode reaction,

DOCUMENT CONTROL DATA - R & D (Continued)

13. ABSTRACT (Continued)

the agreement is only fair (experimental: 13 kcal/mole; theoretical: 9 kcal/mole). Theory and experiment both show that the free energy of activation for an electrode reaction is about half of that for its homogeneous counterpart when the most probable distance of separation between the reactant and the electrode in the activated state is twice the radius of the reactant.

DOCUMENT CONTROL DATA - R & D (Continued)

14. KEY WORDS

Electrochemistry

Electrode kinetics

Linear sweep voltammetry

Mercuty electrode

Chromous-Chromic couple

Redox reactions

Rate constants

Activation free energies

Ionic double layer effects

TABLE OF CONTENTS

LIST OF FIGURES

LIST OF FIGURES (cont.)

LIST OF FIGURES (cont.)

LIST OF FIGURES (cont.)

LIST OF FIGURES (cont.)

LIST OF TABLES

CHAPTER I

HOMOGENEOUS AND ELECTROCHEMICAL CHROMIUM(II)/(III) DATA

Introduction

The purpose of this research is to establish a quantitative understanding of the mechanism by which heterogeneous redox processes proceed. Attention is directed to the chromium(II)/(III) couple for the following reasons: its kinetics are usually sufficiently slow to measure easily[1]; the potential range over which the redox reactions proceed is accessible with mercury electrodes; the higher and lower valency states occur as simple aquo complexed ions with little hydrolysis[2] at a reasonable acidic pH; and the complexes are relatively easy to prepare. Of particular importance in clarifying the mechanism of chromium(II) oxidation and chromium(III) reduction at electrodes is the influence of prior and post coupled chemical steps, ligand bridging, and double layer effects with and without chloride or bromide ions sharing the inner and/or outer coordination sphere of chromium with water.

Homogeneous electron transfer studies of transition metal complexes such as vanadium[3,4], cobalt[3-7], ruthenium[4], iron[8], and chromium[3,5,8,9] have substantial relevance to electrode electron transfer kinetic studies of the type undertaken in the present research. All of these complexes exhibit large changes in homogeneous redox rate constants with different ligands in their inner coordination spheres. Detailed work performed on the chromium(II)/(III) couple[10] with a Cr^{51} tracer in acidic aqueous media has estab-

lished that ligands such as fluoride, chloride, bromide, thiocyanate, and azide are transferred into the inner coordination sphere of the newly formed chromium(III). Earlier experiments with tagged chloride ions in solution demonstrated that the chloride ion which finally coordinated to chromium(III) came from the inner sphere of the original chromium(III) and not from the solution. Reaction (I-1) shows the transfer and redox reaction.

$$[Cr^*(H_2O)_5L]^{2+} + [Cr(H_2O)_6]^{2+} = [Cr^*(H_2O)_6]^{2+} + [Cr(H_2O)_5L]^{2+} \quad (I\text{-}1)$$

where L = some ligand which facilitates the charge transfer. At 0°C and an ionic strength of 1.0 maintained by $LiClO_4$, the second order rate constants for L = F^-, N_3^-, Cl^-, and Br^- are 1.2×10^{-2}, > 1.2, 9, and >60 $\underline{M}^{-1}sec^{-1}$ respectively. When L = H_2O, the rate constant[11] at 0°C in 1 $\underline{M}$ $HClO_4$ is 4.0×10^{-6} $\underline{M}^{-1}sec^{-1}$.

Electron transfer reactions range from those with weak orbital interactions between reactants to those with appreciable energy interactions as evidenced by bond rupture and formation. Chloride transfer from one chromium complex to another is a case of strong interaction and has been placed in a subdivision of electron transfer reactions called atom transfer reactions. The term atom transfer suggests that the ligand is essentially a neutral species when it transfers from one complex to another. This is in contrast to the ligand behaving as a bridge for the electron to move across.

For the weak interaction case, Marcus has quantitatively discussed[12] the theory of homogeneous and electrode electron transfer

reactions and derived expressions for calculating the free energy of activation for each case from fundamental considerations of interaction and reorganizational energies of reactant and solvent. The close similarity between the derived free energy expressions for the homogeneous and electrode cases helped Marcus in deriving another expression, $(k_h/Z_h)^{\frac{1}{2}} \simeq k_{el}/Z_{el}$, which compares the homogeneous rate constant, k_h, to the standard electrochemical rate constant, k_{el}, for the same redox couple. Z_h and Z_{el} are the homogeneous and electrochemical frequency factors, respectively. The true standard electrochemical rate constant should be used for comparison with the homogeneous rate constant, but the latter must be corrected for electrostatic work terms (see Ch. V). This expression is theoretically valid only when several conditions are met: specific electrode effects are absent; work terms for both reactants are negligible; the square root, β, of the ratio of the mean-square deviation of the distance of closest approach of the two reactants to the mean-square deviation of the perpendicular distance from the reaction hypersurface in configurational space is unity; κ, the velocity-weighted transition probability, is unity; and the average reactant-electrode distance in the activated complex is one-half that of the separation of the homogeneous reactants.

Since the atom transfer case is not one of weak interaction between reactants, more complete expressions are necessary for calculating the free energies of activation for both the homogeneous and electrode cases. This has been done for homogeneous atom trans-

fer reactions in solution[13], but has not yet been accomplished for the electrochemical counterpart. In addition to the presence of the degree of reaction and bond energy parameters in the more complete homogeneous expressions, the electrochemical expressions must contain factors describing adsorbed ion electrode interactions. These factors could become quite sophisticated, considering the nature of conduction bands in a metal and the complicated and not completely understood nature of the compact double layer. Consequently Marcus' relationship comparing homogeneous and electrochemical rate constants for weak interaction reactions do not apply to the atom transfer case. The first and last conditions listed earlier for weak interaction electron transfer are the ones most violated: considerable specific electrode effects are present; and the electrode-reactant distance in the activated complex is larger than half of that distance for the homogeneous reactants.

Chromium(III) Dinuclear Formation

Chromium(III) complexes in water are generally stable[2,9,15] and comparatively easy to prepare[9,10,14], purify, and analyze[16,17]. Chromium(II) complexes, by contrast, are quite labile in water[9] and are sensitive to a wide range of oxidants[19,20] such as H_2O_2, HClO, $H_2Cr_2O_7$, O_2, and Tl^{3+}. Oxygen and Tl^{3+} will oxidize chromium(II) to a dinuclear species[19] which is believed to have the structure $[(H_2O)_4Cr(OH)_2Cr(H_2O)_4]^{4+}$ [18]. The remaining oxidizing agents produce a mixture of the dimer and $Cr(H_2O)_6^{3+}$. The dimer

has a visible spectrum[21] almost identical to that for the hydrolysis product of $[Cr(H_2O)_6](ClO_4)_3$ in a perchlorate solution and is deceptively similar to the spectrum[17] of green $[Cr(H_2O)_5Cl]^{2+}$. The mechanism of dinuclear species formation is unclear. When reviewing papers on chromium(II)/(III), the above complications must be remembered, since some authors have not considered them.

Chromium(II)/(III) Electrochemistry

The hexaaquochromium(II)/(III) couple at 18°C has an effective standard potential[22] in V vs SHE evaluated from data on platinum and tin in 0.02 N acetate of -0.403 ± 0.003 V, in 0.003 N H_2SO_4 of -0.412 ± 0.002 V, in slightly acidified 0.02 N Cl^- of -0.398 ± 0.001 V, and in slightly acidified 0.4 N Cl^- of -0.454 V. Latimer[23] reports -0.41 V as the best value for the standard potential at 25°C.

In a perchlorate supporting electrolyte with a pH of 2 or less (to avoid hydrolysis[2]), the couple exhibits an irreversible polarographic wave. Under the same conditions the chloropentaaquochromium(II)/(III) couple is still irreversible, but less so. The anodic polarographic wave on mercury is shifted toward more negative potentials and the cathodic wave is shifted toward positive potentials. The bromopentaaquochromium(II)/(III) couple produces anodic and cathodic waves still closer together and is almost polarographically reversible. The iodopentaaquochromium(II)/(III) couple is difficult to study on mercury since its anodic wave co-

incides with the mercury dissolution wave once some free iodide is present in solution. When the supporting electrolyte contains chloride or bromide ions, the hexaaquochromium(II)/(III) couple produces two cathodic waves: one corresponding to the uncomplexed chromium(III) reduction, the other to the complexed chromium(III) reduction. Only a single anodic wave is apparent corresponding to the formation of both the complexed and uncomplexed chromium(III) from chromium(II). Even with the nearly reversible oxidation of chromium(II) in bromide solution, this is the case. Representative voltammetry curves with chloride and bromide are given later.

Table (I-1) lists the rate constant for the hexaaquochromium (II)/(III) couple at the accepted standard potential of -0.65 V vs SCE on various mercury electrodes. The Parsons and Passeron[24] paper is of particular interest because it shows the potential dependence of the transfer coefficient on potential. Unfortunately, the results are questionable due to the high pH of the supporting electrolyte. The transfer coefficient, α, is associated with the reduction process while the transfer coefficient, β, corresponds to the oxidation process.

Table (I-2) lists representative half wave potentials, $E_{\frac{1}{2}}$, and transfer coefficients for the reduction of $Cr(H_2O)_6^{3+}$ on mercury. All of the authors cited, except Jones, did not give rate constants and the published data are insufficient for such a calculation. Table (I-2) shows that $E_{\frac{1}{2}}$ is shifted appreciably away from -0.87 V vs

TABLE (I-1). Chromium(II)/(III) Rate Constants

Chromium in M	Supporting Electrolyte in M	α	Apparent Rate Constant at -0.65 V vs SCE in cm/sec.	Double Layer Corrected Rate Constant at -0.65 V in cm/sec.	Reference Comments
$\sim 1.5 \times 10^{-3}$ Cr^{3+}	0.908 $NaClO_4$ 0.066 $HClO_4$ 27°C	0.63	0.69×10^{-5}	-	Jones[25], polarography
$\sim 1.5 \times 10^{-3}$ Cr^{2+}	0.908 $NaClO_4$ 0.066 $HClO_4$ 27°C	0.63	1.8×10^{-5}	-	Jones,[25] chronocoulometry on HME*
? Cr^{3+} + Cr^{2+}	0.50 $NaClO_4$ pH = 3.4 25°C	0.53	7.08×10^{-6}	-	Parsons and Passeron,[24] polarography
1×10^{-3} Cr^{3+}	0.20 $NaClO_4$ 0.1 $HClO_4$ 25°C	0.69	1.6×10^{-5}	5.0×10^{-7} α_{true}=0.50	Slotter et al.,[26] SME**
$0.5\text{-}7.0 \times 10^{-3}$ Cr^{2+}	1.0 $NaClO_4$ pH = 2 25°C	0.63	7.8×10^{-6}	-	Aikens and Ross,[14] HME*

* HME = hanging mercury electrode

** SME = streaming mercury electrode

TABLE (I-2). $[Cr(H_2O)_6]^{3+}$ Reduction in Various Media

$Cr(H_2O)_6^{3+}$ in M	Supporting Electrolyte in M	$E_{1/2}$ vs SCE	α	Reference, Comments
1×10^{-3}	0.1 $CaCl_2$ pH = 2.9[2] 20°C	-0.82	0.60	Kemula and Rakowska,[27] cyclic voltammetry on HME
1×10^{-3}	Sat. $CaCl_2$(~10 M) pH = 5.5; 25°C 0.005% gelatin	-0.51	–	Pecsok and Lingard,[28] polarography wave is polarographically reversible
1×10^{-3}	0.908 $NaClO_4$ 0.006 $HClO_4$ 27°C	-0.87	0.63	Jones,[25] polarography
$10^{-4} - 10^{-3}$	0.50 $HClO_4$ 25°C	-0.85	0.76	Elving and Zemel,[29] polarography
$10^{-4} - 10^{-3}$	1.9 $NaClO_4$ 0.1 $HClO_4$ 25°C	-0.89	0.75 before $E_{1/2}$ 0.48 after $E_{1/2}$	Elving and Zemel,[29] polarography
1×10^{-3}	2.0 KCl; 0.005% gelatin. pH not given, estimate at 6; temp. not given, estimate at room temp.	-0.81	-	Abubacker and Mali,[30] polarography. Traces of alcohol probably present.

SCE only in a very concentrated chloride solution. Frequent use of gelatin as a maximum suppressor makes much of the available polarographic data questionable.

Table (I-3) contains suspect data with both the higher and lower valency states of chromium present. Abubacker and Malik[31] formed $[Cr(H_2O)_6]^{2+}$ from chromic chloride by a method which, in all probability, left traces of alcohol in solution. To obtain the desired ratios of oxidation states, a portion of the lower valency state was oxidized with H_2O_2, which will produce not only $[Cr(H_2O)_6]^{3+}$, but also 14% of the chromium(III) in the dinuclear form.[19] Srinivasan et al.[32] prepared the lower valency state from chromic chloride by zinc reduction and permitted the zinc ion, whose ($E_{\frac{1}{2}}$) cathodic is about 150 mv more negative than the $E_{\frac{1}{2}}$ of $[Cr(H_2O)_6]^{3+}$, to remain in the supporting electrolyte. To further cause their data to be questioned, they attempted to reoxidize a portion of the chemically generated $[Cr(H_2O)_6]^{2+}$ to $[Cr(H_2O)_6]^{3+}$ with air, and unknowingly produced virtually 100% of the chromium(III) in the dinuclear form[19]. The rate constants from Abubacker and Malik, and Srinivasan et al. are about an order of magnitude higher than those previously cited. Randles and Somerton[33] did not specify that the pH of their supporting electrolyte, KCl, was anything other than neutrality. Significant hydrolysis[2] of $[Cr(H_2O)_6]^{2+}$ occurs at this high a pH. Their rate constant, however, is reasonable.

TABLE (I-3). Kinetic Data with Chromium(II) and Chromium(III) Both Present in Supporting Electrolyte

$\frac{Cr^{3+}}{Cr^{2+}}$	Total Cr in M	Supporting Electrolyte in M	$(E_{\frac{1}{2}})_c$ cathodic V vs SCE	α	$(E_{\frac{1}{2}})_a$ anodic V vs SCE	β	Reference, Comments
0.431 3.290	2.146×10^{-3} 2.146×10^{-3}	1 KCl; 0.005% gelatin. Temp. and pH not given, est. 25°C and acid soln.	-1.09 -1.00	0.48 -	-0.53 -0.52	0.25 -	Abubacker and Malik[31], polarography. Dinuclear species present.
1.146	2.146×10^{-3}	1 H_2SO_4 Other conditions same as above	-1.02	-	-0.54	0.18	Abubakcer and Malik,[31] polarography. Dinuclear species present.
0.22	0.1	1 KCl 25°C acidic	-	0.50	$K^{\circ}_{apparent} = 9.5 \times 10^{-5}$ cm/sec.	-	Srinivasan et al.,[32] (SME). Dinuclear species present.
5.90	0.1	Same as above	-	0.78	$K^{\circ}_{apparent} = 1.8 \times 10^{-4}$ cm/sec.	-	Srinivasan et al.,[32] (SME). Dinuclear species present.
1.0	10^{-3}	1 KCl; 20°C pH not given, est. at 6	-	-	$K^{\circ}_{apparent}$ at -0.716 V vs SCE = 1×10^{-5} cm/sec.	-	Randles and Somerton,[33] polarography

Table (I-4) demonstrates the sensitivity of chromium(II) oxidation to the composition of the supporting electrolyte. Rate constants and transfer coefficients increase on descending the Periodic Table for the halogens. In the last entry of the table, the shape of the polarographic wave was changed as well as its position. $(CH_3)_4NBr$ and KSCN in solution produced waves which appear more polarographically reversible than do the other two. These data strongly suggest that certain ligands facilitate the electron transfer process through double layer effects, bridging, atom transfer, or prior or post chemical reactions. Aquo complexed chromium(II) is labile and can exchange water for various ions in its inner coordination sphere. Chromium(III) is not labile and as Table (I-1) shows, its reduction is virtually independent of the composition of the supporting electrolyte except in extreme cases. The higher the dipole moment and polarizability of the ion, the more likely it is to enter into the inner coordination sphere of chromium(II) and present a more favorable energy barrier for electron transfer.

If ligands other than water are present in chromium(III), transfer coefficients and rate constants for the cathodic process change considerably from those for $[Cr(H_2O)_6]^{3+}$. Table (I-5) lists kinetic data for the reduction of chromium(III) complexes.

TABLE (I-4). $[Cr(H_2O)_6]^{2+}$ Oxidation in Various Media

$Cr(H_2O)_6^{2+}$ in M	Supporting Electrolyte in M	$E_{\frac{1}{2}}$ V vs SCE	β	Apparent Rate Constant in cm/sec vs SCE	Reference, Comments
~1.5 x 10^{-3}	0.908 $NaClO_4$ 0.066 $HClO_4$ 27°C	-	0.37	1.8 x 10^{-5} at -0.65 V	Jones[25] polarography
0.5-7 x 10^{-3}	1.0 $NaClO_4$ pH = 2 25°C	-	0.37	6.77 x 10^{-5} at -0.5 V	Aikens and Ross[14] HME
0.5-7 x 10^{-3}	0.95 $NaClO_4$ 0.005 NaCl pH = 2 25°C	-	0.43	9.5 x 10^{-5} at -0.5 V	Aikens and Ross[14] HME
0.5-7 x 10^{-3}	0.95 $NaClO_4$ 0.005 NaI pH = 2 25°C	-	0.50	1.67 x 10^{-4} at -0.5 V	Aikens and Ross[14] HME
1 x 10^{-4}	Sat. $CaCl_2$ (~ 10 M) pH = 5.5; 25°C 0.005% gelatin	-0.51	-	polarograph. reversible	Pecsok and Lingane[28] polarography

[continued]

TABLE I-4 (continued)

$Cr(H_2O)_6^{2+}$ in M	Supporting Electrolyte in M	$E_{\frac{1}{2}}$ V vs SCE	β	Apparent Rate Constant in cm/sec vs SCE	Reference, Comments
10^{-3}	1.0 KCl; 0.005% gelatin 25°C; pH not given, est. at 6	-0.40	-	-	Pecsok and Lingane,[28] polarography
10^{-3}	1.0 KSCN; 0.005% gelatin, 25°C; pH not given, est. at 6	-0.80	-	-	Pecsok and Lingane,[28] polarography
10^{-3}	0.5 HCOOH; 0.005% gelatin; 25°C	-0.30	-	-	Pecsok and Lingane,[28] polarography
10^{-3}	0.1 $(CH_3)_4NBr$; 0.005% gelatin; 25°C; pH not given, est. at 6	-	-	-	Pecsok and Lingane,[28] polarography
10^{-3}	0.1 KBr pH = 2.9 20°C	~-0.4	-	-	Kemula and Rakowska.[27] Cyclic voltammetry on HME. Wave is polarographically reversible.

TABLE (I-5). Chromium(III) Complex Reduction

Chromium(III) in M	Supporting Electrolyte in M	$E_{\frac{1}{2}}$ V vs SCE	α	Apparent Rate Constant in cm/sec	Reference, Comments
$[Cr(H_2O)_5Cl]^{2+}$	$NaClO_4$ (I = 1.0) pH = 2 25°C	-	0.39	-	Aikens and Ross[34] polarography
10^{-4} - 10^{-3} $[Cr(H_2O)_4Cl_2]^{+}$	0.1 HCl 25°C	-0.55	0.55	-	Elving and Zemel[29] polarography
10^{-4} - 10^{-3} $[Cr(H_2O)_4Cl_2]^{+}$	0.1 KCl 25°C pH not given; est. at 6	-0.55	0.48	-	Elving and Zemel[29] polarography
10^{-3} $[Cr(H_2O)_5Br]^{2+}$	0.91 NaBr 0.066 $HClO_4$ 27°C	-	0.48	1.82×10^{-3} at -0.50V vs SCE	Jones[25] polarography

Before an interpretation is given for the presented data, three more types of experimental results must be considered. Kemula and Rakowska[27] observed with cyclic voltammetry that $[Cr(H_2O)_6]Cl_3$ in 0.1N KCl at 20°C and a pH of 2.9 on a hanging mercury electrode (HME) will produce $[Cr(H_2O)_5Cl]Cl_2$ on the anodic sweep following the first cathodic sweep. The complex's presence is evident from the appearance of a new reduction peak on the second cathodic sweep. This phenomenon does not occur when the supporting electrolyte is $HClO_4$ or K_2SO_4. The perchlorate ion does not coordinate in the inner sphere with chromium(II) and the sulfate ion, which can be a member of the inner coordination sphere, is only weakly adsorbed in the potential range scanned. The import of this statement will become evident in the following section.

Jones[25,35] oxidized $[Cr(H_2O)_6]^{2+}$ at room temperature on a large mercury surface in an air-free solution of 2M $HClO_4$ containing a known amount of NaCl. The potential was held at -0.012V vs SCE since that was found to be the potential at which $Cr(H_2O)_6^{2+}$ oxidation is diffusion limited in the absence of chloride. Current integration determined the amount of $[Cr(H_2O)_6]^{2+}$ oxidized. Free chloride present in solution at the conclusion of the oxidation was determined by silver titration. The difference between final and initial chloride concentration gave the amount of $[Cr(H_2O)_5Cl]^{2+}$ in the product. Although the solution was not analyzed directly for $[Cr(H_2O)_5Cl]^{2+}$, (which could easily be accomplished spectrophotometrically[17] when most of the product is in that form),

$[Cr(H_2O)_5Cl]^{2+}$ is the most probable product. This explains the disappearance of the free chloride and is consistent with the results of homogeneous electron transfer studies,[10] the results of Kemula and Rakowska,[27] and the fact that $[Cr(H_2O)_4Cl_2]^+$ aquates quickly at so low a pH. Mass balance considerations demonstrate that $[Cr(H_2O)_4Cl_2]^+$ is not formed in any measurable amount. Jones further showed[25,36] with chronopotentiometric measurements in chloride and bromide solutions during $[Cr(H_2O)_6]^{2+}$ oxidation and current reversal for both oxidation and reduction that electron transfer is not preceded by a slow chemical reaction.

Qualitative Interpretation of Existing Data

The chromium(II)/(III) couple in an acidic fluoride or perchlorate supporting electrolyte under an inert atmosphere is a simple one-electron transfer reaction having very irreversible kinetics. When ions such as the halides, fluoride excluded, are present in the supporting electrolyte, the increasing reversibility of the couple is due to surface adsorption of the ion which subsequently transfers to the inner sphere of the approaching labile $[Cr(H_2O)_6]^{2+}$. The resulting redox couple differs from the simple $[Cr(H_2O)_6]^{2+}/[Cr(H_2O)_6]^{3+}$ in that $[Cr(H_2O)_5L]^{2+}$, where L = a ligand facilitating charge transfer, becomes involved. Since the anodic branch is positive to the point of zero charge on mercury and most anions are specifically adsorbed at such potentials, the above hypothesis is the most probable. $[Cr(H_2O)_6]^{3+}$ is too slow to inner sphere sub-

stitution for the halide to complex with it, and reasonable arguments suggest it is unlikely that the ligand complexes with the labile $[Cr(H_2O)_6]^{2+}$ in the bulk part of the solution prior to approaching the electrode. With a negative one charge on L, a chemical reaction prior to an electrode reaction can be represented as

$$[Cr(H_2O)_6]^{2+} + L^- \underset{k_r}{\overset{k_f}{\rightleftharpoons}} [Cr(H_2O)_5L]^+ \xrightarrow{-e} [Cr(H_2O)_5L]^{2+} \quad \text{(I-2)}$$

Voltage-time curves would show evidence of control by the homogeneous chemical process if $K[L^-](k_f[L^-] + k_r)^{\frac{1}{2}}$ is smaller[37] than 500 $sec^{-\frac{1}{2}}$. K is the equilibrium constant for the homogeneous reaction and is equal to k_f/k_r. $[L^-]$ is the ligand concentration in M. Since the present work is limited to ligands of chloride and bromide, the following discussion will be limited to them. Chloride will be considered first. Although exact values of K, k_f and k_r are not available, limits for them can be set by the following reasoning.

If the rate of diffusion of the complexing species toward each other is much faster than the rate of inner sphere complexing,

$$k_f = K_o k_{in} \; ; \; \text{where } K_o = \frac{C_{[Cr(H_2O)_6]Cl^+}}{C_{[Cr(H_2O)_6]^{2+}} C_{Cl^-}} \quad \text{(I-3)}$$

and k_{in} is the rate constant for transfer of the ligand from the outer to inner coordination sphere. Limits can be set for k_{in} and K_o from the following data. Eigen[38] reports a k_{in} of 2 to 3 x 10^8 sec^{-1}, but he has not published the experimental or theoretical

details concerning the procurement of this value. Connick[39] reports a water exchange rate constant for a specific water on $[Cr(H_2O)_6]^{2+}$ of 7×10^9 sec^{-1}. This value may be open to some question because of other factors contributing to the NMR line breadth. The rate of exchange of a water ligand on chromium(II) is certainly fast, with 10^8 sec^{-1} being a conservative estimate of k_{in}. For the present discussion, the Eigen value of 2×10^8 sec^{-1} will be used to determine whether or not Jones could have detected control by the homogeneous reaction (I-2).

The outer coordination sphere association constant K_o can be calculated from ionic association theory.[40-42]

$$K_o = \frac{4\pi Na^3}{3000} \exp\left(-\frac{z_A z_B e_o^2}{DakT}\right) \qquad \text{(I-4)}$$

where N = Avogadro's number, a = the encounter distance in cm, $z_A = z_B$ = valence of species, e_o = elementary charge in absolute electrostatic units, D = dielectric constant of solvent, k = Boltzmann's constant, and T = absolute temperature. At 25°C in an aqueous solution of D = 80 and a = 4Å (corresponding to the outer coordination sphere), $K_o = 5\ \underline{M}^{-1}$. With $K_o = 5\ \underline{M}^{-1}$ and $k_{in} = 2 \times 10^8$ sec^{-1}, $k_f = 1.0 \times 10^9\ \underline{M}^{-1}\ sec^{-1}$.

Knowledge of the equilibrium constant K for the homogeneous reaction will yield a value for the reverse rate constant k_r. Pecsok and Bjerrum[43] state that spectrophotometric analysis of chromium(II) solutions show no detectable amount of inner coordination sphere complexes forming for solutions less than 6 $\underline{M}$ in

chloride. This would suggest an equilibrium constant $k < 0.1$ $\underline{M}^{-1}$. From experimental kinetic data, Reynolds and Lumry[44] set an upper limit of 5.5×10^{-2} $\underline{M}^{-1}$ for K. Using this upper limit of 5×10^{-2} $\underline{M}^{-1}$ for K, k_r for the dissociation of $[Cr(H_2O)_5Cl]^+$ has a lower limit of 2×10^{10} $\underline{M}^{-1}sec^{-1}$.

When $k_f = 10^9$ $\underline{M}$ sec^{-1}, $k_r = 2 \times 10^{10}$ sec^{-1} and $K = 0.05$ $\underline{M}^{-1}$, $K[Cl](k_f[Cl^-]+k_r)^{\frac{1}{2}}$ ranges from 560 to 700 $sec^{-\frac{1}{2}}$ for chloride solutions of 0.08 to 0.10 $\underline{M}$, which Jones employed. If the activity coefficient for a 1$\underline{M}$ $NaClO_4$ supporting electrolyte is considered, $K[Cl^-]\gamma_\pm(k_f[Cl^-]\gamma_\pm+k_r)^{\frac{1}{2}}$ ranges from 350 to 440 $sec^{-\frac{1}{2}}$. These values, with or without the activity coefficient correction, are on the borderline for detection with chronopotentiometry. Jones' abundant data are consistent and appear reliable in concluding that a homogeneous reaction prior to electron transfer is not an important factor in the kinetics.

For other transition metal ions such as Co^{2+}, Cd^{2+}, Fe^{2+}, and Ni^{2+}, the stability constants with a bromide ion are just about equal to or less than those with a chloride ion. Consequently, contribution from Reaction (I-2) is even less significant with bromide than with chloride, unless a very high bromide concentration is used.

When $[Cr(H_2O)_6]^{2+}$ approaches an electrode surface which is not uniformly covered by the adsorbed ion, it can either approach an occupied site or an unoccupied site. If an unoccupied site is approached, reaction (I-5) occurs.

$$[Cr(H_2O)_6]^{2+} \xrightarrow{k_1} [Cr(H_2O)_6]^{3+} + e^- \qquad \text{(I-5)}$$

If an occupied site is approached by $[Cr(H_2O)_6]^{2+}$, reaction (I-6) occurs.

$$[Cr(H_2O)_6]^{2+} + X^-_{ad} \xrightarrow{k_2} [Cr(H_2O)_5X]^{2+} + e^- \qquad \text{(I-6)}$$

where X = chloride or bromide ion.

An overall rate constant which is contributed to by k_1 and k_2 is observed. Since the kinetics of (I-6) are faster than those of (I-5), the observed apparent rate constants for chromium(II) oxidation will be larger in the presence of ligands which specifically adsorb on mercury and which complex inner sphere with chromium(II).

For weak interaction of reactants, Marcus[45] states that the transfer coefficient is 0.5 for small activation overpotentials when the work terms are negligible. For strong interaction homogeneous reactions, the transfer coefficient can still be expected to be 0.5 in certain cases. The strong interaction case for electrode reactions has not been treated. In a perchlorate medium, α for $[Cr(H_2O)_6]^{3+}/[Cr(H_2O)_6]^{2+}$ is 0.63 uncorrected for double layer effects,[25] and 0.5 when corrected[26]. For $[Cr(H_2O)_5Cl]^{2+}/[Cr(H_2O)_6]Cl^{+}$ α uncorrected[34] is 0.39. Both of these reactions are polarographically irreversible with the half wave potentials sep-

arated by at least 120 mv. The first couple cited could be considered an example of weak interaction, if no water molecule is transferred between chromium(II) and chromium(III), but the second couple is definitely an example of strong interaction. With $[Cr(H_2O)_5Br]^{2+}/[Cr(H_2O)_6]Br^{+}$, which is another example of strong reactant interaction, α uncorrected[25] is 0.48 and the system is almost polarographically reversible.

Since the thermodynamically most stable form of the labile chromium(II) is the one whose inner-sphere is coordinated with six water molecules. in this work the reduction product of $[Cr(H_2O)_5Cl]^{2+}$ will be written as $[Cr(H_2O)_6]Cl^{+}$, not as $[Cr(H_2O)_5Cl]^{+}$, and the reduction product of $[Cr(H_2O)_5Br]^{2+}$ will be written as $[Cr(H_2O)_6]Br^{+}$, not as $[Cr(H_2O)_5Br]^{+}$.

CHAPTER II

MATHEMATICAL ANALYSIS

General Kinetic Considerations

Cyclic voltammetry on a hanging mercury electrode was the principal experimental method used in this work. Except for the sensitivity of chromium(II) to air, obtaining cyclic voltammetry data was experimentally uncomplicated. Evaluation of current-potential curves, on the other hand, is rather awkward because of diffusion problems. For irreversible reactions on plane electrodes with at least partial mass transfer control, several approximate analytical functions are available. For spherical electrodes or quasi-reversible reactions, explicit solutions are, for the most part, lacking and tabulated numerical solutions must be used.

To simplify mathematical analysis and to minimize the number of assumptions, an expression derived directly from first principles was used to convert experimentally obtained current-time data into reactant species concentration at the interface. The concentrations so obtained were used to find the apparent rate constant at a given potential.

The advantage of first calculating reactant species concentrations at the interface and then determining the apparent rate constants was that neither numerical tabulated functions nor a priori assumptions concerning the dependence of the apparent rate constant on

potential need be made. The most obvious manner in which to treat the apparent rate constants was to make a semi-log plot of them vs applied potential to ascertain if Tafel linearity was observed. Subsequently the rate constants for the parallel processes were separated with certain assumptions and double layer corrections applied, as will be shown later.

When the anodic and cathodic waves are distorted sufficiently from reversible behavior, the back reaction can be neglected for rate constant calculations. This is the case for the $[Cr(H_2O)_6]^{2+}/[Cr(H_2O)_6]^{3+}$ couple and the $[Cr(H_2O)_6]Cl^{+}/[Cr(H_2O)_5Cl]^{2+}$ couple. Under such conditions the net current is

$$i = nFACk_a \qquad \text{(II-1)}$$

The observed current i at a particular potential is proportional to an apparent rate constant k_a for that same potential. Current is in amperes and k_a is in cm/sec. The other symbols are defined as F the Faraday, A the electrode area in cm^2, C the concentration in $mole/cm^3$ of the reacting species at the interface, and n the number of electrons.

For $[Cr(H_2O)_6]Br^{+}/[Cr(H_2O)_5Br]^{2+}$, the couple is almost reversible and at any particular potential near its reversible potential, both an anodic and cathodic component of the current must be considered. For

$$[Cr(H_2O)_6]^{2+} + Br^{-}_{ad} \underset{k_{-4}}{\overset{k_4}{\rightleftharpoons}} [Cr(H_2O)_5Br]^{2+} + e^{-} \qquad \text{(II-2)}$$

k_4 and k_{-4} are the effective first order rate constants with the surface concentration of Br^-_{ad} included in k_4 (i.e., $k_4 = k'_4\theta_{Br^-}$ where θ_{Br^-} is the fractional electrode surface coverage for bromide). For any particular potential, simultaneous rate equations can be written for the anodic i_a and cathodic i_c currents. The current corresponding to the anodic wave is

$$\frac{i_a}{nFA} = [C'_{Cr(H_2O)_5Br^{2+}}]k_{-4} - [C'_{Cr(H_2O)_6^{2+}}]k_4 \qquad \text{(II-3)}$$

and that for the cathodic wave is

$$\frac{i_c}{nFA} = [C_{Cr(H_2O)_5Br^{2+}}]k_{-4} - [C_{Cr(H_2O)_6^{2+}}]k_4 \qquad \text{(II-4)}$$

The primed concentrations refer to the concentrations observed on the anodic wave; the unprimed concentrations refer to the concentrations observed on the cathodic wave. Anodic currents are taken as negative and cathodic currents are positive. These simultaneous rate equations can be solved and each rate constant expressed at a particular potential in terms of the anodic and cathodic currents and reacting species concentrations.

$$k_{-4} = \frac{[i_a(C_{Cr(H_2O)_6^{2+}}) - i_c(C'_{Cr(H_2O)_6^{2+}})]}{(nFA)[C'_{Cr(H_2O)_5Br^{2+}})(C_{Cr(H_2O)_6^{2+}}) - (C_{Cr(H_2O)_5Br^{2+}})(C'_{Cr(H_2O)_6^{2+}})]}$$

$$k_4 = \frac{[k_{-4}(C_{Cr(H_2O)_5Br^{2+}}) - i_c/(nFA)]}{[C_{Cr(H_2O)_6^{2+}}]} \qquad \text{(II-5)} \qquad \text{(II-6)}$$

The constancy of k_4 at a given potential is contingent on θ_{Br^-} remaining constant. Such will be true provided the concentration of bromide is sufficiently large that no large change in bromide concentration

in the solution adjacent to the electrode occurs. The adsorption-desorption of bromide should be very fast and not cause any complications.

Observed Current-Concentration Relationship

In order to use either Eq. (II-1) or Eqs. (II-5) and (II-6), the concentration of the reactant species at the interface must be calculated. This can be accomplished by considering the following. For a plane electrode with a reaction of the form

$$O + ne \underset{\overleftarrow{k_a}}{\overset{\overrightarrow{k_a}}{\rightleftharpoons}} R \qquad \text{(II-7)}$$

the differential equations and associated boundary conditions are[46]

$$\partial C_o/\partial t = D_o(\partial^2 C_o/\partial x^2) \qquad \text{(II-7a)}$$

$$\partial C_R/\partial t = D_R(\partial^2 C_R/\partial x^2) \qquad \text{(II-7b)}$$

At $t = 0$ and $x \geq 0$, $C_o = C_o^*$ and $C_R = C_R^* = 1$. (II-7c)

At $t \geq 0$ and $x \to \infty$, $C_o \to C_o^*$ and $C_R \to 0$. (II-7d)

At $t > 0$ and $x = 0$,

$$D_o(\partial C_o/\partial x) = -D_R(\partial C_R/\partial x) = \frac{i}{nFA} = [\overrightarrow{k_a}C_o - \overleftarrow{k_a}C_R] \qquad \text{(II-7e)}$$

C_o and C_R are the concentrations of O and R at the distance x from the electrode, t is time, C_o^* and C_R^* are the bulk concentrations, and D_o and D_R are the diffusion coefficients.

When the back reaction is negligible, Eq. (II-7e) becomes

$$D_o(\partial C_o/\partial x) = \overrightarrow{k_a}C_o = i/nFA \qquad \text{(II-8a)}$$

for $t > 0$ and $x = 0$.

The apparent rate constant k_a in the forward and reverse directions are related to the apparent standard rate constant k_a° by

$$k_a = k_a^\circ \exp [(\alpha nF/RT)(E-E^\circ)] \qquad \text{(II-8b)}$$

where the usual assumption is made that the electrochemical free energy of activation is a linear function of the overall change in the electrochemical free energy of the reaction. The applied electrode potential is E, the standard electrode potential is E°, and R, T, and F have their usual significance.

By taking Laplace transforms of Eqs. (II-6a to d), determining the transform of the surface concentrations as a function of the transform of the surface fluxes and then using the convolution theorem, the following[46] is obtained for the concentration in the solution immediately outside of the diffuse double layer at time t:

$$C = C^* \pm \left[\frac{1}{nFA(D\pi)^{1/2}}\right] \int_0^t \frac{i}{(t-\tau)^{1/2}}\, d\tau \qquad \text{(II-9)}$$

where i corresponds to a particular time τ and C* is the bulk concentration for whichever polarizable species is present at t=0. (The experimentally obtained current-potential data from the cyclic voltammetry curves can be translated easily into current-time data by viewing the process as occurring on a continuous, unidirectional time scale with time zero corresponding to the potential at which the scan was begun.) The sign of the second term in Eq. (II-9) depended upon which process, oxidation or reduction, was followed. For example, when $[Cr(H_2O)_6]^{3+}$ was present in solution at t=0 and

its reduction was followed, the second term was negative; when the reoxidation of the generated $[Cr(H_2O)_6]^{2+}$ was followed, the second term was positive. For all of the experiments in the present work, chromium was initially present only in the chromium(III) form so that the concentration of the chromium(II) form at t=0 was always zero.

Several assumptions[47] are implicit in the derivation of Eq. (II-9). Diffusion toward the spherical electrode was described by semi-infinite linear diffusion equations. The use of a supporting electrolyte in large excess over the concentration of the polarizable species enabled ionic migration under the influence of an electric field to be neglected. Convection complications were not considered. The diffusion coefficient was assumed the same for chromium(II) and chromium(III) in using Eq. (II-9). This assumption was based on the knowledge that the diffusion current constants measured in nearly identical solutions for chromium(II) and chromium(III) were 1.50 and 1.54 respectively.[14] The diffusion coefficient for $[Cr(H_2O)_6]^{3+}$ at 25°C in 0.5M $NaClO_4$ at a pH of 3 to 4 was calculated to be 5.82×10^{-6} cm^2/sec from the experimentally measured diffusion current constant.[48] This calculation was accomplished with the simple Ilkovic equation[49] which is correct to within 5%.

Experimental Conditions Corresponding to Calculation of Interface Concentrations

The current-time data from the initial cycle sweeps are the only really safe data to use for Eq. (II-9), since the assumptions used for its derivation -- negligible convection and spherical corrections --should then be valid. The initial cycle sweeps were completed in 10 to 20 sec whereas generally 30 sec is required for natural convection to develop. Consequently convection complications were not taken into account. To ascertain how large the correction for spherical divergence of the electrode was, published tables of Nicholson and Shain[46] can be used. From these tables, the contribution to the total current for the spherical divergence of the electrode for the first cathodic or anodic sweep of an irreversible or of a reversible reaction can be calculated. Such was done for the three different couples considered in this work.

For the first sweep for the irreversible $[Cr(H_2O)_6]^{2+}/[Cr(H_2O)_6]^{3+}$ couple, the parameters used for this calculation were scan rate = 0.2 V/sec, diffusion coefficient = 5.82×10^{-6} cm^2/sec, transfer coefficient = 0.5, radius of electrode = 0.028 cm, apparent standard rate constant = 10^{-5} cm/sec, and standard potential = -0.65V vs SCE. The correction for spherical divergence amounted at most to only 0.2% of the total observed current. For the potential range from which most of the apparent rate constants were obtained, the spherical correction was less than 0.1% of the total observed current.

For the $[Cr(H_2O)_6]Cl^+/[Cr(H_2O)_5Cl]^{2+}$ couple which can be analyzed by neglecting the back reaction, the spherical correction over the potential range of the greatest interest was again about 0.1% of the total observed current. For this calculation the standard apparent rate constant was taken as 3×10^{-4} cm/sec, and the standard potential as -0.46V vs SCE. The other parameters were the same as the ones listed above.

For the almost reversible $[Cr(H_2O)_6]Br^+/[Cr(H_2O)_5Br]^{2+}$ couple, an estimate of the spherical contribution could be made from the Nicholson and Shain tabulated data for a reversible reaction. In this case the spherical contribution to the total current was at most about 1%. For this calculation $(E-E_{1/2})$ was ± 30 mV, with the other parameters needed for the calculation being the same as those already given. Since the spherical contributions were so small for each of the three couples, the spherical contributions could be disregarded for the initial sweep voltammetry curves.

A significant portion of this work was done with the initial sweep data. However, much data was recorded in earlier phases of this work after 3 or 4 complete cyclic scans had produced voltammetry curves of constant shape. Since it was desirable to also use these "steady-state" data, the necessity arose for determining how different the rate constants and Tafel slopes obtained from the "steady-state" data were from the initial sweep data.

The method for determining these differences was to compare the apparent rate constants calculated from initial cycle current-

time data with the apparent rate constants calculated from the "steady-state" curve for the same run. For the calculation of the apparent rate constants from the initial cycle scan, the integration in Eq. (II-9) was begun at the true time zero when the concentration of chromium(III) at the interface was equal to the concentration of chromium(III) in the bulk and the concentration of chromium(II) was equal to zero. For the calculation of the apparent rate constants from the "steady-state" cycle, a point on the curve was designated as t=0, which will be termed pseudo-time zero, and the assumption was made that at this point the concentration of chromium(III) at the interface was equal to the concentration of chromium(III) in the bulk and that the concentration of chromium(II) was equal to zero. The integration in Eq. (II-9) was then begun from the pseudo-time zero.

If the pseudo time zero for the "steady-state" curve is selected from a flat portion of the curve preceding a voltammetry peak where the net current was zero or close to it, the concentration gradient would also be close to zero. The other errors resulting from using a "steady-state" curve instead of an initial cycle curve are difficult to predict. Some natural convection should have set in. Furthermore, the concentration gradient may extend further from the electrode surface than during the initial sweep and hence the spherical correction may not necessarily be small. The actual proof that the differences in apparent rate constants and Tafel slopes between initial and "steady-state"

cycles were small, is the comparison of these parameters for the initial and "steady-state" cycles in a number of test cases.

The first critical case is that with no halogen present in the supporting solution. The cyclic voltammetry curve beginning at the true time zero and continuing until the "steady-state" has been reached is shown in curve A of Fig. II-1. The apparent rate constants for the $[Cr(H_2O)_6]^{2+}/[Cr(H_2O)_6]^{3+}$ couple were calculated by the computer program (described in the following section) for two different typical initial cycle voltammetry curves which began at the true time zero and for each of their "steady-state" cycle voltammetry curves which began at a pseudo time zero. For the initial cycle curves, the total electrolysis times were 20 sec and for the steady-state cycle curves, the pseudo time zero was either 60 or 80 sec after the true time zero. The pseudo time zero was selected from a flat portion of the curve preceding the cathodic peak, where the net current was zero or close to it. In this manner an attempt was made to begin the integration when the concentration gradient was close to zero. The pseudo time zero and true time zero are indicated by the vertical arrows in Fig. II-1.

A semi-log plot of apparent rate constants vs applied potential calculated from the initial cycle and the "steady-state" cycle are given in Fig. II-2. The apparent rate constants on the cathodic branch for the initial and steady-state cycles were virtually identical. On the anodic branch, the steady-state cycle's rate constants

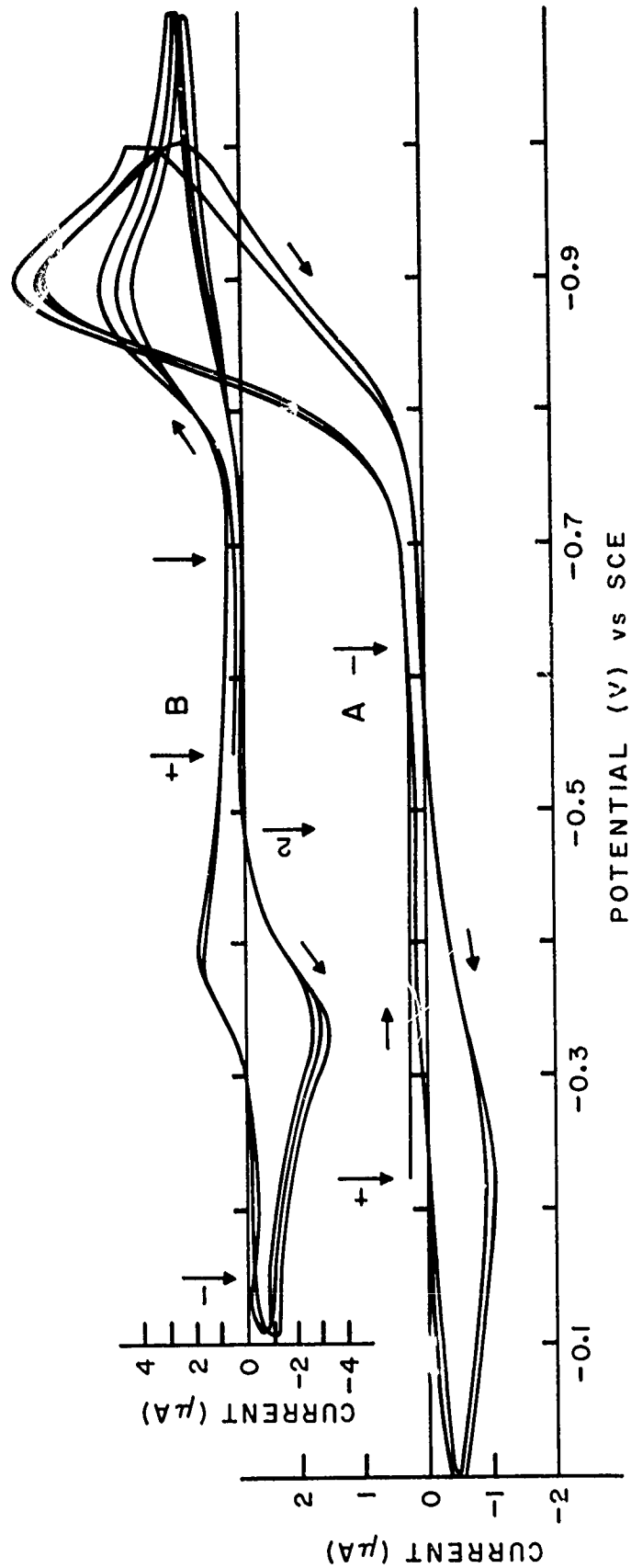

Fig. II-1. Initial and "steady-state" cyclic voltammetry curves in pure perchlorate and mixed bromide-perchlorate solutions. Curve A: initial $[Cr(H_2O)_6](ClO_4)_3$ concentration = 2.46 mM in 0.33 M $NaClO_4$ at pH of 2.20. Scan rate = 0.0982 V/sec, HME area = 0.02236 cm^2. Curve B: initial $[Cr(H_2O)_6](ClO_4)_3$ concentration = 2.41 mM in 0.316 M $NaClO_4$ and 0.0107 M NaBr at pH of 2.13, HME area = 0.01278 cm^2, scan rate = 0.1793 V/sec. T = 25°C for both. In both cases, the potential scal has been translated into a continuous, unidirectional time scale. The true time zero corresponds to the time at which the potential is first applied to the cell. The → and → are pseudo time zeroes which correspond to the point selected on the "steady-state" curve at which the concentration gradient has been assumed to be zero. For the pseudo time zeroes, an explanation is given at the end of Appendix II.

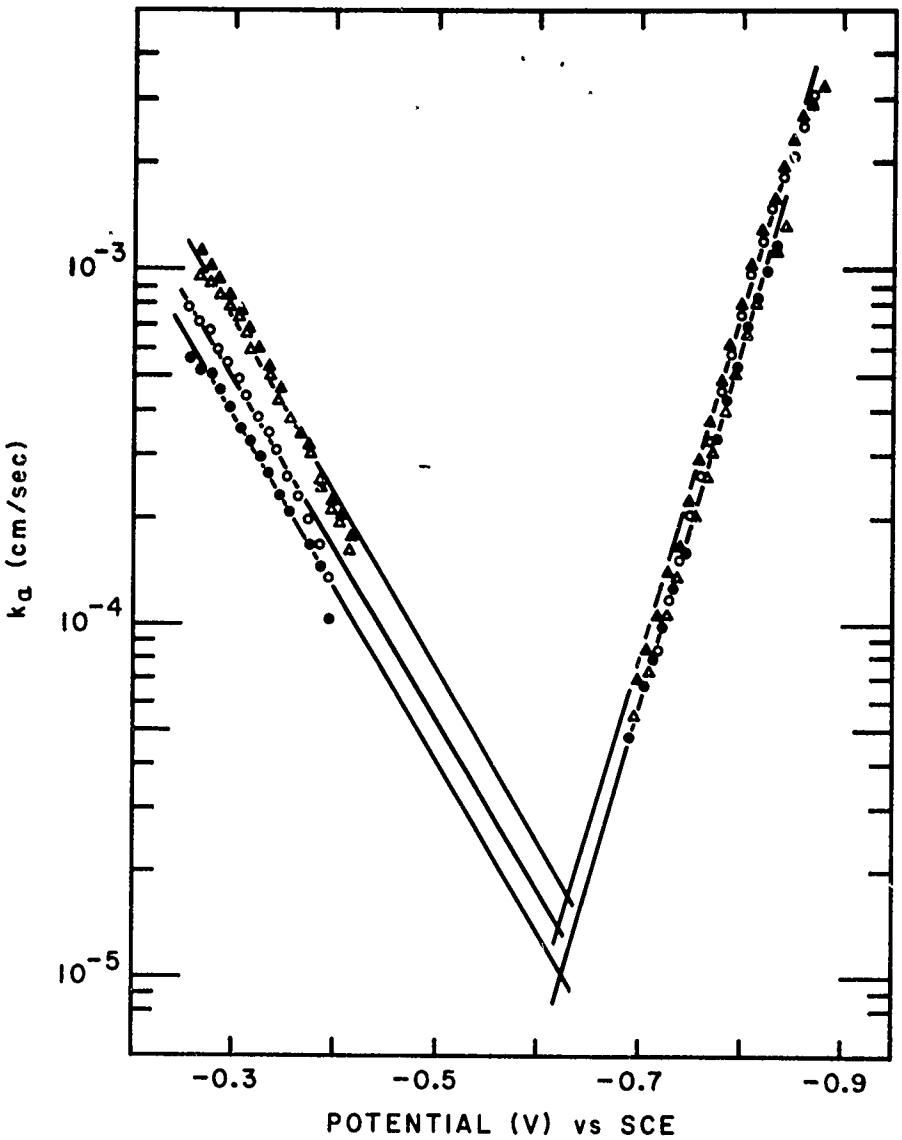

Fig. II-2. Log of apparent rate constants from initial and "steady-state" cycle scans vs applied potentials for $[Cr(H_2O)_6]^{2+}/[Cr(H_2O)_6]^{3+}$. Initial $[Cr(H_2O)_6](ClO_4)_3$ concentration = 2.46 mM in 0.33 M $NaClO_4$ at pH = 2.20, T = 25°C, scan rate = 0.0982 V/sec, and HME areas were: ● 0.02381 cm^2; X 0.02236 cm^2. ● and o are the initial cycle apparent rate constants and ▲ and △ are the corresponding "steady-state" apparent rate constants.

were between a factor of 1.5 to 2 times larger than the rate constants for the initial cycle. The values of the Tafel slopes did not change between the initial and steady-state cycles. When the standard apparent rate constants and standard potential were calculated from initial cycle and steady-state cycle data, the question of which set of data to use became relatively minor. The difference in apparent standard rate constants was a factor of 1.4 and the difference in standard potential was 10 mV. The larger discrepancy between apparent rate constants for the anodic branch than for the cathodic branch was a result of assuming the chromium(II) concentration to be zero at the electrode surface and extending out into the solution at the pseudo time zero. These were zero only at the true time zero.

The second critical case evaluated was with bromide present in the supporting electrolyte. The voltammetry curves with bromide present in the supporting electrolyte are significantly different from those with only perchlorate present. The cyclic voltammetry curve in bromide-perchlorate solutions beginning at the true time zero and continuing until the "steady-state" was reached are shown in curve B of Fig. II-1. The true and pseudo time zeroes are indicated with vertical arrows.

Another computer program (described in the next section) was used to calculate apparent rate constants for two typical runs with bromide present in the supporting electrolyte for the $[Cr(H_2O)_6]^{2+}/[Cr(H_2O)_6]^{3+}$ couple and for the $[Cr(H_2O)_6]Br^{+}/$

$[Cr(H_2O)_5Br]^{2+}$ couple from both the initial cycle and "steady-state" cycle current-time data. A semi-log plot of these apparent rate constants is given in Fig. II-3. The intersection of extrapolated lines at more negative potentials corresponds to the apparent standard rate constant for the $[Cr(H_2O)_6]^{2+}/[Cr(H_2O)_6]^{3+}$ couple, while the intersection of lines at less negative potentials corresponds to the apparent standard rate constant for the $[Cr(H_2O)_6Br^{+}/[Cr(H_2O)_5Br]^{2+}$ couple.

For the $[Cr(H_2O)_6]Br^{+}/[Cr(H_2O)_5Br]^{2+}$ couple, the Tafel slopes were identical for the initial cycle and "steady-state" cycle curves. The apparent standard rate constants differed by a factor of 1.8 and the standard potentials differ by 8 mV. For the $[Cr(H_2O)_6]^{2+}/[Cr(H_2O)_6]^{3+}$ couple, the Tafel slopes for the cathodic branch differed for the initial cycle and "steady-state" cycle curves, but the difference was relatively small.

Since the Tafel slopes, standard apparent rate constants and standard potentials calculated with Eq. (II-9) from "steady-state" cycle voltammetry data (even with no spherical divergence correction) do not differ substantially from those values calculated from the initial cycle voltammetry data for the critical cases, the use of "steady-state" cycle data appears acceptable.

Computer Program to Generate Reactant Species Concentrations at the Interface and the Apparent Rate Constants

To facilitate the integration in Eq. (II-9) and the use of the resulting concentrations in Eq. (II-1), (II-5), or (II-6) for

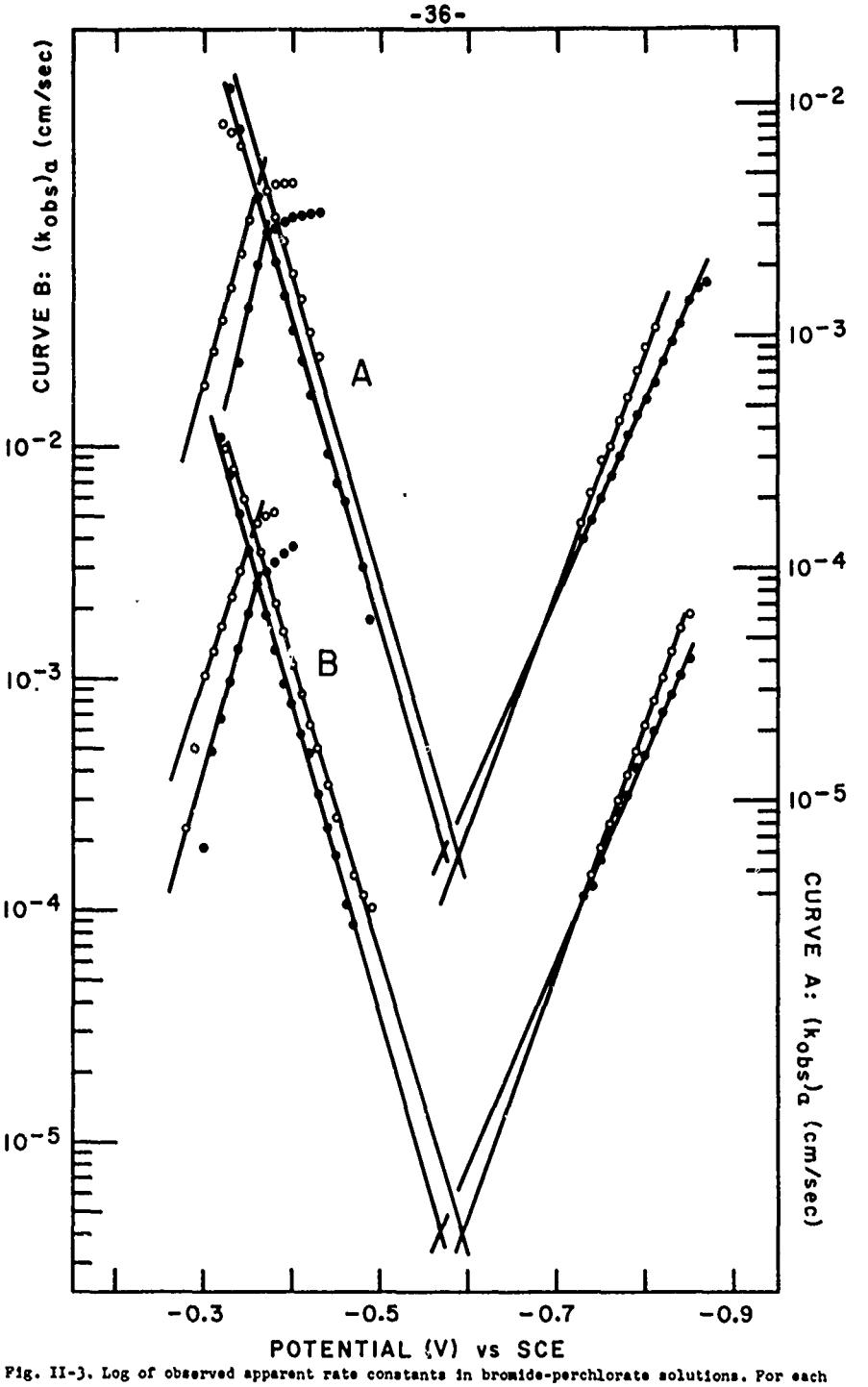

Fig. II-3. Log of observed apparent rate constants in bromide-perchlorate solutions. For each run O is for the initial cycle and ● is for the "steady-state" cycle. Initial concentration of $[Cr(H_2O)_6](ClO_4)_3$ = 2.41 mM in 0.316 M $NaClO_4$ at pH = 2.13, scan rate = 0.1793 V/sec. Curve A: 0.0107 M NaBr, HME area = 0.01278 cm^2 Curve B: 0:00773 M NaBr, HME area = 0.01404 cm^2.

the calculation of apparent rate constants, a digital computer (Univac 1108) was used. From the following considerations, computer programs were written.

Typically the potential was swept from zero to a -1 V vs SCE and then reversed. Since the same potential was passed twice in one complete cycle, the procedure was viewed as occurring on a continuous, unidirectional time scale. The function within the integral sign for Eq. (II-9) was calculated for closely spaced equal time intervals corresponding to 0.01 V and summed according to the method of trapeziums. Once the interface concentration values were obtained, Eqs. (II-1) or (II-5) and (II-6) were used to calculate apparent rate constants at predetermined voltages of interest.

The current values used in Eq. (II-9) were the Faradaic, not the total observed currents. The assumption was made that the Faradaic and non-Faradaic components of the total current are additive and that the non-Faradaic component could simply be subtracted from the total observed current. Thus

$$i_{\text{total observed}} = (i_{\text{Faradaic}}) + (i_{\text{non-Faradaic}}) \quad \text{(II-10)}$$

At a sweep rate of 0.2V/sec, one of the fastest sweep rates used in this work, the non-Faradaic current was only about 1×10^{-5} A/cm^2 while the Faradaic peak currents were about 3×10^{-4} A/cm^2. The size of the non-Faradaic current for each voltammetry curve was obtained from the change in current values at the points where

the scan direction was reversed. The non-Faradaic current was assumed constant over the entire potential range scanned. Therefore a small error was introduced since the double layer capacity was not constant over the voltage range under consideration. The error, however, in the final double layer corrected standard rate constants was quite small, being no greater than 2.5%. This error estimate was made on the basis that the non-Faradaic component was usually not greater than 3% of the current averaged over the voltammetry peak and used in the integration of Eq. (II-9).

Appendix I contains the program mainline for obtaining apparent rate constants when the back reaction can be neglected. Appendix II contains the program mainline for obtaining apparent rate constants when the back reaction must be considered. An explanation of each mainline is given. Both programs were written in Fortran V and executed on a Univac 1108.

Double Layer Corrections

Double layer corrections can be substantial with higher valency ions like chromium(II) and chromium(III) at millimolar concentrations, even in the presence of a supporting electrolyte with an ionic strength near 0.35. Double layer corrections derived by Frumkin for the apparent rate constants consider the fact that only a portion of the potential drop across the interface occurs between the electrode and the outer Helmholtz plane, and that the concentration of reacting species at the outer Helmholtz plane is

substantially different from what it would be in the bulk. The following equation[50] can be used to correct apparent rate constants at any given potential to true rate constants for the same potential.

$$k_a = k_t \exp[(\alpha n - Z) F \phi_2 / (RT)] \qquad \text{(II-11)}$$

The charge with sign of the reducing species is Z; α is the true transfer coefficient; and ϕ_2 is the potential at the outer Helmholtz plane relative to the bulk of the solution. In Eq. (II-11) the assumption is made that the distance of closest approach to the electrode of the reacting species before charge transfer corresponds to the outer Helmholtz plane.

The true transfer coefficient α_t can be calculated from[51] the apparent transfer coefficient α_a for a one-electron transfer by

$$\alpha_t = \frac{\alpha_a - Z \frac{\partial \phi_2}{\partial E}}{1 - \frac{\partial \phi_2}{\partial E}} \qquad \text{(II-12)}$$

where $\partial \phi_2 / \partial E$ is the value over the potential range where the apparent rate constants were used to calculate α_a. The use of Eqs. (II-11) and (II-12) for determining the double layer corrected rate constants for the cathodic branch is correct and does not depend upon $(\alpha + \beta)$ equalling one. Using these equations for the anodic branch is open to question, since then the assumption that $(\alpha + \beta) = 1$ is necessary. If all effects which influence the redox kinetics are properly accounted for, $(\alpha + \beta)$ should indeed equal one. The α_t which is used in Eq. (II-11) for the correction of the anodic branch rate constants is obtained from Eq. (II-12) with the α_a being

$(1-\beta_a)$. Here the β_a is the apparent transfer coefficient for the anodic branch. Some question exists about how to consider the reduction of the inner sphere halogen chromium(III) complex with respect to α_t. A discussion of the reduction of the inner-sphere halogen chromium(III) complex will be given later.

ϕ_2 data on mercury for pure perchlorate, chloride,[52] and bromide[53] solutions over a concentration range of about 0.01 to 4 M are available. The previously unpublished double layer data of R. Payne for perchlorate solutions are listed in Appendix III. The author is indebted to Dr. Payne for making these data available.

ϕ_2 data for the experimentally used mixed electrolytes of perchlorate and chloride, or bromide, are not available. Dutkiewicz and Parsons[54] presented a partial solution to the problem. With different mixtures of KI and KF at constant ionic strength, they found that the dependence of the iodide adsorption data on the activity of the salt $(a_{KI}) = (a_{K^+})(a_{I^-})$ was the same, independent of the concentration of the KF. Such was not the case when the dependence of the iodide adsorption on the iodide activity ($a_{I^-} = \gamma_{\pm} C_{I^-}$) was considered. Isotherms of electrode charge coincided for solutions of pure KI and mixtures of KI and KF when the charge due to specific adsorption was plotted vs the log of the salt activity, a_{KI}, and not vs the log of the iodide ion activity. Consequently, ϕ_2 data for pure iodide solutions can be plotted vs the salt activity and then the ϕ_2 data for a mixed electrolyte of iodide

and fluoride for a certain total salt activity can be determined from the graph.

Iodide strongly adsorbs on mercury whereas fluoride does not adsorb. The same experimental correlation for two adsorbing anions probably would not be exactly the same as that for one strongly adsorbing anion and a non-adsorbing anion. Teppema et al.[55a] used the method of Dutkiewicz and Parsons for bromide-chloride mixtures at potentials where the chloride adsorption is almost negligible. The mixtures were then treated as if chloride did not specifically adsorb. The method worked well since their measured capacity-potential curves for KCl + KI mixtures were identical to the capacity-potential curves of KF + KI mixtures at potentials more negative than -1.0 V vs NCE for mole fractions of KI in KI + KCl mixtures of 0, 0.01, and 0.1.

They also suggested that the method of Dutkiewicz and Parsons would not work well if the ratio of strongly adsorbing anion to weakly adsorbing anion in a solution was less than 0.2. This is because the presence of the more weakly adsorbing ion in the inner part of the compact double layer would make a substantial contribution to the ϕ_2 values.

Since the perchlorate specific adsorption is weaker than the chloride or bromide specific adsorption, the method of Dutkiewicz and Parsons was applied to the mixed electrolytes used in the present work. For the chloride-perchlorate mixtures, the method worked well except at low ($<4\%$) percentages of chloride in per-

chlorate at potentials negative to the point of zero charge, which is -0.490 V vs SCE in 0.33 M $NaClO_4$ at a pH of 2.0 according to Payne's data (Appendix III). For this range, ϕ_2 data for pure perchlorate solutions were used. For the bromide-perchlorate mixtures, the method did not work as well. The details of the separation of apparent rate constants for the parallel oxidation reactions and the details of double layer corrections will be presented with the data analysis.

The ϕ_2 data used to correct apparent rate constants were not obtained in the presence of chromium ions, whereas the solutions used in the present work contained chromium. Even though the supporting electrolyte was 0.33 M $NaClO_4$ and the bulk chromium(III) concentration was $\leq 5 \times 10^{-3}$ M, some of the ϕ_2 values were sufficient in some cases to cause very high chromium(III) and chromium(II) concentrations at the electrode. The ϕ_2 values would be expected to differ somewhat with and without chromium ions present. For the correction of apparent rate constants, the effect of chromium on ϕ_2 was not taken into account. The consequences of this omission will be further discussed in the last chapter.

CHAPTER III

EQUIPMENT, CHEMICALS, AND TECHNIQUES

Electronic and Glass Equipment

A Hewlett-Packard function generator (model 3300A) was used in conjunction with a scanner modified[55b] Wenking fast rise potentiostat (model 61R) and Hewlett-Packard X-Y recorder (model 7030A) for the cyclic voltammetry studies on a hanging mercury electrode (HME). (Some preliminary studies were made on a mercury pool electrode which is shown in Fig. III-1.) The slewing rate (20 in/sec) of the X-Y recorder was such as to enable the recording of the current-voltage curves with no distortion at accuracies of 0.3% up to the fastest voltage sweep used in the present work. This was generally 0.2V/sec (equivalent to 2"/sec pen travel). One run only was at 0.47V/sec (equivalent to 4.7"/sec pen travel) and the apparent rate constants calculated from these voltammetry curves agreed with those of slower sweep rates.

The Kemula Assembly for the HME was modified to improve electrical contact by placing a bit of silver solder between the center shaft and outer hull. Mercury drops of reproducible size were formed at the end of precision bore tubing (Wilmid Glass Co.) of 0.004 inch internal diameter. Drop size was controlled by turning the micrometer of the Kemula Assembly the same distance for each drop formation. After the experiment was completed, about a dozen

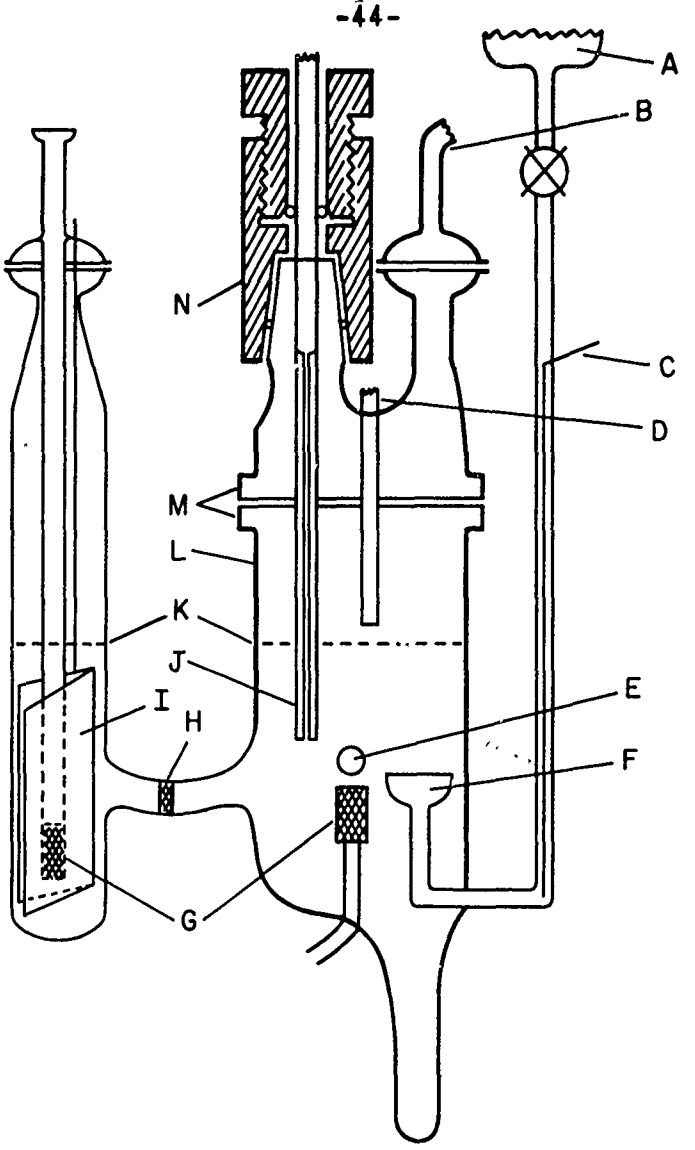

Fig. III-1. Electrochemical cell showing the working electrode compartment on the right and the counter electrode compartment on the left. A = Mercury reservior for Hg pool electrode; B = Helium gas exit; C = Tungsten lead to Hg pool electrode; D = Inlet tube from storage pipettes; E = Opening to reference electrode compartment; F = Hg pool electrode; G = Bubblers; H = Sintered glass disc; I = Platinum foil; J = Capillary for HME; K = Liquid level; L = Level of oil in oil bath surrounding cell; M = 2" joint pressure clamp (not pictured); N = Kel-F adapter.

drops of mercury were formed in the same solution used for the voltammetry studies and knocked off the tip of the capillary. There was no evidence of residual mercury outside of the capillary. These drops were individually weighed (the standard deviation in the average drop weight was about 3%) and the electrode area calculated from the average weight assuming sphericity of the drop.

The experiments were performed in a three compartment, air-tight Pyrex glass cell shown in Figs. III-1 and III-2. The temperature of the electrochemical cell was held at 25 ± 0.1°C by means of a silicone oil bath. The only 2 inch ball and socket type joint (West Glass Co.) near the top of the working electrode compartment was fitted with a Teflon sleeve and a Teflon O-ring. All stopcocks were Teflon and all other ball and socket joints (West Glass Co.) were vacuum tight with inserted Teflon O-rings. A Kel-F adaptor was located on the working electrode compartment for introduction of the HME into the cell. Another was located on the reference electrode compartment for introduction of the NaCl saturated calomel reference electrode. Both adaptors were fitted securely into the taper joints of the cell with Teflon O-rings embedded in the Kel-F. Around each of the electrodes were Teflon O-rings which seated when the inner Kel-F fitting was screwed into the outer. The reference electrode and counter electrode compartments were separated from the working electrode compartment with medium and coarse sintered glass discs, respectively.

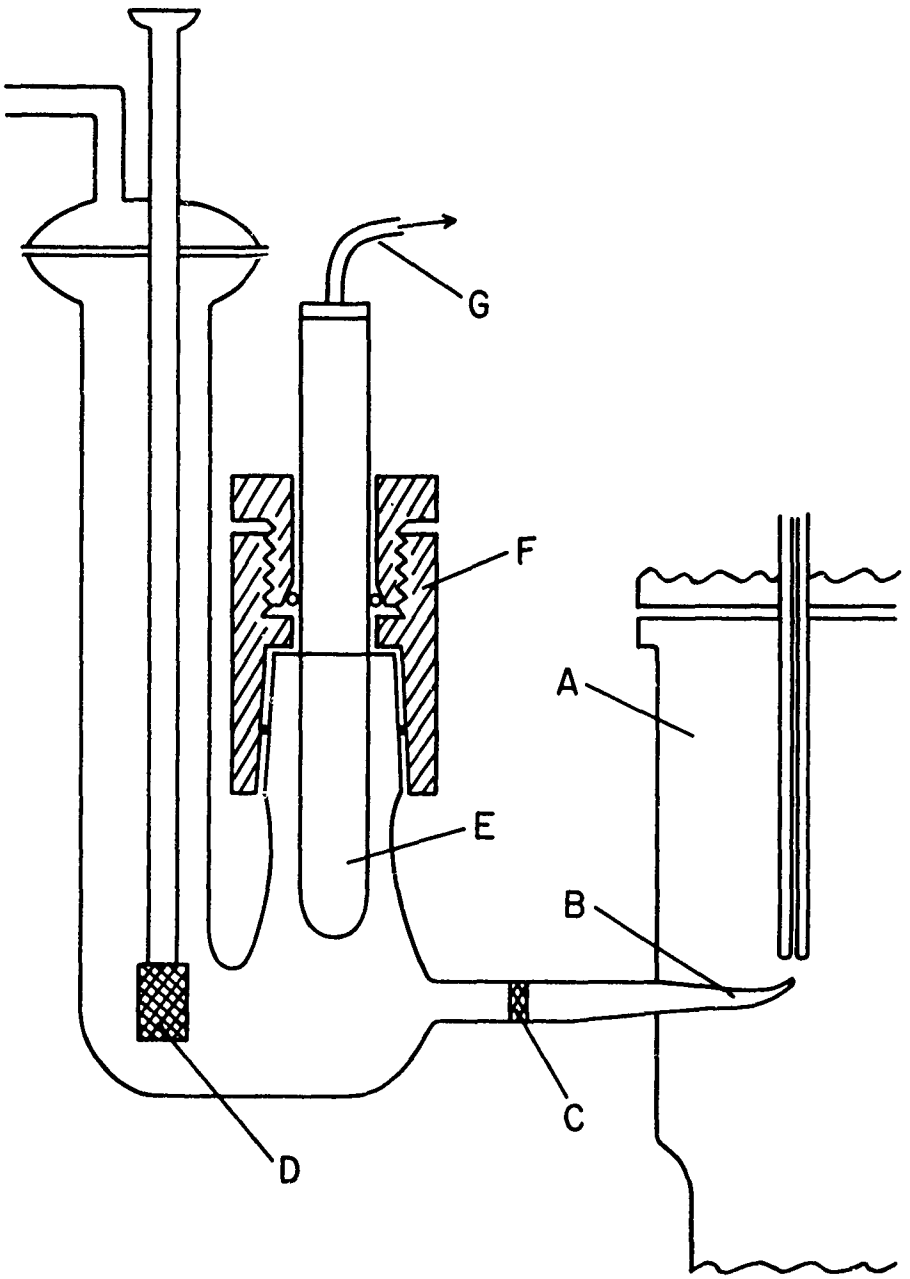

Fig. III-2. Reference compartment of electrochemical cell. A = Working electrode compartment; B = Luggin capillary; C = Sintered glass disc; D = Bubbler; E = SCE; F = Kel-F adapter; G = Electrocal lead from reference electrode.

Purified helium gas (Ohio Chemical - water pumped) was introduced into each compartment of the cell through bubblers. The helium gas exited from each compartment through water filled traps to avoid back diffusion of the air. Oxygen was removed from the tank helium by passing it through heated copper turnings maintained at 600°C in a Sargent furnace (model S36517). For further removal of O_2 and other trace impurities, the helium was then passed through a TiO trap submerged in liquid nitrogen. Finally the helium was passed through a bubbler containing conductivity water in order to saturate the gas with water and minimize evaporation of water from the cell. The helium train was made entirely of Pyrex glass and copper tubing. Graded Kovar seals were used at the copper-glass junctions. All stopcocks were Teflon.

The working electrode compartment was fitted with two pipettes, one calibrated in 0.1 ml units and holding a total volume of 10 ml, and the other calibrated in 1 ml units and holding a total volume of 70 ml. These pipettes were used for the introduction of reagents to the cell without exposing the cell to the atmosphere. The larger pipette was fitted with a purified helium supply identical to the one already described for the electrochemical cell. The helium was introduced below the liquid level of the reagent and exited through the working electrode compartment near the 2 inch joint. Thus the working electrode compartment effectively had two sources of helium: one from its own bubbler and the second from the

larger reagent storage pipette. The smaller pipette was closed on top with a Teflon plug. Since very small volumes of reagents were added to the electrochemical cell from this pipette, prior purging of the reagents while they were still in the small pipette was considered unnecessary. After the reagent was added to the working electrode compartment, it was purged of oxygen by means of the bubbler in that compartment.

All glassware, except the electrochemical cell, was cleaned first with a biodegradable detergent, Alconox, rinsed thoroughly with singly distilled water, soaked at least 24 hrs in a 1:1 mixture of concentrated HNO_3-H_2SO_4, rinsed well with triply distilled conductivity water, and further soaked in conductivity water for at least a few hours. If the water did not run freely off the glass surfaces, the piece was recleaned. The electrochemical cell was only acid cleaned as described above. Because of the porosity of the bubblers in the cell, the detergent would have been extremely difficult to rinse out. Teflon parts of the cell and of the helium lines were also acid cleaned as described above, but soaked for several days in continually changed conductivity water and not used until all of the adsorbed acid was removed. This was determined with pH paper.

Chemicals

Triply distilled conductivity water was used for all solutions. Commercially available $NaClO_4$ is contaminated as evidenced by

a broad cathodic peak centering on -1 V vs SCE. Consequently the supporting electrolyte used in this work was prepared from reagent grade $HClO_4$ (J. T. Baker Chemical Co.) and NaOH pellets (Fisher Scientific Co.) freshly dissolved in water to a strength of about 10 M. This clear NaOH solution was very hot (80-90°C) and was quickly added to standardized $HClO_4$ (~ 10 M) until the solution reached a pH of 7 as indicated by pH paper. The high temperature of the NaOH solution helped to prevent dissolution of CO_2 in the solution from the air. The neutral $NaClO_4$ solution was cooled to room temperature and diluted to the desired molarity (~ 0.23 - 0.33 M). It was acidified to a pH of about 2 which was precisely measured with a Beckman Expandomatic pH meter (model 76A).

There is a fair probability that iron contamination greater than that reported by the manufacturer was present in the NaOH which was used to prepare the $NaClO_4$ supporting electrolyte. Strong evidence which is discussed in a following section indicates that the iron caused no complications since H_2 evolution occurred at the expected potential and the voltammetry curves were extremely reproducible.

Impure mercury can cause extraneous peaks in the voltammetry curves as well as maxima. Whenever the voltammetry curves appeared distorted, the reason was generally unclean mercury. Commercially distilled mercury was filtered, washed with dilute HNO_3 for at least 24 hrs, rinsed with conductivity water, dried by filtering, distilled

under a continuous stream of air, then finally vacuum distilled. Mercury so cleaned cannot be stored in a closed glass container for more than 2 or 3 months without needing recleaning because of oxide formation.

The salt $[Cr(H_2O)_6](ClO_4)_3$ was prepared[9] by adding unstabilized 30% H_2O_2 (Baker Analyzed) to $Na_2Cr_2O_7 \cdot 2H_2O$ (Fisher Certified) in $HClO_4$ (Baker Analyzed). The reaction is

$$8HClO_4 + Na_2Cr_2O_7 \cdot 2H_2O + 3H_2O_2 + 3H_2O \longrightarrow$$

$$2[Cr(H_2O)_6](ClO_4)_3 + 3O_2 + 2NaClO_4 \qquad \text{(III-1)}$$

The highly exothermic reaction was kept at moderate temperatures by placing the reaction vessel in ice water. To avoid formation of the green colored chromium dimer, the solution was kept very acid. After the formation of $[Cr(H_2O)_6](ClO_4)_3$ was apparent by the appearance of a violet colored solution, excess H_2O_2 was boiled off with gentle heating.

NaCl and NaBr (Baker Analyzed) were purified by several recrystallizations. In the case of NaBr, the first crystals were discarded since they contained a higher percentage of the chloride impurity than did the mother liquor.

Reagent grade (Mallinckrodt Chemical Works) $CrCl_3 \cdot 6H_2O$ was the source for $[Cr(H_2O)_5Cl]^{2+}$. The commercially available salt[9] is at least 98% in the form $[Cr(H_2O)_4Cl_2]Cl$ which aquates to a stable form $[Cr(H_2O)_5Cl]Cl_2$ in an acidic solution. Spectrophoto-

metric analysis was used to determine when the complex was in the desired form and the solution was used without further purification.

Chromic bromide (K&K Laboratories) was the source[25] for $[Cr(H_2O)_5Br]^{2+}$. The commercial salt very quickly aquates to the desired form, as was spectrophotometrically determined, and was stable for several hours before further aquation. No further purification was employed.

Spectrophotometric Analysis

The molar extinction coefficient for $[Cr(H_2O)_6]^{3+}$ at 4070Å was determined to be 15.6 $\underline{M}^{-1}cm^{-1}$. This was accomplished by measuring the absorption of a $[Cr(H_2O)_6](ClO_4)_3$ solution in $HClO_4$ at a pH of 1, oxidizing the chromium(III) to CrO_4^{2-} with H_2O_2 in NaOH, and then determining the chromium concentration from the well-known chromate extinction coefficient[56,16] of 4830 at 3730Å. All spectrophotometric measurements were made with a Cary-15 spectrophotometer. The wavelengths corresponding to the absorption maxima and the corresponding molar extinction coefficients[9,17] used for $[Cr(H_2O)_5Cl]^{2+}$, $[Cr(H_2O)_4Cl_2]^{+}$ and $[Cr(H_2O)_5Br]^{2+}$ were 21.6 at 4300Å, 27.9 at 4500Å, and 22.4 at 4320Å, respectively.

Purity and Reproducibility

.If the manufacturer's analysis of reagent impurities is to be believed, the prepared 1 $\underline{M}$ $[Cr(H_2O)_6](ClO_4)_3$ contained a maximum of 1×10^{-3} $\underline{M}$ impurities as Cl^-, SO_4^{2-}, H_2SO_4, NO_3^-, and PO_4^{2-}. Since the electrochemical experiments contained a chromium concen-

tration in the millimolar range, the impurity level introduced via the chromium stock solution was in the micromolar range. A comparable impurity level composed of Cl^-, SO_4^{2-}, Pb, Fe and insoluble matter was introduced through the supporting electrolyte. Even if the supporting electrolyte (pH = 2) were exposed to an atmosphere containing 0.5 atm of CO_2 the CO_3^{2-} concentration[57] in the solution would be less than 10^{-14} M and thus only dissolved CO_2 need be considered. Carbonate introduced with the NaOH solution when it was added to the $HClO_4$ would be in the form of CO_2. It is rather unlikely that sufficient CO_2 would be adsorbed on the electrode to have any significant effect on the results.

Evidence that impurity effects were not important is presented in Figs. III-3 and III-4. Figure III-3 shows that no detectable adsorption, desorption, or Faradaic peaks, other than hydrogen evolution, were present in the background curve on a HME in acidic $NaClO_4$ solutions with no chromium present. Figure III-4 shows reproducible $[Cr(H_2O)_6]^{3+}$ reduction waves taken at various time intervals. Impurity effects usually lead to irreproducibility.

Procedure

A typical experiment was performed in the following manner. Conductivity water was kept in the Pyrex cell when the cell was not being used. The Pyrex cell was emptied of conductivity water with a large pipette and filled with a known volume of $NaClO_4$. All bubblers and joints were fitted into place and helium passed

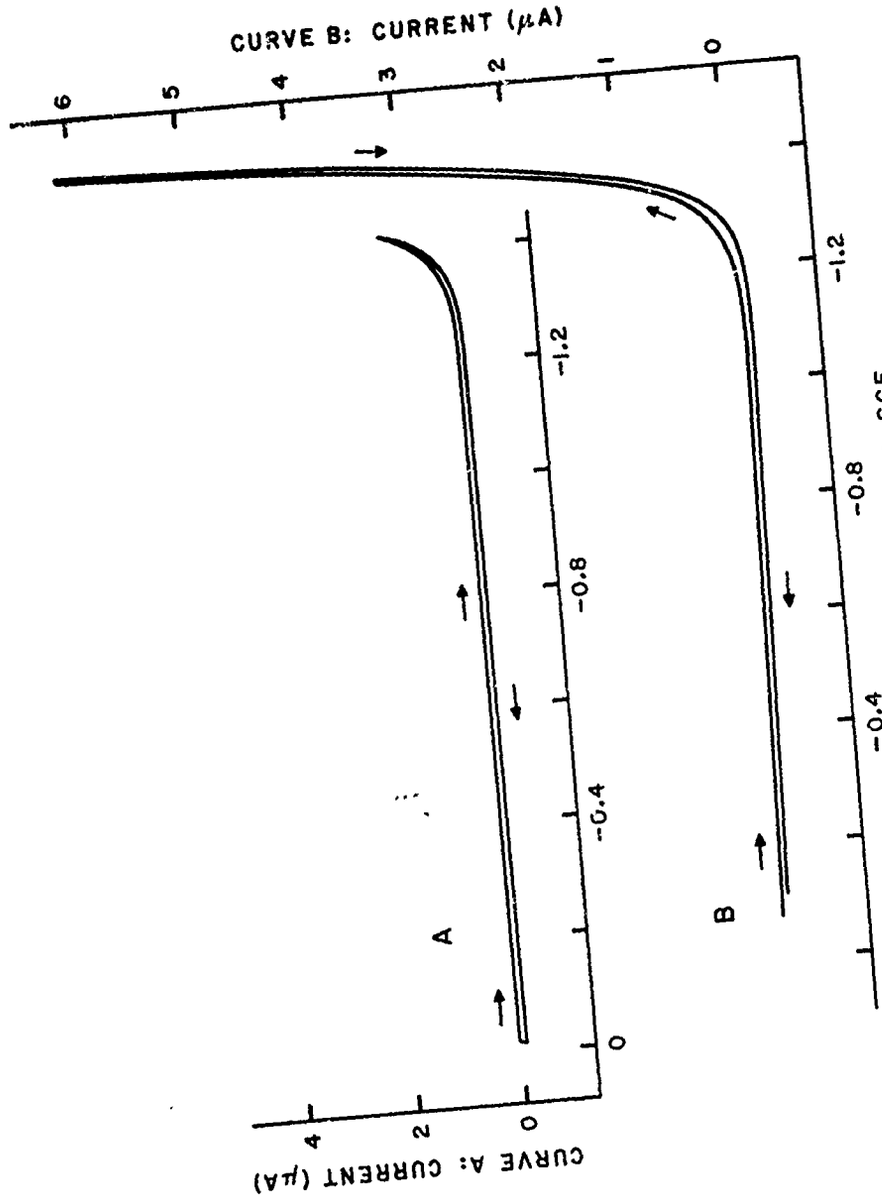

Fig. III-3. Background curve of $NaClO_4$ on HME. Curve A: 0.32 M $NaClO_4$, pH = 2.045, HME area = 0.0230 cm^2, scan rate = 0.1400 V/sec, 25°C, Pt counter electrode. Curve B: 1.013 M $NaClO_4$, pH = 1.5, HME area = 0.0256 cm^2, scan rate = 0.0333 V/sec, Pt counter electrode, 25°C.

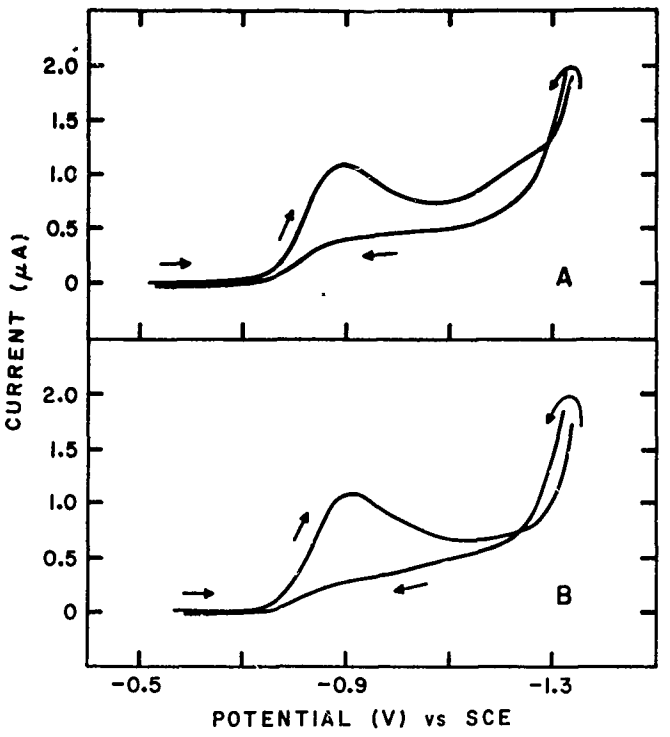

Curve A was obtained 4 hrs after curve B. Concentration of $[Cr(H_2O)_6](ClO_4)_3$ = 0.250 mM, HME area = 0.0232 cm^2, scan rate = 0.0333 V/sec.

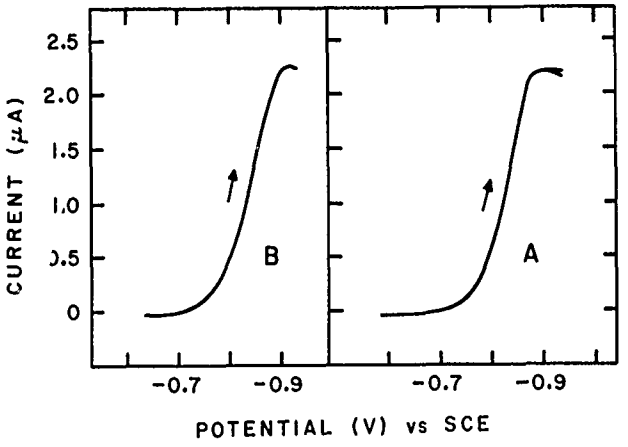

Curve B was obtained 16.5 hrs after curve A. Concentration of $[Cr(H_2O)_6](ClO_4)_3$ = 0.500 mM, HME area = 0.0245 cm^2, scan rate = 0.0333 V/sec.

Fig. III-4. Time effects of $[Cr(H_2O)_6]^{3+}$ reduction in 0.42 M $NaClO_4$, pH=2.0, T=25°C.

through the solution for a few hours to remove O_2. Any reagents to be added were placed in the pipette above the working electrode compartment. Helium was passed through the larger pipette. Chromium concentrations were spectrophotometrically determined prior to the complexes being introduced to the cell. Only one chromium complex isomer was spectrophotometrically analyzed and added to the cell at a time. The purified NaCl or NaBr crystals were carefully weighed and solutions of the desired molarity prepared. About 20 min before the run began, the bright platinum foil counter electrode was fitted into place, and the SCE reference electrode (Fisher calomel electrode, cat. no. 13-639-52) was checked against an identical unused electrode with a Hewlett-Packard (419A) DC null voltmeter and fitted into place.

For $[Cr(H_2O)_6]^{3+}$ solutions containing chloride, the potential was scanned from 0.00 to -1.0 V vs SCE and for solutions containing bromide, the potential was swept from -0.1 to -1.1 V vs SCE. For other chromium isomers the potential sweep range was shortened. $[Cr(H_2O)_5Br]^{2+}$ was examined over a potential range of -0.1 V to -0.6 V vs SCE and $[Cr(H_2O)_5Cl]^{2+}$ was studied over a potential range of 0.0 to -0.75 V vs SCE.

With only $NaClO_4$ and no chromium in the cell, background curves were recorded at typical scan rates to check solution purity. If the background curve was acceptable, the run proceeded. When the mercury was beginning to form oxides, the background curve

would indicate the presence of impurities by showing extraneous peaks, maxima, or a distortion of the H_2 evolution peak. A known volume of the solution containing the chromium complex, usually 1 M in strength, was introduced into the cell. Their volumes were typically 2 ml and measurable to ± 0.002 ml. Voltammetry curves were used to determine if all experimental conditions were proper and if the run should continue. Known volumes of NaCl or NaBr at concentrations of 0.01 to 4 M were added. These were typically from 0.5 to 5 ml and measurable to ± 0.01 ml.

After introduction of a reagent to the working electrode compartment, the solution was mixed by permitting helium to bubble through it. During the voltammetry sweeps, the solution was quiescent.

CHAPTER IV

EXPERIMENTAL DATA AND THEIR ANALYSIS

The Hexaaquochromium Couple in a $NaClO_4$ Supporting Electrolyte

The "steady-state" cyclic voltammetry curve of $[Cr(H_2O)_6]^{3+}$ on an HME with a bright Pt foil counter electrode is shown by curve A in Fig. IV-1 for 0.33 M $NaClO_4$ at a pH of $\sim$ 2. The semi-log plot of the apparent rate constants for the $[Cr(H_2O)_6]^{2+}$/ $[Cr(H_2O)_6]^{3+}$ couple at various potentials for many runs is the upper graph in Fig. IV-2. The points in the plot were obtained with the computer program in Appendix I which utilized Eqs. (II-1) and (II-9). The best straight line was drawn through these points and extrapolated to the apparent standard rate constant at the apparent standard potential $(E_s^o)_a$. The activity coefficients for $[Cr(H_2O)_6]^{2+}$ and $[Cr(H_2O)_6]^{3+}$ were assumed to be equal.

Rather than double layer correct each experimentally obtained point shown in the upper graph of Fig. IV-2, the line itself was double layer corrected at a number of different potentials along the line. The double layer corrections at any given potential were made by solving for k_t in Eq. (II-11):

$$k_a = k_t \exp\left[\frac{(\alpha n - Z) F \phi_2}{RT}\right]$$

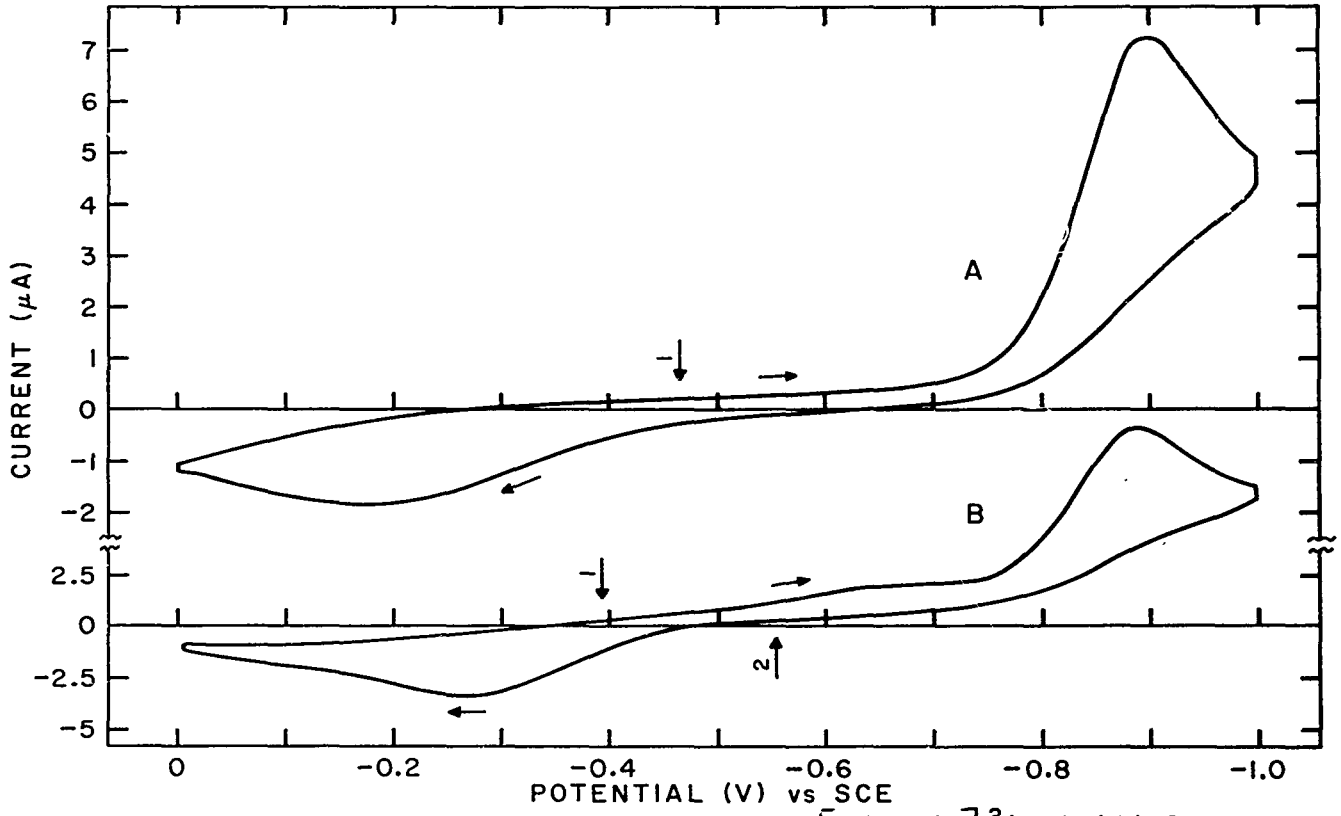

Fig. IV-1. Cyclic voltammetry curve for $[Cr(H_2O)_6]^{3+}$. Initial $[Cr(H_2O)_6](ClO_4)_3$ concentration = 2.46 mM in 0.33 M $NaClO_4$ at pH of 2.20 and 25°C. Curve A- scan rate = 0.1594 V/sec and HME area = 0.0185 cm^2. Curve B- 3.22 mM NaCl present in addition to the 0.33 M $NaClO_4$, scan rate = 0.1388 V/sec and HME area = 0.02381 cm^2. $\rightleftharpoons$ $\rightleftharpoons$ = pseudo time zeroes (1),(2).

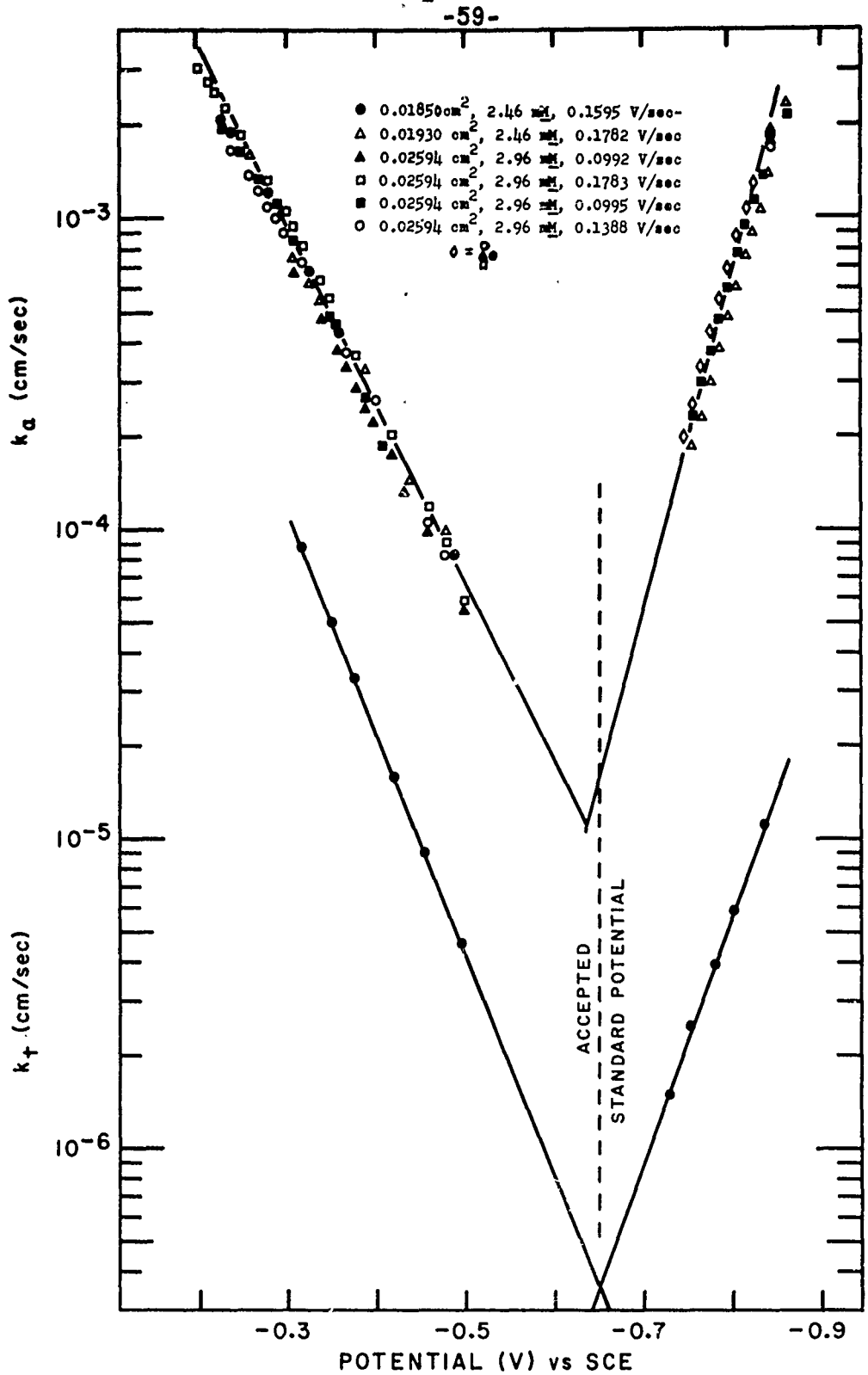

Fig. IV-2. Log of apparent (upper) and double layer corrected (lower) rate constants vs applied potential for the $[Cr(H_2O)_6]^{2+}/[Cr(H_2O)_6]^{3+}$ couple. All runs at 25°C in 0.33 M $NaClO_4$ at pH of 2.20 on a HME with the areas, initial $[Cr(H_2O)_6](ClO_4)_3$ concentrations, and scan rates as above.

For Eq. (II-11) the k_a for any given potential was obtained from the plot in Fig. IV-2. The true transfer coefficient was calculated from the appropriate apparent transfer coefficient from Fig. IV-2 with Eq. (II-12). For the cathodic branch α_t was 0.48. For the anodic branch α_t was 0.43. The double layer corrected curve shown as the lower graph in Fig. IV-2 was extrapolated to the true standard rate constant at the standard potential $(E_s^o)_t$. For the double layer corrections in $NaClO_4$, ϕ_2 data from $HClO_4$ solutions were used in lieu of the unavailable ϕ_2 data for $NaClO_4$. No serious error resulted from this since the ϕ_2 data for these two electrolytes should be essentially the same, as will be discussed in the last chapter.

The above treatment does not consider that some of the electrode sites are covered with adsorbed perchlorate ions rather than water. As long as the perchlorate ions do not facilitate charge transfer, their presence would not be expected to cause any serious error provided double layer corrections reflect their effects on the potential distribution at the interface. Even at quite anodic potentials, not more than 10% of the total surface would be expefted to be covered with the rather weakly adsorbed perchlorate. For the calculation of rate constants, the electrode sites were considered to be covered by either water, water and chloride, or water and bromide, whichever was applicable. The perchlorate ion will be further discussed in the last chapter.

Cyclic Voltammetry of $[Cr(H_2O)_6]^{3+}$ in a Mixed Chloride-Perchlorate Supporting Electrolyte

When increasing concentrations of NaCl were added to the $NaClO_4$ supporting electrolyte, with the ionic strength held constant, the resulting cyclic voltammetry curves for $[Cr(H_2O)_6]^{3+}$ were different from the ones shown in Fig. IV-1 for the simple $[Cr(H_2O)_6]^{2+}/[Cr(H_2O)_6]^{3+}$ couple in a pure perchlorate solution. For the chloride-perchlorate solutions the anodic peak was shifted toward more negative potentials and the original cathodic peak appeared more drawn-out because of a new cathodic wave superimposed near its foot. Its position, however, was unchanged. The "steady-state" cyclic voltammetry curves for increasing chloride concentrations are shown in Figs. IV-1, 3 and 4a. In all cases the counter electrode was a bright Pt foil.

Small differences between the initial cycle and "steady-state" cycle curves and resulting observed apparent rate constants existed in the mixed chloride-perchlorate electrolytes. Figure IV-4b shows the cyclic voltammetry curve beginning at the true time zero and continuing until a "steady-state" was reached. Figure IV-4c shows the resulting observed apparent rate constants. The details concerning the two different pseudo time zeroes are explained along with the computer program at the end of Appendix II. Figure IV-4c also shows that the new cathodic peak appeared only after $[Cr(H_2O)_6]^{2+}$ was oxidized.

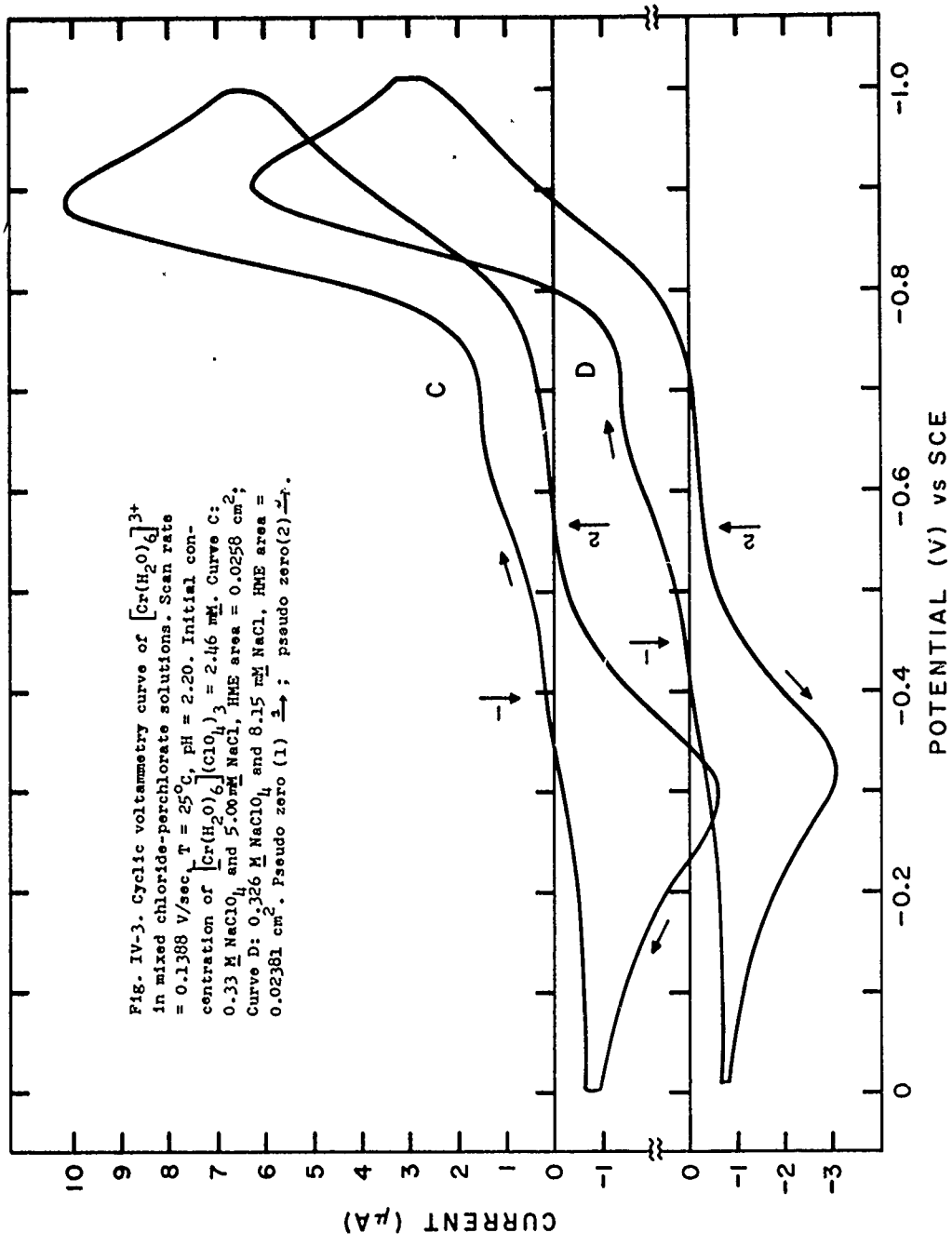

Fig. IV-3. Cyclic voltammetry curve of $[Cr(H_2O)_6]^{3+}$ in mixed chloride-perchlorate solutions. Scan rate = 0.1388 V/sec, T = 25°C, pH = 2.20. Initial concentration of $[Cr(H_2O)_6](ClO_4)_3$ = 2.46 mM. Curve C: 0.33 M $NaClO_4$ and 5.00 mM NaCl, HME area = 0.0258 cm^2; Curve D: 0.326 M $NaClO_4$ and 8.15 mM NaCl, HME area = 0.02381 cm^2. Pseudo zero (1) ⟶; pseudo zero(2) ⟵.

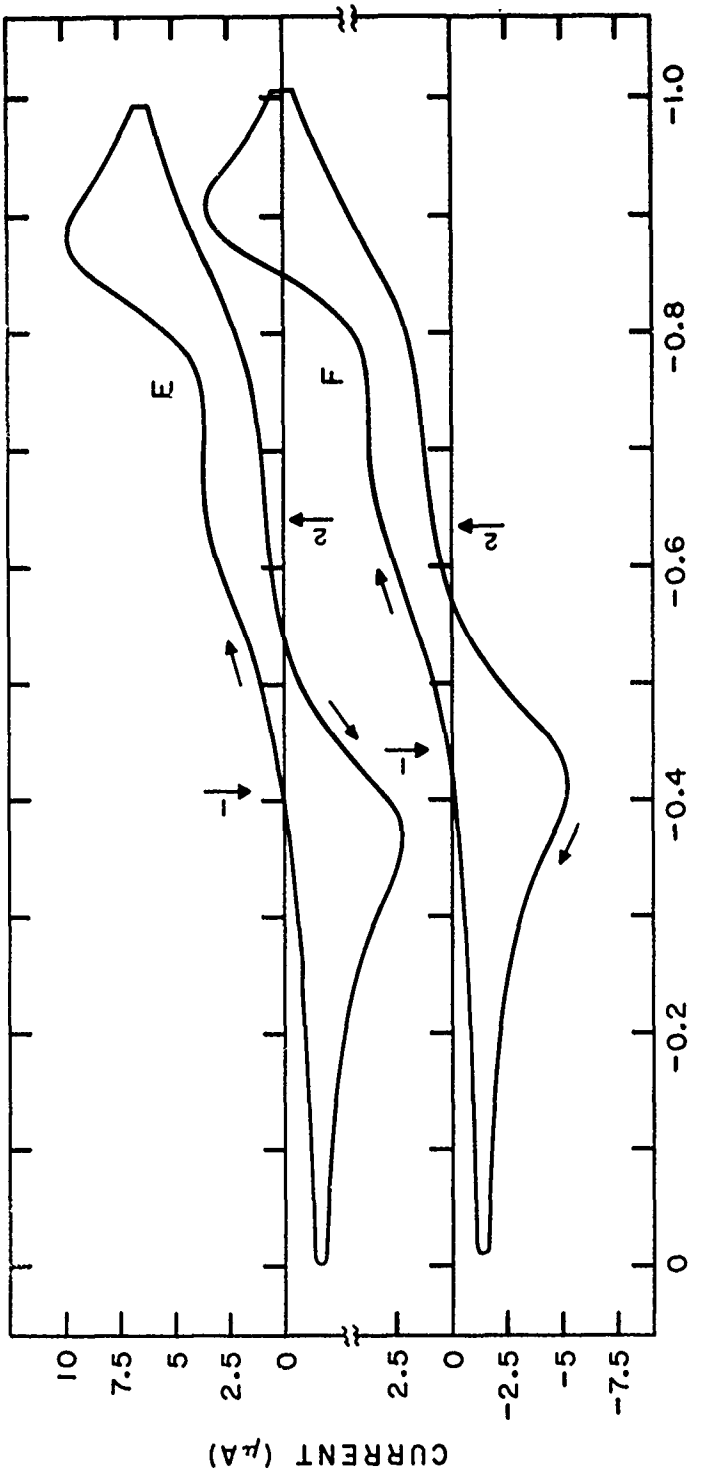

Fig. IV-4a. Cyclic voltammetry curve for $[Cr(H_2O)_6]^{3+}$ in mixed chloride-perchlorate solutions. HME area = 0.02236 cm^2, pH = 2.20, 25°C. Curve E-initial $[Cr(H_2O)_6](ClO_4)_3$ concentration = 2.46 m$\underline{M}$ in 0.28 $\underline{M}$ $NaClO_4$ and 0.0472 $\underline{M}$ NaCl with scan rate of 0.1380 V/sec; Curve F-initial $[Cr(H_2O)_6](ClO_4)_3$ concentration = 2.96 m$\underline{M}$ in 0.24 $\underline{M}$ $NaClO_4$ and 0.0899 $\underline{M}$ NaCl with a scan rate of 0.1381 V/sec. $\xrightarrow{1}$, $\xrightarrow{2}$ = pseudo zero(1),(2).

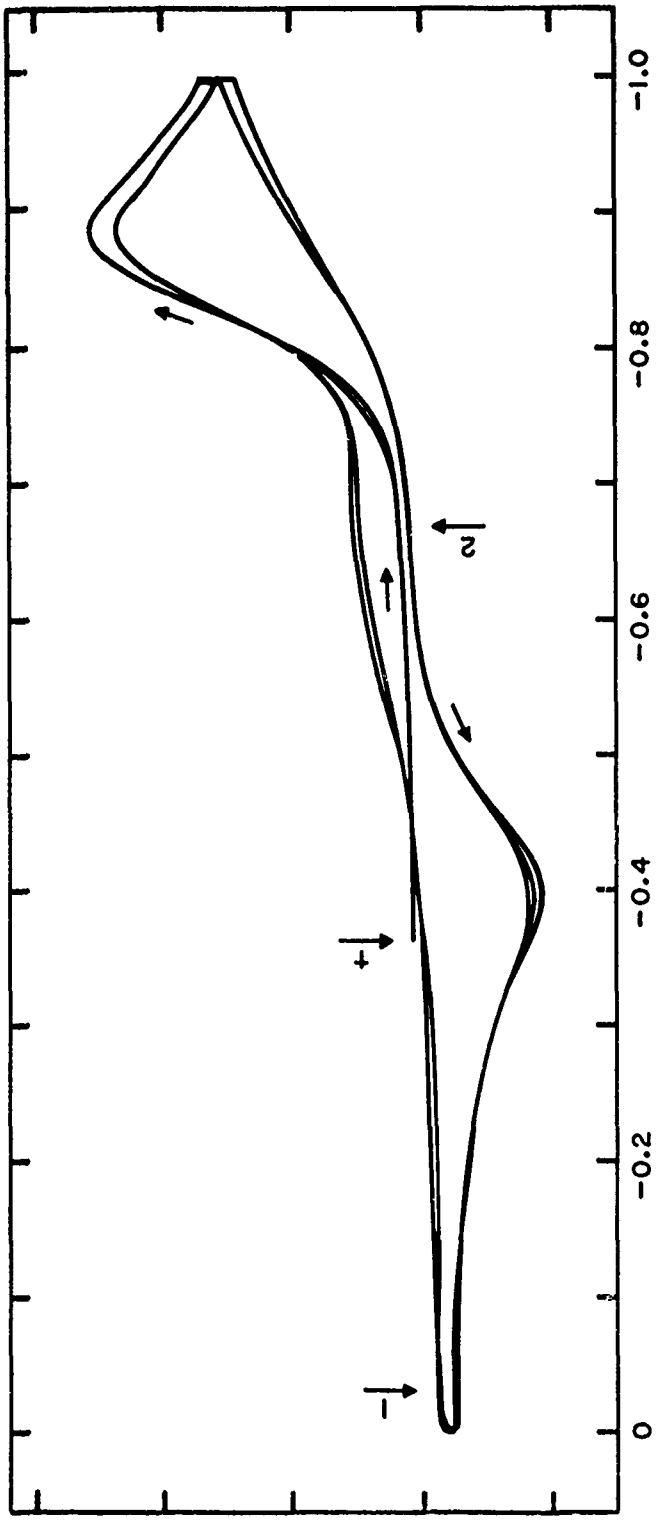

Fig. IV-4b. Cyclic voltammetry in mixed chloride-perchlorate solutions for initial and "steady-state" curves. Initial $[Cr(H_2O)_6](ClO_4)_3$ concentration = 2.46 mM in 0.24 M $NaClO_4$ and 0.0899 M NaCl, scan rate = 0.1397 V/sec, HME area = 0.0217 cm^2, pH = 2.20, T = 25°C. True time zero (1) → ; pseudo time zero (2) → ; pseudo time zero (1) → ; pseudo time zero (2) →

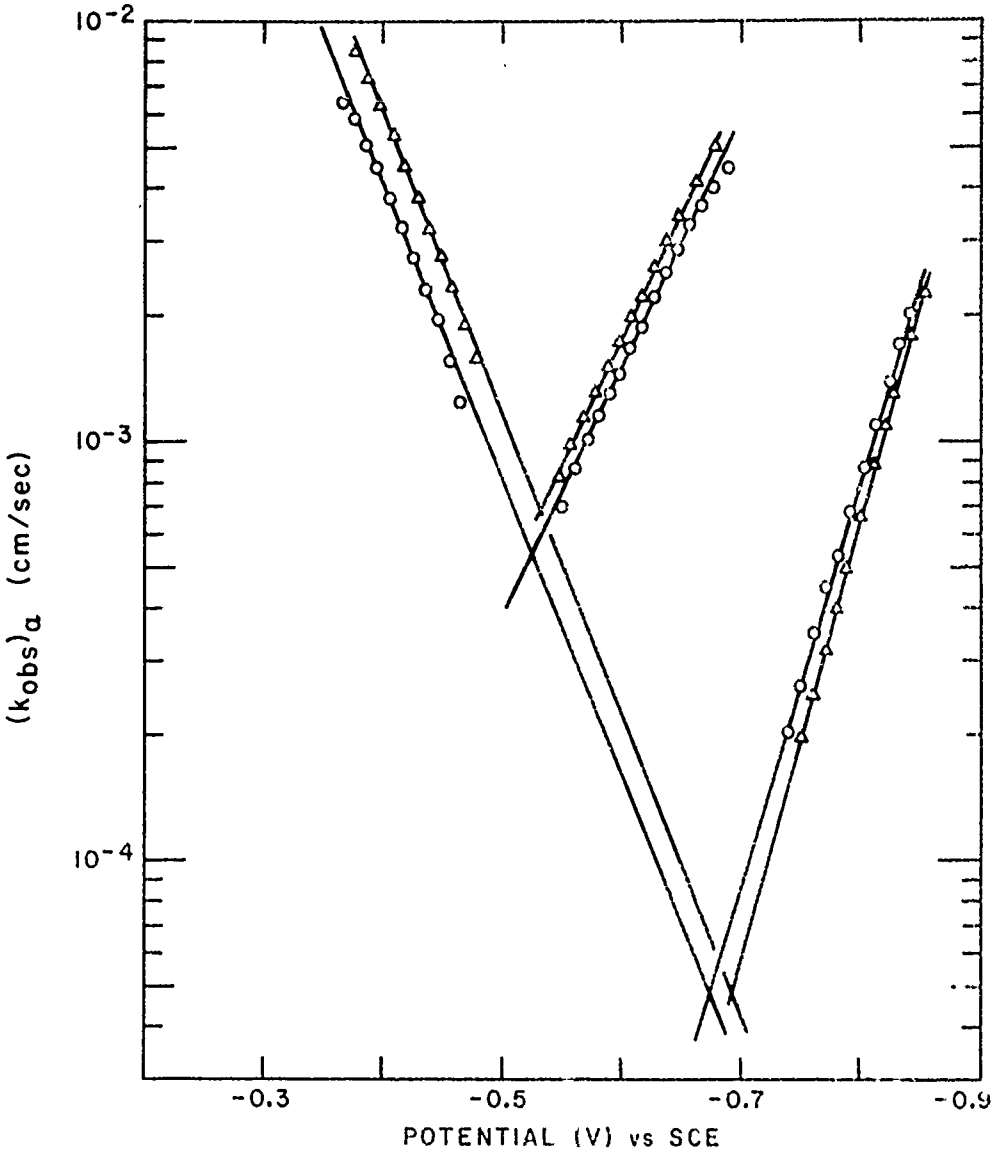

Fig. IV-4c. Log of observed apparent rate constants in mixed chloride-perchlorate solution for initial (Δ) and "steady-state" (o) scan. Experimental conditions given in Fig. IV-4b. The cathodic branch occurring at higher observed apparent rate constants corresponds to the reduction of $[Cr(H_2O)_5Cl]^{2+}$. The cathodic branch occurring at lower observed apparent rate constants corresponds to the reduction of $[Cr(H_2O)_6]^{3+}$. The anodic branch corresponds to the oxidations of $[Cr(H_2O)_6]Cl^{+}$ + $[Cr(H_2O)_6]^{2+}$.

The anodic peak was a composite of two different electrochemical oxidations: the oxidation of $[Cr(H_2O)_6]^{2+}$ at sites covered with water and at sites covered with chloride. The reaction which occurred at a water-covered site can be written as

$$[Cr(H_2O)_6]^{2+} \xrightarrow{k_1} [Cr(H_2O)_6]^{3+} + e^- \qquad \text{(IV-1)}$$

where $k_1 = k_1'\theta_{H_2O}$ with θ_{H_2O} being the fractional surface coverage for water. The oxidation which occurred at a chloride covered site can be written as

$$[Cr(H_2O)_6]^{2+} + Cl^-_{ad} \xrightarrow{k_2} [Cr(H_2O)_5Cl]^{2+} + e^- \qquad \text{(IV-2)}$$

where $k_2 = k_2'\theta_{Cl^-}$ with θ_{Cl^-} being the fractional surface coverage for chloride. Since the electrode coverage with water is close to unity even at quite anodic potentials in halogen containing solutions, θ_{H_2O} will be set equal to unity as a good approximation. The original cathodic peak was, of course, the reduction of $[Cr(H_2O)_6]^{3+}$ and the reverse of reaction (IV-1). The new cathodic peak was the reduction of $[Cr(H_2O)_5Cl]^{2+}$ and was the reverse of reaction (IV-2). The experimental data which proves the identity of the new cathodic peak will be given later. Each peak will be discussed beginning with the anodic peak.

Since the anodic voltammetry peak was a composite of two different processes, the apparent rate constants calculated from it with the computer program in Appendix I were composite apparent

rate constants. To separate the composite apparent rate constants into k_1 and k_2, k_1 must be subtracted from the composite apparent rate constant, leaving k_2. The apparent rate constant k_1 for the mixed chloride-perchlorate supporting electrolyte could be calculated from the apparent rate constant of $[Cr(H_2O)_6]^{2+}$ oxidation in a pure perchlorate medium if the change in double layer potentials between the pure perchlorate and mixed chloride-perchlorate solutions were taken into account. The calculation of k_1 was accomplished by considering the following. In a pure $NaClO_4$ supporting electrolyte, only reaction (IV-1) occurred. At any given potential the relationship between the true and apparent rate constants was

$$(k_a)_{ClO_4^-} = (k_t)_{ClO_4^-} \exp\left\{\frac{[(\alpha_{ClO_4^-})n-Z]F(\phi_2)_{ClO_4^-}}{RT}\right\} \qquad \text{(IV-3)}$$

The transfer coefficient α was always taken as the same α which is in Eq. (IV-1), and Z was always taken as the charge with sign, of the reducing species. For the simple hexaaquochromium couple of reaction (IV-1) occurring at a water-covered site in the mixed electrolyte, the relationship between the true and apparent rate constants at any given potential was

$$(k_a)_{Cl^-+ClO_4^-} = (k_t)_{Cl^-+ClO_4^-} \exp\left\{\frac{[(\alpha_{Cl^-+ClO_4^-})n-Z]F(\phi_2)_{Cl^-+ClO_4^-}}{RT}\right\} \qquad \text{(IV-4)}$$

The assumption will be made that the true transfer coefficient and true rate constant in the mixed electrolyte for discharge on

water-covered sites are identical to those for discharge on water-covered sites in the pure perchlorate electrolyte. Division of Eq. (IV-4) by Eq. (IV-3) yielded

$$(k_a)_{Cl^-+ClO_4^-} = (k_a)_{ClO_4^-} \exp\left\{\frac{(\alpha n - Z)\left[(\phi_2)_{ClO_4^-+Cl^-} - (\phi_2)_{ClO_4^-}\right]}{RT}\right\} \qquad \text{(IV-5)}$$

The rate constant $(k_a)_{Cl^-+ClO_4^-}$ was identical to k_1 of reaction (IV-1) when the reaction occurred in the mixed chloride-perchlorate supporting electrolyte. The apparent rate constant at any given potential in a pure perchlorate supporting electrolyte was known, as was also the true transfer coefficient. The difference in ϕ_2 potentials for pure perchlorate and chloride-perchlorate was found after the ϕ_2 values for the mixed electrolyte were obtained as was described in Chapter II. For Eq. (IV-5) the transfer coefficient α was 0.43. The calculated k_1 was then double layer corrected using ϕ_2 data from the mixed electrolyte.

When the calculated k_1 was subtracted from the composite apparent rate constant, the difference was k_2 or the apparent rate constant for reaction (IV-2) in the mixed chloride-perchlorate supporting electrolyte. The apparent rate constant k_2 was double layer corrected with the ϕ_2 data calculated for a mixed chloride-perchlorate electrolyte. The apparent transfer coefficient for the oxidation of $[Cr(H_2O)_6]Cl^{+}$ for each run was corrected to the true transfer coefficient with Eq. (II-12) and the true transfer coefficient for each particular run was used for the double layer

corrections.

The second voltammetry peak to be discussed is the new cathodic peak which corresponded to the reduction of $[Cr(H_2O)_5Cl]^{2+}$. This was not a composite peak and the apparent rate constants calculated for it with the computer program in Appendix I were the apparent rate constants for the $[Cr(H_2O)_5Cl]^{2+}$ reduction

$$[Cr(H_2O)_5Cl]^{2+} + e^- \xrightarrow{k_{-2}} [Cr(H_2O)_6]^{2+} + Cl^-_{ad} \qquad \text{(IV-6)}$$

where $k_{-2} = k'_{-2}\theta_{H_2O} \simeq k'_{-2}$. Reaction (IV-6) written in this manner is simply the reverse of reaction (IV-2), but perhaps representing the reduction as such is misleading. For Cl^-_{ad} to be one of the reduction products, $[Cr(H_2O)_5Cl]^{2+}$ reduction must occur at the electrode with the chloride oriented toward the electrode. If the complex is in the opposite orientation when charge transfer occurs, the chloride bound inner-sphere to the chromium would dissociate from the labile $[Cr(H_2O)_6]^{2+}$ simultaneously with or subsequent to the reduction. The dissociated chloride would not be specifically adsorbed. While adsorption equilibrium exists between Cl^-_{ad} and free Cl^- ions, kinetically the two possibilities for reduction of $[Cr(H_2O)_5Cl]^{2+}$ are quite different.

The negative charge on the electrode would not encourage the $[Cr(H_2O)_5Cl]^{2+}$ complex to approach chloride first, but the tendency for specific adsorption of Cl^- may result in the chloride of the

complex taking a position equivalent to the electrode's inner coordination sphere with the chromium being in the outer. If the complex does not orient with the chloride toward the electrode, the large difference in apparent rate constants between $[Cr(H_2O)_6]^{3+}$ and $[Cr(H_2O)_5Cl]^{2+}$ is difficult to explain. The question of the $[Cr(H_2O)_5Cl]^{2+}$ complex orientation prior to reduction is important not only from the standpoint of bridging but also because of the double layer corrections. If the chloride part of the complex adsorbs onto the electrode, the ϕ_2 data is certainly insufficient. The ϕ_2 data and α_t will be discussed at greater length in the last chapter.

The apparent rate constants were double layer corrected with the mixed electrolyte ϕ_2 data when the chloride concentration was greater than 4% of the perchlorate concentration. When the chloride concentration was less than 4% of the perchlorate concentration, the ϕ_2 data for a pure perchlorate electrolyte was used. A further discussion of a refinement needed for the calculation of k_{-2} will be given after appropriate figures are presented later in this chapter.

Some comments are in order as to why the mixed electrolyte ϕ_2 data was not used on the cathodic branch for low chloride concentrations, whereas the mixed electrolyte ϕ_2 data was used on the anodic branch for the same low chloride concentrations. The double layer corrected rate constants from the cathodic branch were

obviously fallacious when the mixed electrolyte ϕ_2 data were employed. The slope of the cathodic branch, double layer corrected, was zero or even negative. This fallacious cathodic slope could be explained in one of two ways: either the calculated ϕ_2 values for such low chloride concentrations in a potential range negative to the point of zero charge on mercury were too large in absolute value, or the double layer correction itself was no longer valid because the $[Cr(H_2O)_5Cl]^{2+}$ ion had approached the inner Helmholtz plane with the chloride part immediately adjacent to the electrode. Perhaps both effects were occurring. A factor which must be emphasized is that this cathodic branch occurs over a potential range which passes through the point of zero charge and for which the ϕ_2 values change by a factor of 4.

Correcting ϕ_2 values from pure chloride or bromide solutions to what they would be in mixed bromide-perchlorate or mixed chloride-perchlorate solutions without taking the effective ionic strength of the chromium(II) or chromium(III) at the electrode surface into account is likely to yield ϕ_2 values that are too large. As was stated at the end of Chapter II, the chromium effect on ϕ_2 was not taken into account for the double layer corrections presented in this chapter. Therefore the double layer corrections in the mixed electrolytes should be viewed with caution. In Chapter V the shortcomings of the double layer corrections will be discussed and a semi-quantitative analysis given of how the

double layer corrections made in this chapter should be altered.

The final voltammetry peak to be evaluated is the original cathodic peak which corresponded to the reduction of $[Cr(H_2O)_6]^{3+}$.

$$[Cr(H_2O)_6]^{3+} + e^- \xrightarrow{k_{-1}} [Cr(H_2O)_6]^{2+} \qquad \text{(IV-7)}$$

where $k_{-1} = k'_{-1}\,\theta_{H_2O} \simeq k'_{-1}$. This reduction was the reverse of the oxidation reaction (IV-1). Since the end of the cathodic peak of the $[Cr(H_2O)_5Cl]^{2+}$ reduction was superimposed on the foot of the $[Cr(H_2O)_6]^{3+}$ reduction peak, the apparent rate constants for the $[Cr(H_2O)_6]^{3+}$ could not be calculated validly unless the current contribution from the $[Cr(H_2O)_5Cl]^{2+}$ reduction was subtracted from the experimentally observed $[Cr(H_2O)_6]^{3+}$ cathodic peak. Even with this subtraction performed, the question still remained as to how much the chloride in the supporting electrolyte affected the $[Cr(H_2O)_6]^{3+}$ reduction peak and how to double layer correct for it at low chloride concentrations.

Fortunately from an analysis point of view, the initial cycle peaks for the $[Cr(H_2O)_6]^{3+}$ reduction in the presence of chloride, with no $[Cr(H_2O)_5Cl]^{2+}$ reduction peak to interfere, were identical to those in the pure perchlorate media. A comparison of these voltammetry curves is given in Fig. IV-5. Consequently it did not appear necessary to make any corrections for the presence of chloride in the supporting electrolyte or to subtract the current

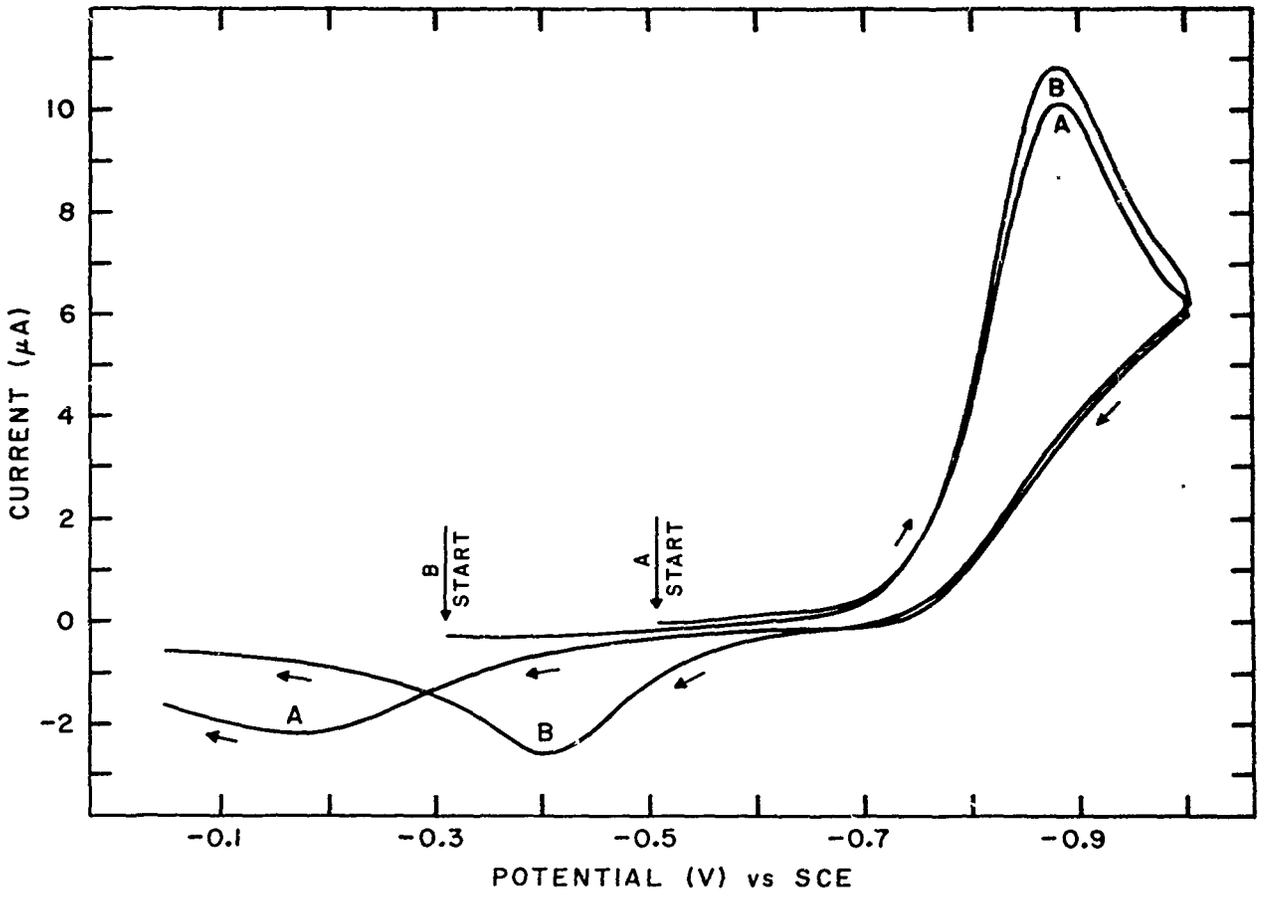

Fig. IV-5. Comparison of initial cycle scans for $[Cr(H_2O)_6]^{3+}$ reduction in mixed and pure electrolytes at 25°C. Curve A: initial $[Cr(H_2O)_6](ClO_4)_3$ concentration of 2.96 mM in 0.33 M $NaClO_4$ at pH of 2.20. Scan rate=0.110 V/sec, HME area=0.0220 cm^2. Curve B: initial $[Cr(H_2O)_6](ClO_4)_3$ concentration of 2.46 mM in 0.28 M $NaClO_4$ + 4.72 mM NaCl at pH of 2.20. Scan rate=0.110 V/sec, HME area=0.02717 cm^2.

for the $[Cr(H_2O)_5Cl]^{2+}$ reduction from the foot of the $[Cr(H_2O)_6]^{3+}$ reduction peak. Instead the $[Cr(H_2O)_6]^{3+}$ reduction peak in the presence of chloride was taken to be identical to that in the perchlorate media.

All of the rate constants so far discussed for the mixed chloride-perchlorate solutions will now be presented in graphical form. In Fig. IV-6 the anodic branch rate constants are the observed composite apparent rate constants, the sum of k_1 and k_2. The cathodic branch rate constants are the apparent rate constants k_{-2}. Since k_1 is so small compared to the composite apparent rate constants at high chloride concentrations, the anodic branch apparent rate constants in Fig. IV-6 are essentially k_2 and Fig. IV-6 can be viewed as representing the apparent rate constants for the $[Cr(H_2O)_6]Cl^+/[Cr(H_2O)_5Cl]^{2+}$ couple. Each pair of lines similarly lettered in Fig. IV-6 corresponds to a different chloride concentration. The curves in these figures are lettered the same as the curves in Fig. IV-6. This lettering of curves also corresponds to the lettering of the cyclic voltammetry curves in Figs. IV-1, 3, and 4 as far as the chloride concentrations are concerned. In Figs. IV-7 and 8 the best straight lines were drawn through the computer calculated apparent rate constants with the points more remote to the point of zero charge being favored. The $(k_1)_a$ and $(k_2)_a$ for each curve in Figs. IV-7 and 8 are shown below the observed composite apparent rate constant lines for the anodic branches.

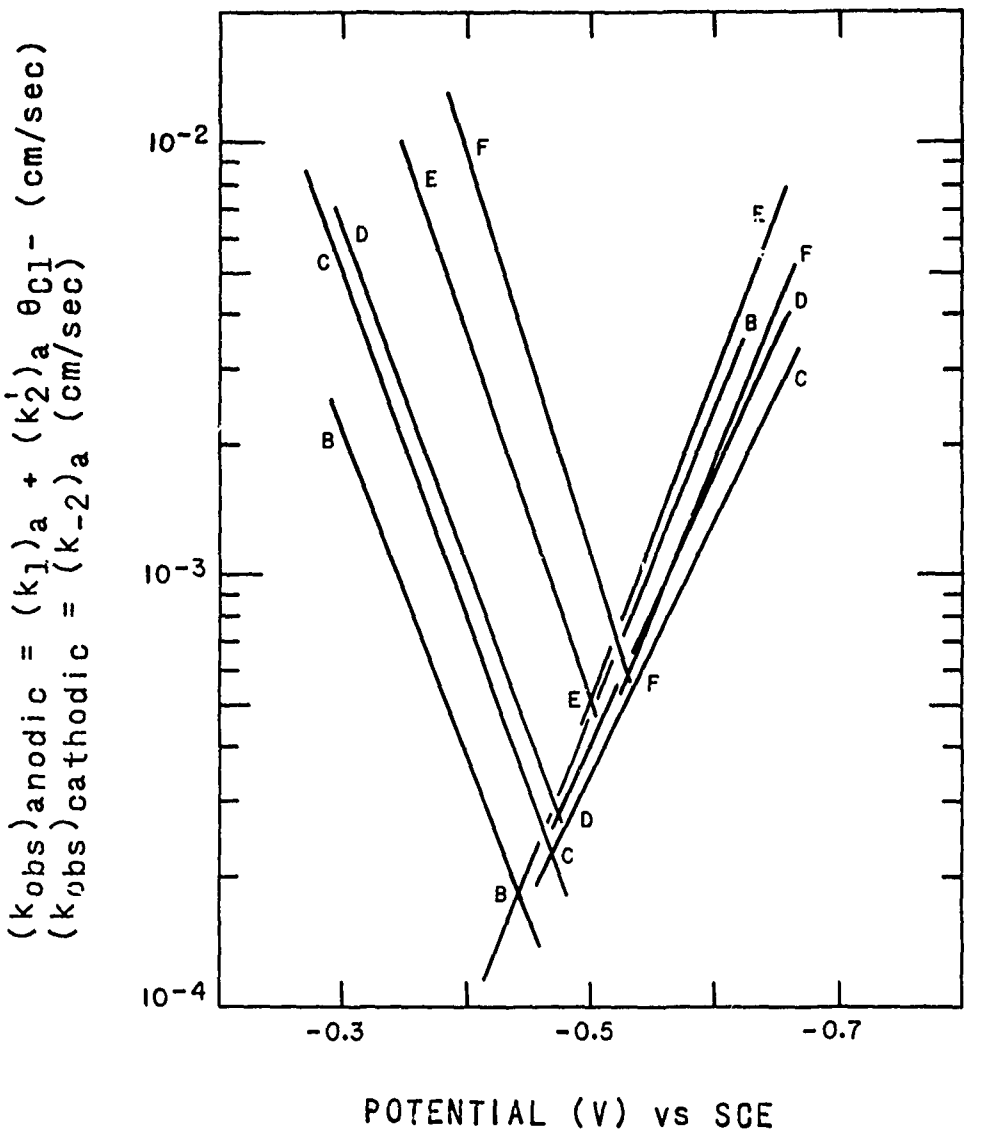

Fig. IV-6. Log of apparent rate constants for $[Cr(H_2O)_6]Cl^+/[Cr(H_2O)_5Cl]^{2+}$ couple in mixed chloride-perchlorate solutions on a HME. T = 25°C, pH = 2.20. The chloride concentrations are B = 3.22 m$\underline{M}$, C = 5.0 m$\underline{M}$, D=8.15 m$\underline{M}$, E=47.2 m$\underline{M}$, F=89.9 m$\underline{M}$.

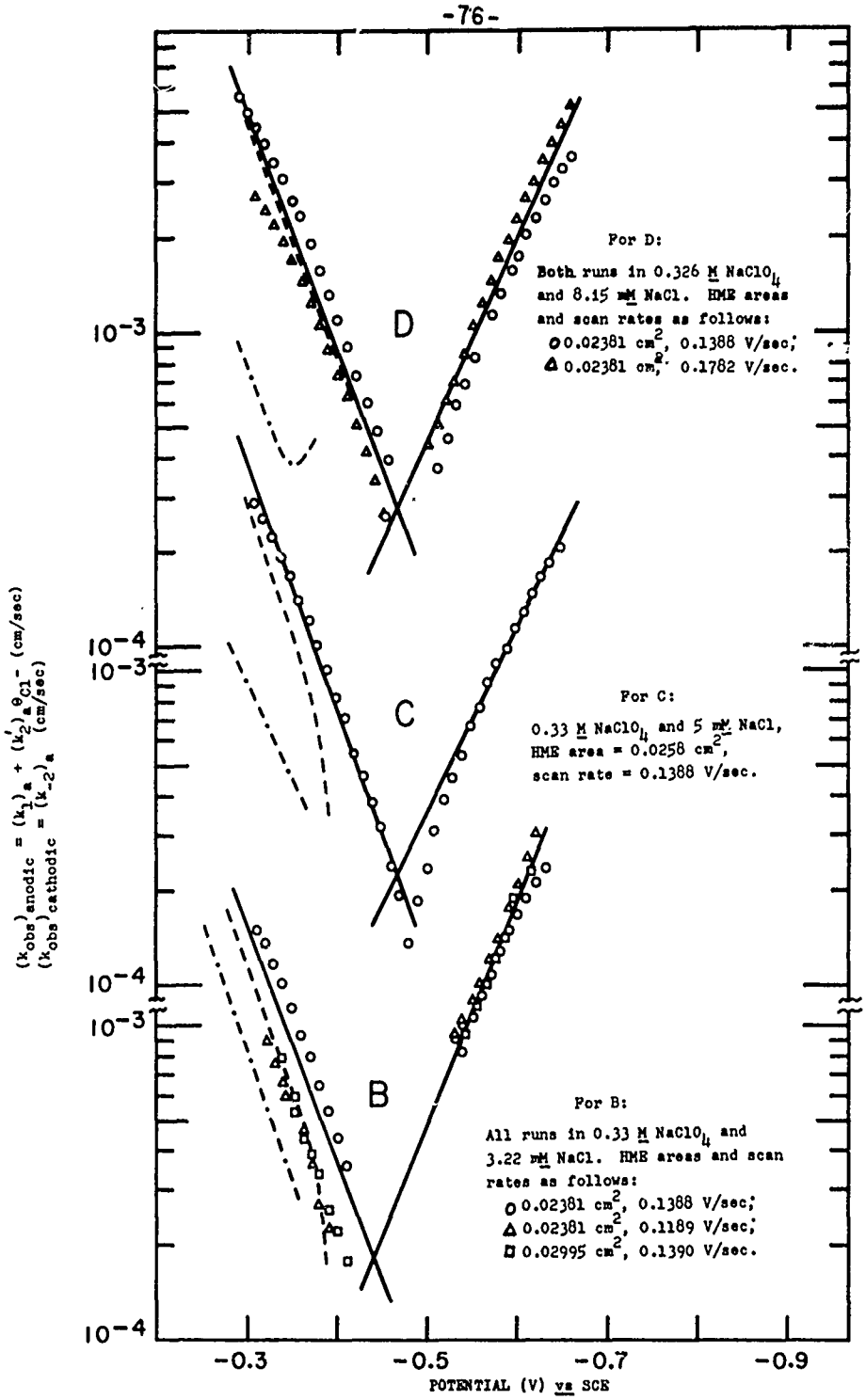

Fig. IV-7. Log of apparent rate constants for the $[Cr(H_2O)_6]Cl^+/[Cr(H_2O)_5Cl]^{2+}$ couple vs applied potentials in chloride-perchlorate solutions. Initial concentration of $[Cr(H_2O)_6](ClO_4)_3$ = 2.46 mM, pH = 2.20, T = 25°C. $(k_2)_a$ ---; $(k_1)_a$ -----.

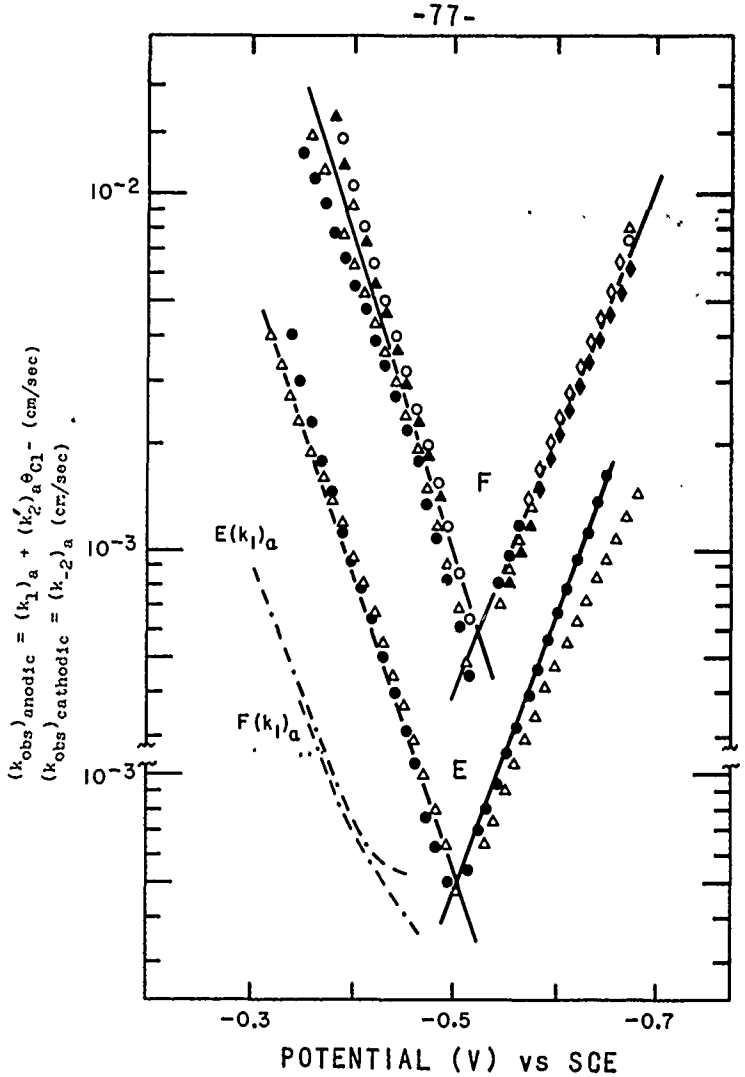

Fig. IV-8. Log of apparent rate constants for the $[Cr(H_2O)_6]Cl^+/[Cr(H_2O)_5Cl]^{2+}$ couple vs applied potentials in mixed chloride-perchlorate solutions at 25°C, pH = 2.20. Plot E- initial $[Cr(H_2O)_6](ClO_4)_3$ concentration = 2.46 mM in 0.28 M $NaClO_4$ and 0.0472 M NaCl. HME areas and scan rates were: ● 0.02236 cm^2, 0.0986 V/sec; Δ 0.02236 cm^2, 0.1380 V/sec. Plot F- initial concentration of $[Cr(H_2O)_6](ClO_4)_3$ = 2.96 mM in 0.24 M $NaClO_4$ and 0.0899 M NaCl. HME areas and scan rates were: ● 0.02594 cm^2, 0.1380 V/sec; Δ 0.02594 cm^2, 0.1380 V/sec; ▲ 0.02594 cm^2, 0.1778 V/sec; ○ 0.02594 cm^2, 0.1778 V/sec,

The line representing $(k_1)_a$ shows a change in direction at the more negative potentials for curves D and E. The change in direction is due to the factor $((\phi_2)_{ClO_4^-+Cl^-} - (\phi_2)_{Cl^-})$ in Eq. (IV-5) changing sign. Ordinarily the magnitude of this factor is quite small, being only 1 or 2 mV at potentials positive to -0.39V vs SCE. At more negative potentials the $\Delta\phi_2$ values can reach 8 or 9 mV and their effect is magnified by the high charge on the chromium ions.

The intersection of each pair of the extrapolated anodic and cathodic rate constant branches in Fig. IV-6 corresponded to the standard apparent rate constant at the apparent standard potential $(E_s^o)_a$ for the $[Cr(H_2O)_6]Cl^+/[Cr(H_2O)_5Cl]^{2+}$ couple. As with the hexaaquochromium(II)/(III) couple already discussed for the pure perchlorate supporting electrolyte, the apparent and the so-called true standard potentials were obtained by assuming that the activity coefficients for the higher and lower oxidation states of the chromium complexes were equal. This assumption was also used for other standard potentials discussed in this chapter. The data shown in Fig. IV-6 is only representative experimental data; not all of the data for all of the different chloride concentrations were used. A log-log plot of all of the standard apparent rate constants obtained for this couple vs their corresponding chloride concentrations is given in Fig. IV-9.

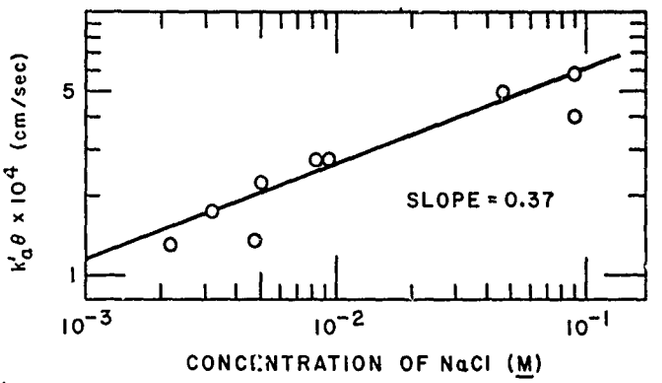

Fig. IV-9. Apparent standard rate constants for the $[Cr(H_2O)_6]Cl^{+}/[Cr(H_2O)_5Cl]^{2+}$ couple vs NaCl concentrations for mixed chloride-perchlorate solutions, T = 25°C, pH = 2.20. (The three points which fell far off the line were felt not to be as reliable as the others for drawing this line.)

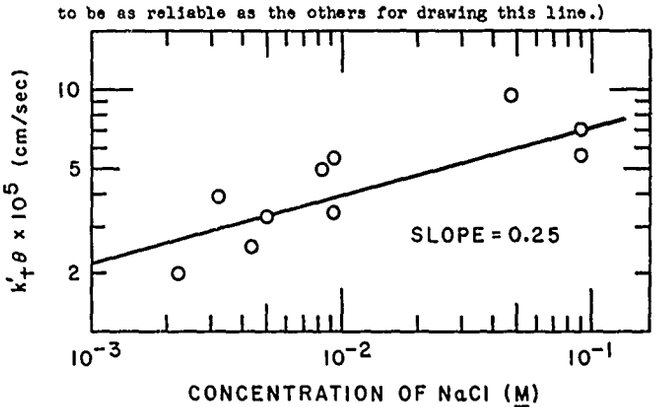

Fig. IV-10. Double layer corrected standard rate constants of Fig. IV-9.

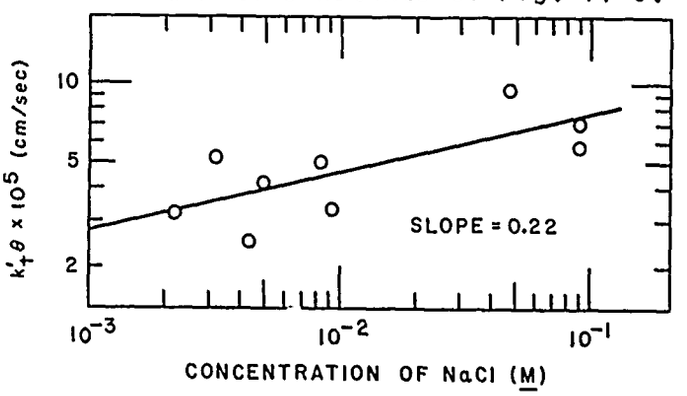

Fig. IV-11. Double layer corrected standard rate constants of Fig. IV-9. Concentration of $[Cr(H_2O)_5Cl]^{2+}$ adjusted to correct value.

Extrapolation of each line of rate constants for the anodic branch in Fig. IV-6 to its intersection with the corresponding line for the rate constants of the cathodic branch for the $[Cr(H_2O)_6]^{3+}$ reduction (not graphically shown for the mixed electrolyte cases) gave the apparent standard rate constant at the apparent standard potential $(E^o_s)_t$ for the $[Cr(H_2O)_6]^{2+}/[Cr(H_2O)_6]^{3+}$ couple in the mixed chloride-perchlorate solutions. A log-log plot of all of the standard apparent rate constants obtained for this couple vs their corresponding chloride concentrations is given in Fig.IV-12.

The double layer corrected rate constants from the observed apparent rate constants of Fig. IV-6 are shown in Fig. IV-11. In Fig. IV-14, the anodic branch of rate constants corresponds to the oxidation of $[Cr(H_2O)_6]^{2+}$ at an electrode site occupied with specifically adsorbed chloride. The cathodic branch of rate constants corresponds to the reverse of this reaction. The points for the anodic branches in Fig. IV-14 were obtained by double layer correcting $(k_2)_a$ points which are represented by the dashed lines in Figs. IV-7 and 8. In Fig. IV-15, the anodic branch of rate constants corresponds to the oxidation of $[Cr(H_2O)_6]^{2+}$ at an electrode site occupied by water. The cathodic branch corresponds to the reverse of this reaction. The points for the anodic branches in Fig. IV-15 were obtained by double layer correcting $(k_1)_a$ points which are represented by the dash-dot lines in Figs. IV-7 and 8. Since the anodic branch lines in Fig. IV-15 fell so close together, only the two extreme lines are shown All others

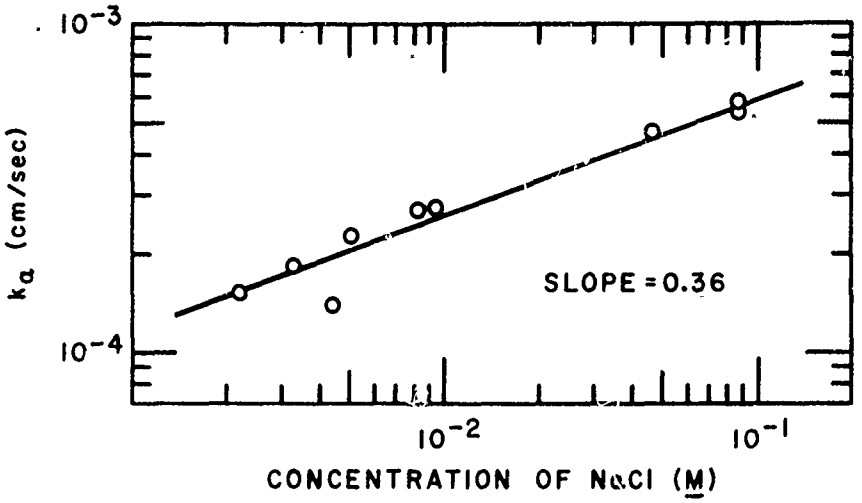

Fig. IV-12. Apparent standard rate constants for the $[Cr(H_2O)_6]^{2+}/[Cr(H_2O)_6]^{3+}$ couple vs NaCl concentrations in mixed chloride-perchlorate solutions of pH=2.2 and T=25°C.

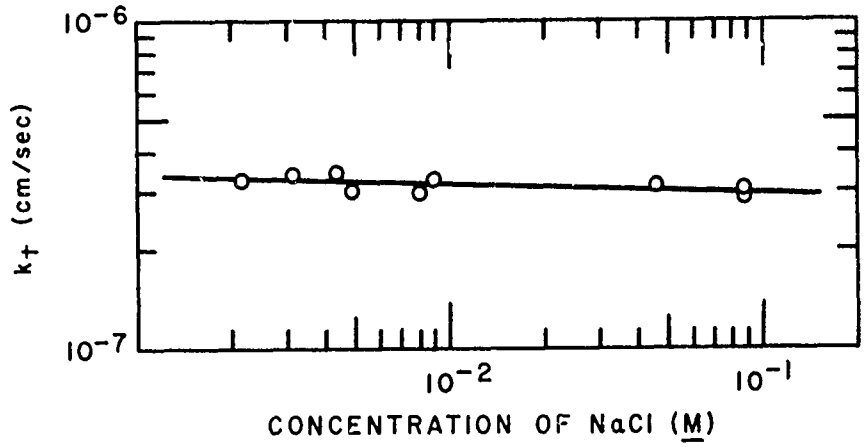

Fig. IV-13. Double layer corrected standard rate constants for the $[Cr(H_2O)_6]^{2+}/[Cr(H_2O)_6]^{3+}$ couple vs NaCl concentrations for mixed chloride-perchlorate solutions.

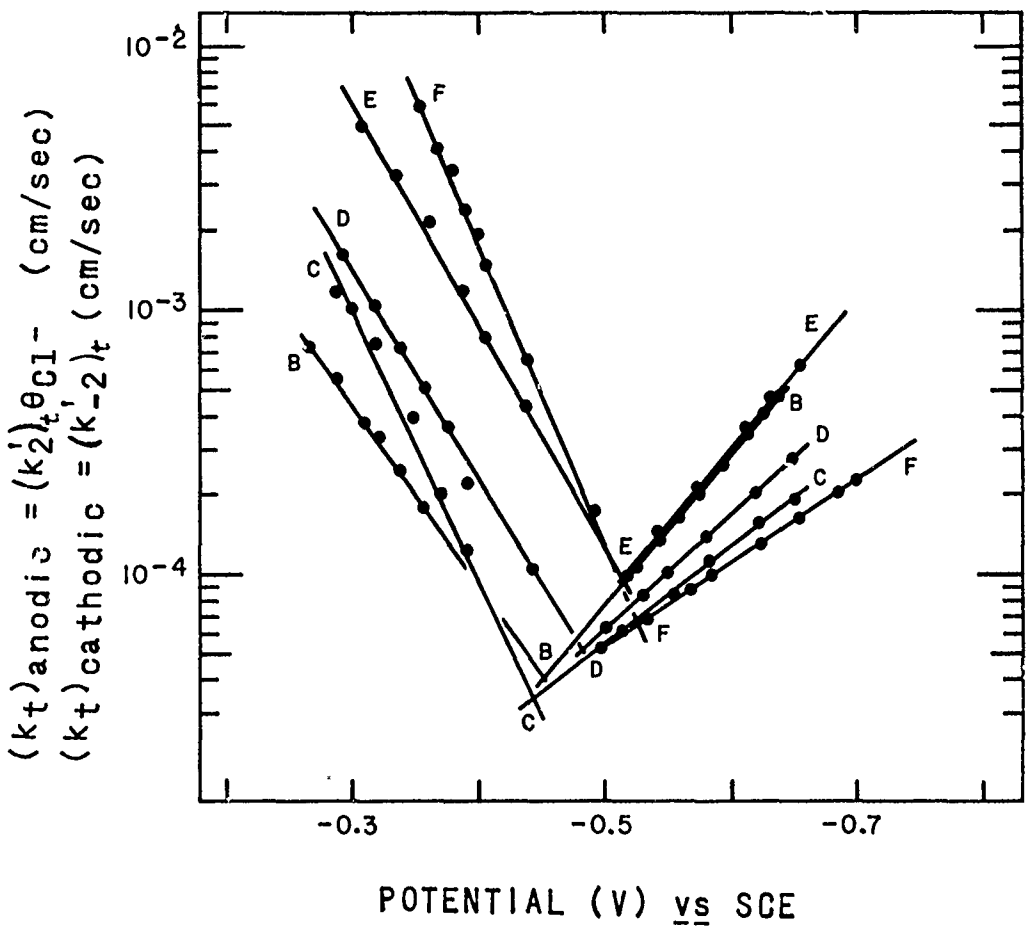

Fig. IV-14. Log of double layer corrected rate constants vs applied potentials for the $[Cr(H_2O)_6]Cl^+/[Cr(H_2O)_5Cl]^{2+}$ couple in mixed chloride-perchlorate solutions of pH = 2.20 and T = 25°C. The letters on the curves correspond to the same letters in Figs. IV-6 to 8.

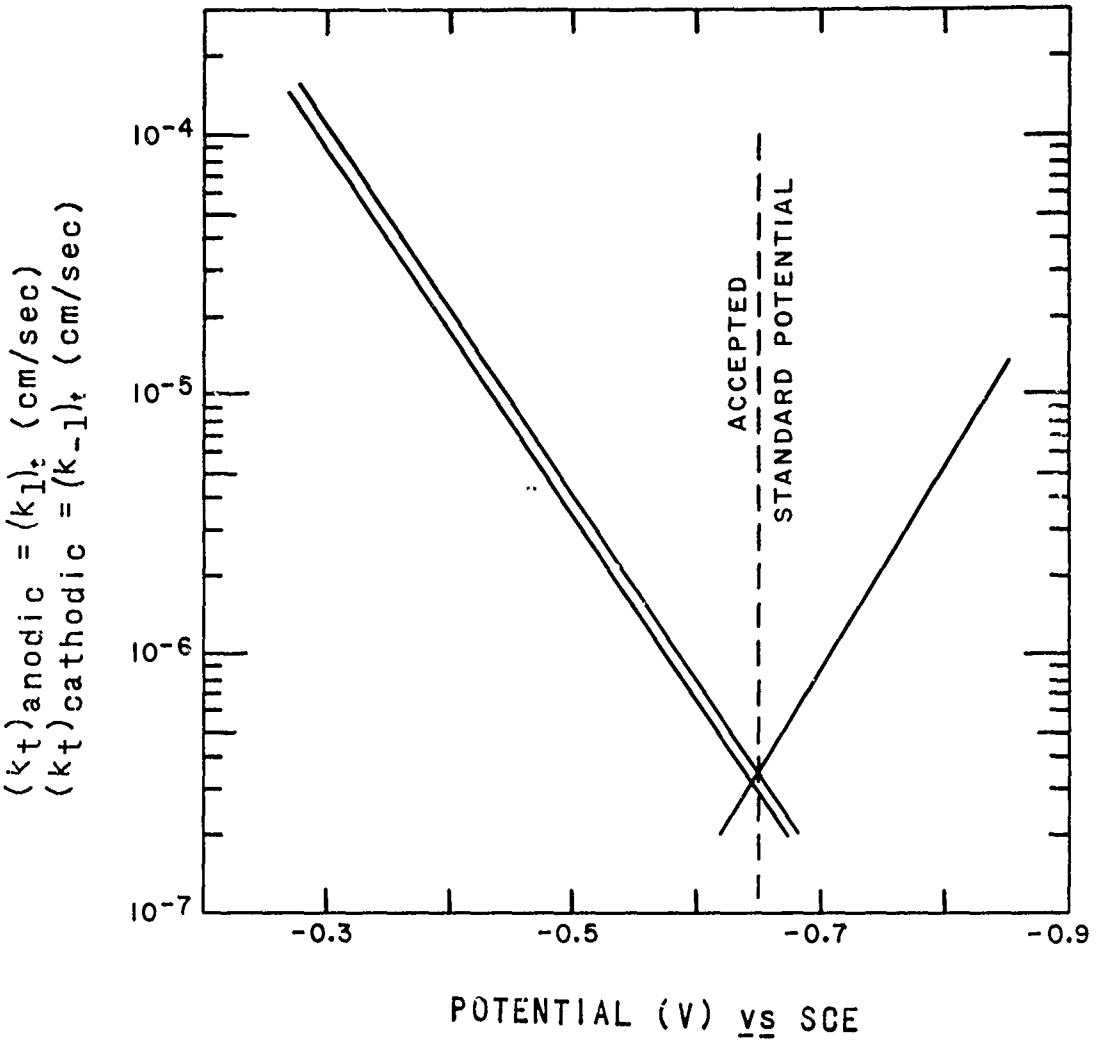

Fig. IV-15. Log of double layer corrected rate constants for $[Cr(H_2O)_6]^{2+}/[Cr(H_2O)_6]^{3+}$ in mixed chloride-perchlorate solutions of pH = 2.2 at 25°C. The anodic branch lines for chloride concentrations B to F (see Fig. IV-6) are contained within the two anodic lines shown here.

fell within these two lines.

Extrapolation of each pair of lines for the anodic and cathodic rate constants in Fig. IV-14 gave the true standard rate constants for the $[Cr(H_2O)_6]Cl^+/[Cr(H_2O)_5Cl]^{2+}$ couple at the standard potential $(E_s^o)_t$. A log-log plot of standard rate constants for this couple vs the corresponding chloride concentrations for all of the chloride concentrations used in this work is presented in Fig. IV-10.

An extrapolation similar to the one performed in Fig. IV-14 for Fig. IV-15 gave the true standard rate constants for the $[Cr(H_2O)_6]^{2+}/[Cr(H_2O)_6]^{3+}$ couple at the standard potential $(E_s^o)_t$. A log-log plot of the standard rate constants for this couple vs the corresponding chloride concentrations for all of the chloride concentrations used in this work is presented in Fig. IV-13.

A discussion of certain necessary refinements is now appropriate. The first is the calculation of the rate constants k_{-2} for the reduction of $[Cr(H_2O)_5Cl]^{2+}$. Unfortunately the calculation of k_{-2} is not as simple as was outlined on page 23. In order to calculate k_{-2}, the concentration of $[Cr(H_2O)_5Cl]^{2+}$ at the interface had to be determined. This concentration was determined by assuming that all of the $[Cr(H_2O)_6]^{2+}$ which was oxidized in the mixed chloride-perchlorate solutions became $[Cr(H_2O)_5Cl]^{2+}$. This assumption is valid only at high chloride concentrations, as is apparent by comparing the observed composite apparent rate con-

stants for the anodic branches with the $(k_1)_a$ values for the anodic branches in Figs. IV-7 and 8. For the lower chloride concentrations, only a fraction of the $[Cr(H_2O)_6]^{2+}$ oxidized became $[Cr(H_2O)_5Cl]^{2+}$. Since all of the $[Cr(H_2O)_6]^{2+}$ had been assumed to be oxidized to the $[Cr(H_2O)_5Cl]^{2+}$ complex even at low chloride concentrations, the rate constants k_{-2} which were calculated were lower than they should have been under such circumstances. The improper calculation of the $[Cr(H_2O)_5Cl]^{2+}$ concentrations was corrected for by comparing the observed composite apparent rate constants with the $(k_1)_a$ apparent rate constants from the anodic branch for the $[Cr(H_2O)_6]^{2+}$ oxidation. Since $[Cr(H_2O)_6]^{2+}$ is the reactant whether the product is $[Cr(H_2O)_6]^{3+}$ or $[Cr(H_2O)_5Cl]^{2+}$, and since the back reactions do not contribute to the anodic part of the cyclic voltammetry curve, this correction could be made by taking the mean value for the difference between the composite rate constants and the $(k_2)_a$ rate constants over the potential range of importance as the average factor by which to increase the k_{-2} rate constants. The final result of this calculation is shown in Fig. IV-11, which is a plot of the double layer corrected standard rate constants vs chloride concentration.

Table IV-1 presents transfer coefficient and standard potential data for the $[Cr(H_2O)_6]^{2+}/[Cr(H_2O)_6]^{3+}$ couple and the $[Cr(H_2O)_6]Cl^{+}/[Cr(H_2O)_5Cl]^{2+}$ couple in mixed chloride-perchlorate solutions. The transfer coefficients for the $[Cr(H_2O)_6]^{2+}/[Cr(H_2O)_6]^{3+}$ couple are very close to being complementary

TABLE IV-1. Transfer Coefficients and Standard Potentials in Chloride-Perchlorate Solutions. pH $\sim$ 2.2, T = 25°C

Chloride in 10^{-3}M	$[Cr(H_2O)_6]^{2+}/[Cr(H_2O)_6]^{3+}$				$[Cr(H_2O)_6]Cl^{+}/[Cr(H_2O)_5Cl]^{2+}$				
	α_t	β_t	$-(E_s^o)_a$ in V vs SCE	$-(E_s^o)_t$	α_t	β_t	$-(E_s^o)_t$	$-(E_s^o)_t$	$-(E_s^o)_t$ *
0	0.48	0.43	0.637	0.650	--	--	--	--	
2.19	(0.48)	0.42	0.638	0.650	0.35	0.54	0.491	0.478	0.482
3.22	(0.48)	0.42	0.623	0.649	0.34	0.41	0.441	0.452	0.430
4.35	(0.48)	0.42	0.643	0.651	0.31	0.46	0.512	0.523	0.503
5.00	(0.48)	0.43	0.634	0.647	0.22	0.62	0.468	0.443	0.435
8.15	(0.48)	0.44	0.645	0.643	0.26	0.49	0.474	0.479	0.469
9.29	(0.48)	0.41	0.648	0.649	0.15	0.52	0.503	0.481	0.471
9.30	(0.48)	0.41	0.650	0.652	0.15	0.69	0.475	0.488	0.478
47.2	(0.48)	0.43	0.663	0.647	0.33	0.51	0.502	0.513	--
89.9	(0.48)	0.42	0.688	0.644	0.13	0.56	0.525	0.513	--
89.9	(0.48)	0.42	0.676	0.645	0.18	0.67	0.528	0.524	--

* $(E_s^o)_t$ obtained from the double layer corrected rate constants after the $[Cr(H_2O)_5Cl]^{2+}$ concentration was corrected for $[Cr(H_2O)_6]^{2+}$ oxidations occurring in solutions with low chloride concentrations.

($\alpha + \beta = 1$), but those for the $[Cr(H_2O)_6]Cl^+/[Cr(H_2O)_5Cl]^{2+}$ couple are not. The α_t for the hexaaquochromium couple in the mixed electrolyte was taken to be the same as α_t in the pure perchlorate solution since no difference existed between the initial sweep curves for the $[Cr(H_2O)_6]^{3+}$ reduction in either the mixed or the pure perchlorate electrolyte (Fig. IV-3).

The potential corresponding to the intersection for the lines drawn through the apparent rate constants has been designated as $(E_s^o)_a$ and the potential corresponding to the intersection for the lines drawn through the double layer corrected rate constants has been designated as $(E_s^o)_t$. In the mixed chloride-perchlorate supporting electrolyte, the apparent and double layer corrected standard potentials are shifted by the activity of the chloride ions present in solution. Assuming that there is no change in the ratio of $[Cr(H_2O)_6]^{2+}$ to $[Cr(H_2O)_5Cl]^{2+}$ activity coefficients as the chloride concentration changes from 3.22 to 89.9 mM, the Nernst equation predicts that the standard potential for the $[Cr(H_2O)_6]Cl^+/[Cr(H_2O)_5Cl]^{2+}$ couple should shift about 95 mV toward more negative potentials. A shift of this magnitude and in the correct direction is evident in Figs. IV-6 or 11 or in Table IV-1. For the $[Cr(H_2O)_6]^{2+}/[Cr(H_2O)_6]^{3+}$ couple, the standard potential should be independent of chloride concentrations and be equal to -0.65 V vs SCE. This was indeed the case for the standard potentials $(E_s^o)_t$ obtained from the extrapolation of the double layer corrected rate constants. The apparent standard potentials

$(E_s^o)_a$ for this couple did show a weak dependence on the chloride concentrations as would be expected since the observed composite apparent rate constants which were extrapolated to $(E_s^o)_a$ still contained a contribution from the $[Cr(H_2O)_6]Cl^+/[Cr(H_2O)_5Cl]^{2+}$ couple.

One additional item needs to be considered: the new cathodic peak which appeared at potentials positive to the $[Cr(H_2O)_6]^{3+}$ reduction peak and which has been treated as the reduction of $[Cr(H_2O)_5Cl]^{2+}$. In a highly acidic perchlorate-chloride solution, the initially introduced $[Cr(H_2O)_6](ClO_4)_3$ was stable. The $[Cr(H_2O)_6]^{3+}$ cation is extremely slow to undergo inner-sphere substitution and at a pH of 2.2, only an insignificant amount[2] of the chromium(III) could exist in a hydrolyzed form. In the course of cyclic voltammetry, the labile $[Cr(H_2O)_6]^{2+}$ was formed. Therefore any new cathodic voltammetry peak which appeared subsequent to the $[Cr(H_2O)_6]^{2+}$ formation must be an inner-sphere complex of chromium(III). Since only ClO_4^-, Cl^-, and H_2O ligands were present in the solution, since the reduction peak of $[Cr(H_2O)_6]^{3+}$ was well known, and since ClO_4^- does not coordinate inner-sphere with $[Cr(H_2O)_6]^{2+}$, the only possible remaining complex is a water-chloride one.

A $[Cr(H_2O)_5Cl]^{2+}$ complex was more likely to be formed than a $[Cr(H_2O)_4Cl_2^+]^+$ complex. To prove the identity of the new cathodic peak, the cyclic voltammetry curve of $[Cr(H_2O)_5Cl]^{2+}$ was run

to learn if it, and its rate constants, agreed with the cyclic voltammetry curve and rate constants of the new cathodic peak. The cyclic voltammetry curve for $[Cr(H_2O)_5Cl]^{2+}$ is given in Fig. IV-16. The cathodic peak of $[Cr(H_2O)_5Cl]^{2+}$ agreed well with the new cathodic peak in the mixed chloride-perchlorate supporting electrolytes. The apparent rate constants for the cyclic voltammetry of $[Cr(H_2O)_5Cl]^{2+}$ were obtained with the computer program in Appendix I. A semi-log plot of the apparent rate constants vs applied potential is given in Fig. IV-17. The best straight line through these apparent rate constants was double layer corrected with ϕ_2 data for a pure perchlorate solution. A semi-log plot of the true rate constants vs applied potential is given in Fig. IV-17.

To determine how much of an effect a second chloride ligand coordinated inner sphere with chromium(II) would have, the cyclic voltammetry of $[Cr(H_2O)_4Cl_2]^{+}$ was studied in an acidic perchlorate supporting electrolyte. This cyclic voltammetry curve is given in Fig. IV-16. The cathodic peak for $[Cr(H_2O)_4Cl_2]^{+}$ was much broader toward more positive potentials than was the cathodic peak for $[Cr(H_2O)_5Cl]^{2+}$. The apparent rate constants for the cyclic voltammetry of $[Cr(H_2O)_4Cl_2]^{+}$ was obtained with the computer program in Appendix I. A semi-log plot of the apparent rate constants vs applied potential is given in Fig. IV-17. The apparent rate constants were double layer corrected with ϕ_2 data for pure

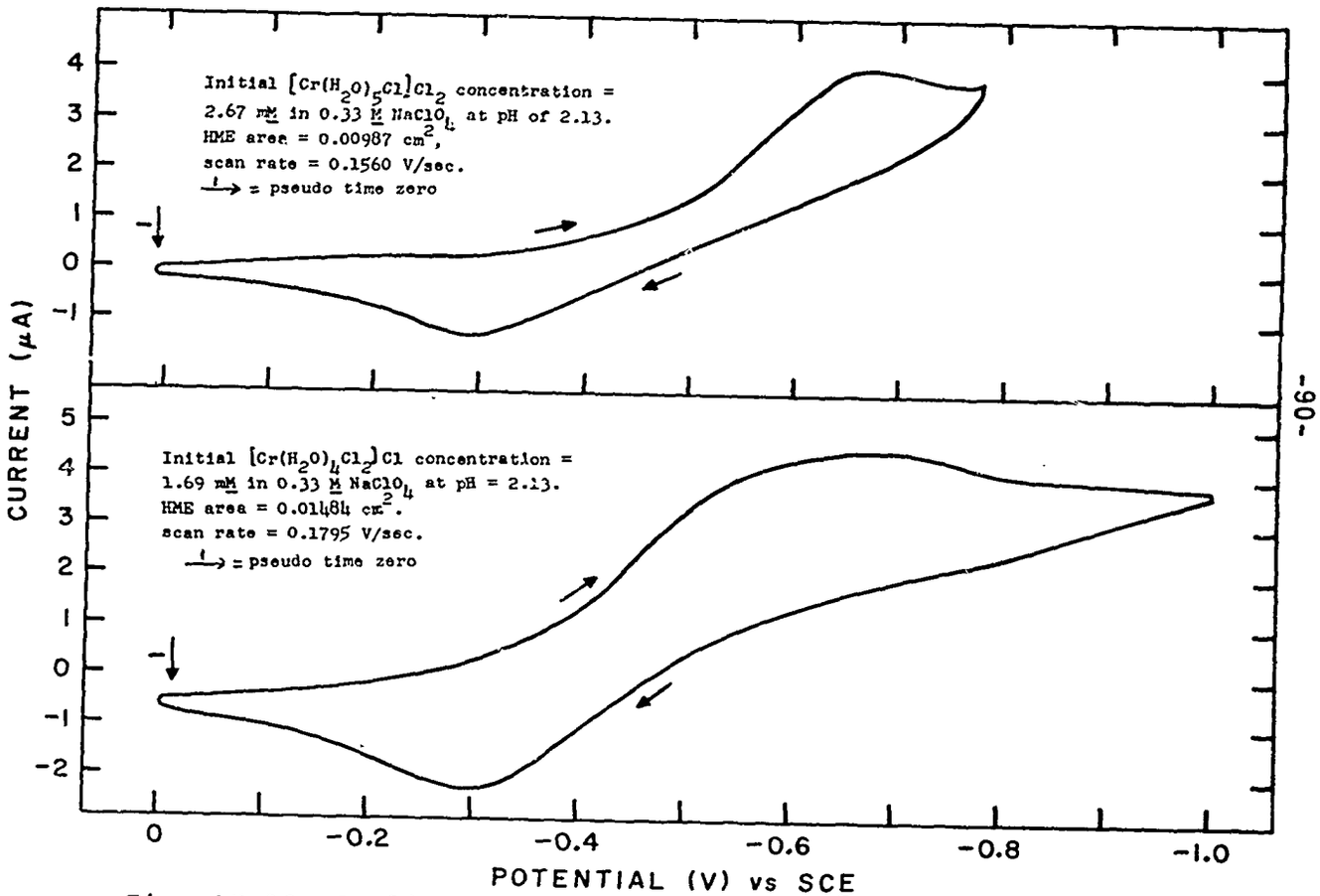

Fig. IV-16. Cyclic voltammetry curve of $[Cr(H_2O)_5Cl]Cl_2$ (upper) and $[Cr(H_2O)_4Cl_2]Cl$ (lower) at 25°C.

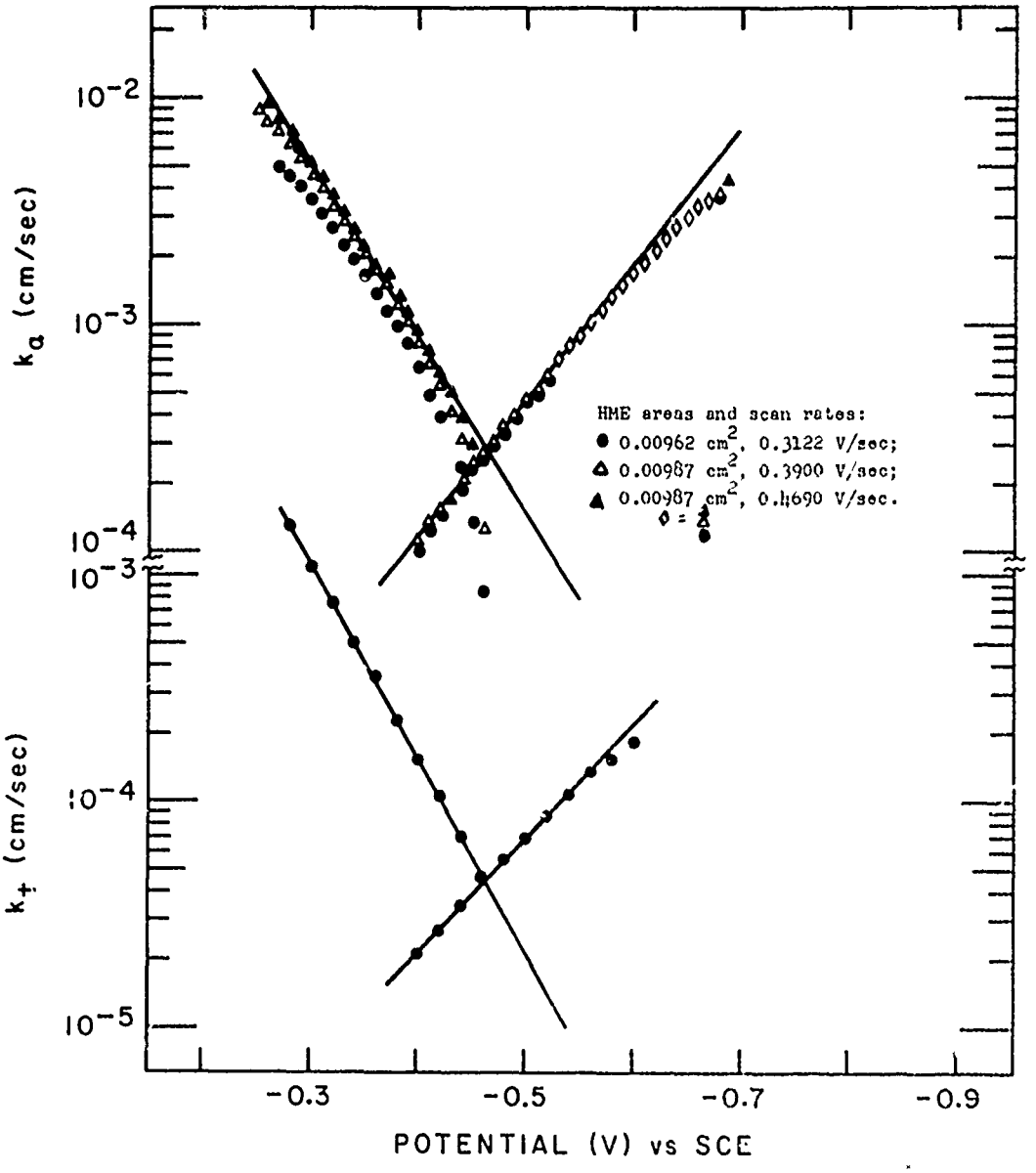

Fig. IV-17. Log of apparent (upper) and double layer corrected (lower) rate constants vs applied potentials for the $[Cr(H_2O)_6]Cl^{+}/[Cr(H_2O)_5Cl]^{1+}$ couple in 0.33 M $NaClO_4$ with pH = 2.13. Initial $[Cr(H_2O)_5Cl]Cl_2$ concentration = 2.67 mM, T = 25°C.

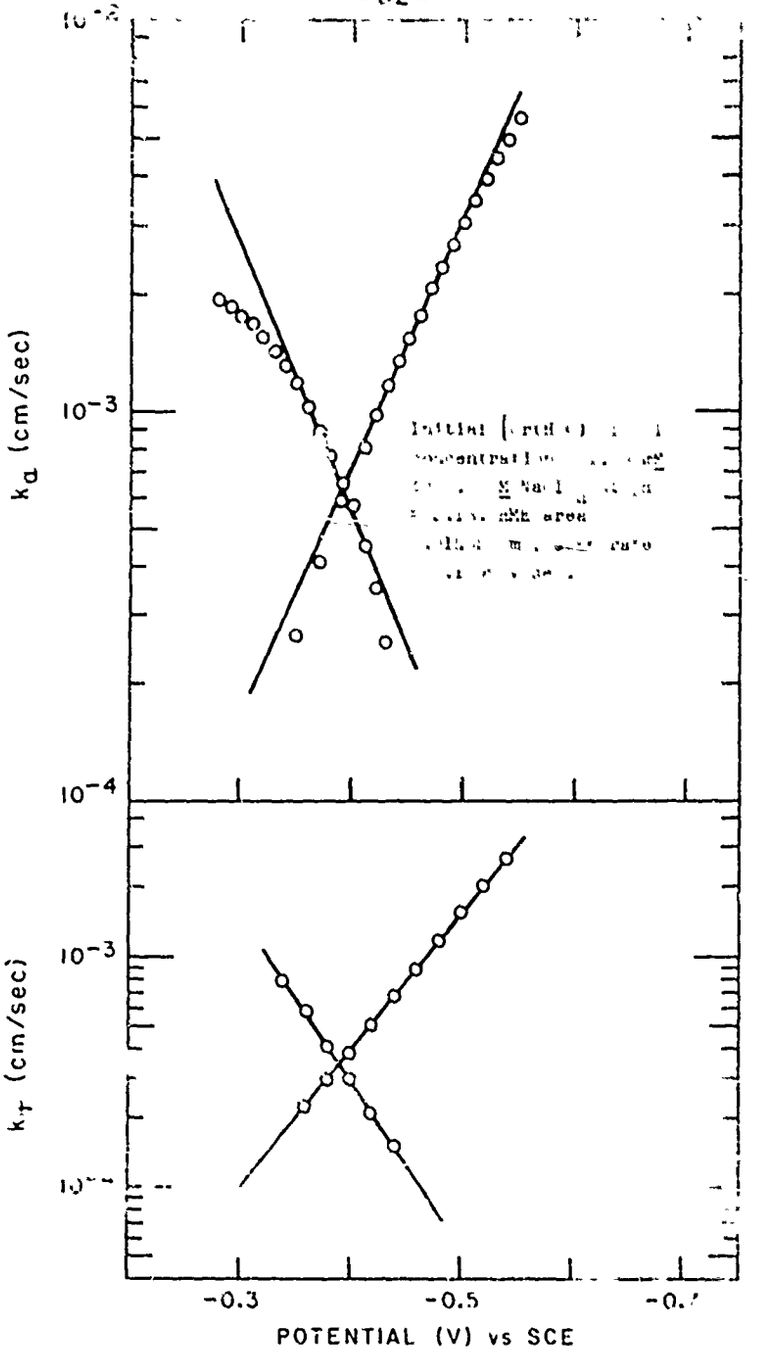

Fig. IV-18. Log of apparent (upper) and double layer corrected (lower) rate constants vs applied potentials for $[Cr(H_2O)_6]Cl_2^{o}/[Cr(H_2O)_4Cl_2]^{+}$ couple at 25°C.

perchlorate solutions and a semi-log plot of the true rate constants vs applied potential is given in Fig. IV-18.

The true transfer coefficients for the $[Cr(H_2O)_6]Cl^+/[Cr(H_2O)_5Cl]^{2+}$ couple at the standard potential of -0.462 V vs SCE were $\alpha_t = 0.30$ and $\beta_t = 0.55$. The true transfer coefficients for the $[Cr(H_2O)_6]Cl_2^o/[Cr(H_2O)_4Cl_2]^+$ couple at the standard potential of 0.0390 V vs SCE were $\alpha_t = 0.35$ and $\beta_t = 0.43$.

Cyclic Voltammetry of $[Cr(H_2O)_6]^{3+}$ in Bromide-Perchlorate Supporting Electrolytes

When NaBr rather than NaCl was added to the $NaClO_4$ supporting electrolyte, with the ionic strength held constant, the cyclic voltammetry curves were changed from what they were in either a pure perchlorate solution or in a mixed chloride-perchlorate supporting electrolyte. For different bromide concentrations, the "steady-state" voltammetry curves of $[Cr(H_2O)_6]^{3+}$ are shown in Figs. IV-19 and 20. Initial cycle curves were given in Chapter II. The original cathodic peak was slightly changed from what it was in the pure perchlorate media, the anodic peak was shifted toward negative potentials, and a new cathodic peak at potentials very positive to the original cathodic peak appeared. Each peak will be discussed.

The anodic peak was a composite peak just as the anodic peak for the cyclic voltammetry of $[Cr(H_2O)_6]^{3+}$ in the mixed chloride-perchlorate supporting electrolyte was. The two oxidation processes involved for the bromide-perchlorate supporting electrolyte included the process which occurred at an electrode site occupied by water

$$[Cr(H_2O)_6]^{2+} \xrightarrow{k_3} [Cr(H_2O)_6]^{3+} + e^- \qquad \text{(IV-8)}$$

where $k_3 = k_3'\theta_{H_2O} \simeq k_3'$ and the process which occurred at an electrode site occupied by adsorbed bromide.

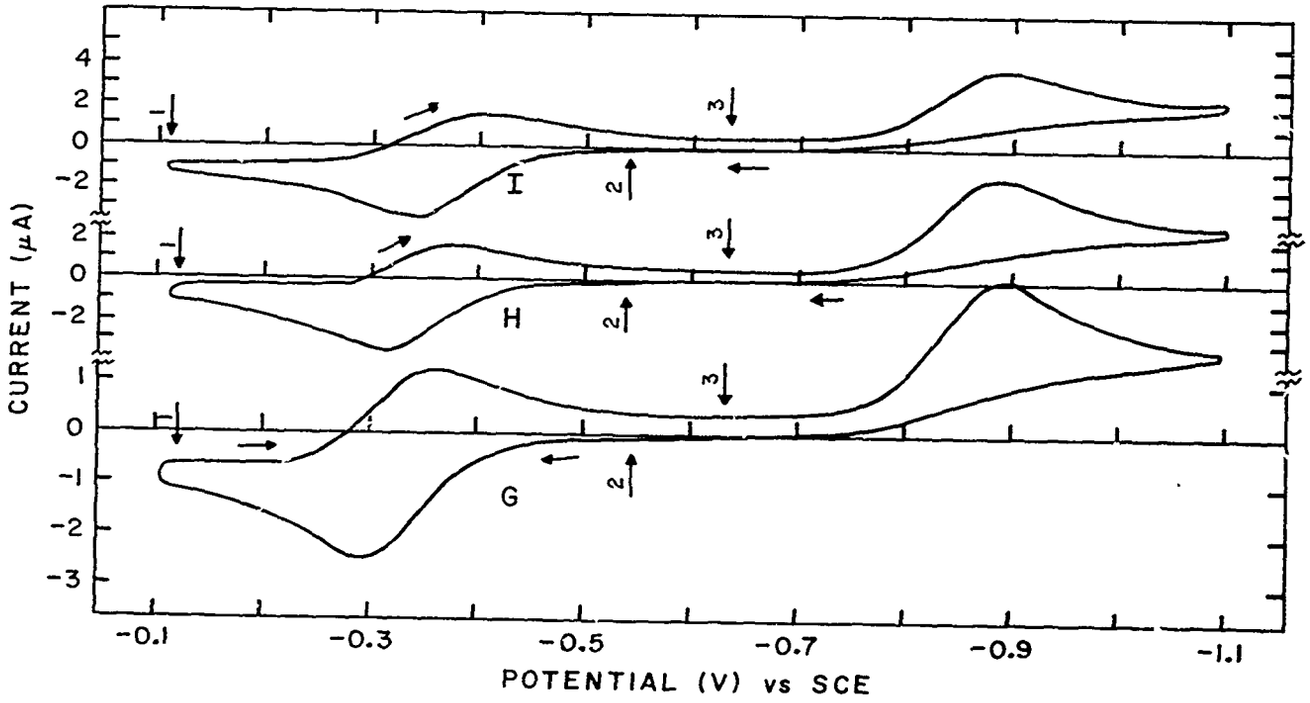

Fig. IV-19. Cyclic voltammetry of $[Cr(H_2O)_6]^{3+}$ in bromide-perchlorate solutions. T=25°C, pH=2.13, initial $[Cr(H_2O)_6](ClO_4)_3$ concentration = 2.41 m$\underline{M}$; Curve G: 0.33 $\underline{M}$ $NaClO_4$ and 3.45 m$\underline{M}$ NaBr, scan rate=0.179 V/sec, HME area=0.00783 cm^2; Curve H: 0.33 $\underline{M}$ $NaClO_4$ and 5.64 m$\underline{M}$ NaBr, scan rate=0.179 V/sec, HME area= 0.01404 cm^2; Curve I: 0.316 $\underline{M}$ $NaClO_4$ and 0.0107 $\underline{M}$ NaBr, scan rate = 0.1791 V/sec, HME area=0.01278 cm^2. $\xrightarrow{1}$ = pseudo zero time (1) $\xrightarrow{2}$ = pseudo zero time (2), $\xrightarrow{3}$ = pseudo time zero (3).

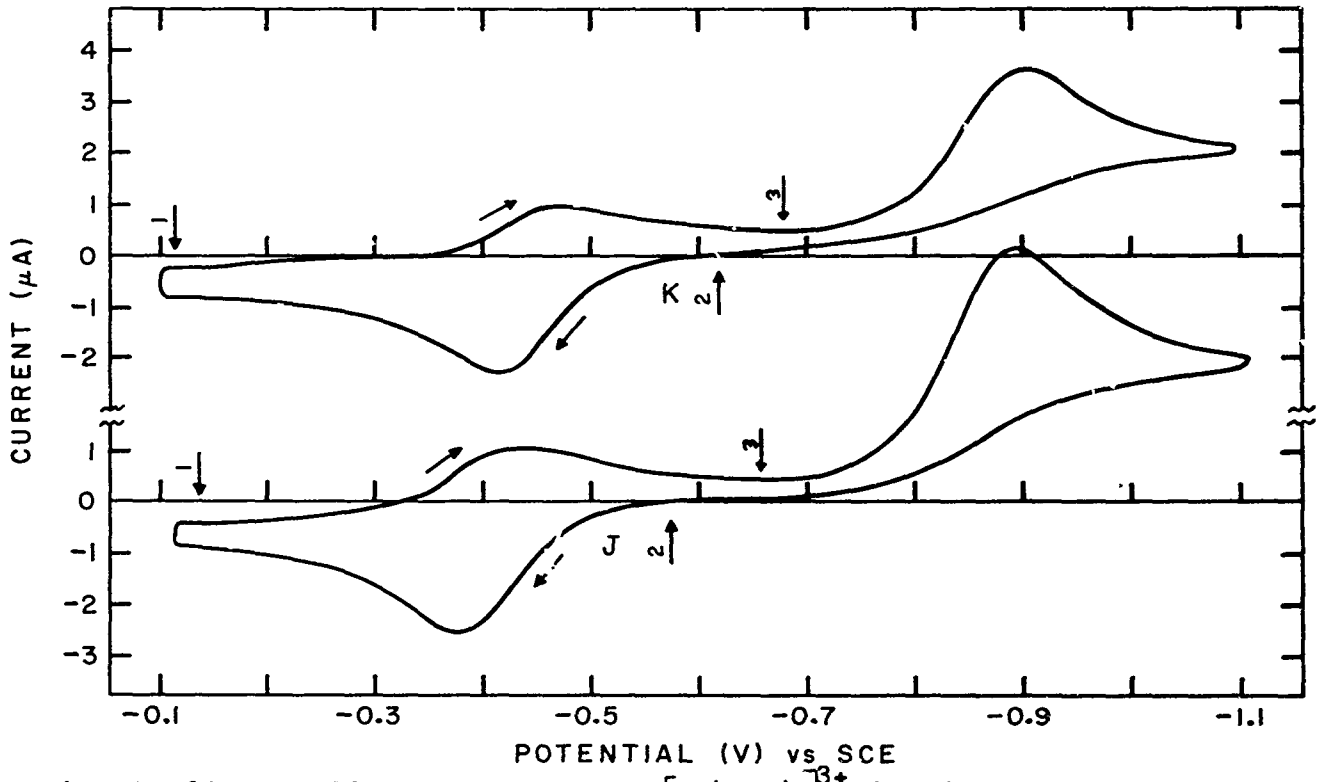

Fig. IV-20. Cyclic voltammetry of $[Cr(H_2O)_6]^{3+}$ in mixed bromide-perchlorate solutions. T=25°C, pH=2.30. Curve J: initial $[Cr(H_2O)_6](ClO_4)_3$ concentration=2.41 m$\underline{M}$ in 0.28 $\underline{M}$ $NaClO_4$ and 0.0428 $\underline{M}$ NaBr, scan rate=0.1393 V/sec, HME area=0.02226 cm^2; Curve K: initial $[Cr(H_2O)_6](ClO_4)_3$ concentration=2.47 m$\underline{M}$ in 0.23 $NaClO_4$ and 0.103 $\underline{M}$ NaBr, scan rate=0.1396 V/sec, HME area = 0.01004 cm^2. $\underline{1}$, $\underline{2}$, $\underline{3}$, = pseudo time zero(1),(2),(3), respectively.

$$[Cr(H_2O)_6]^{2+} + Br^-_{ad} \xrightarrow{k_4} [Cr(H_2O)_5Br]^{2+} + e^- \qquad \text{(IV-9)}$$

where $k_4 = k_4'\theta_{Br^-}$. This anodic peak was also strongly influenced by the back reaction from the new cathodic peak which corresponded to the reduction of $[Cr(H_2O)_5Br]^{2+}$. Proof of the identity of the new cathodic peak will be given later. The computer program given in Appendix II utilizes Eqs. (II-5), (II-6), and (II-9) and was used to calculate the composite apparent rate constants. In this program the back reaction is taken into account.

To separate the composite apparent rate constants into k_3 and k_4, the value of k_3 for any given potential must be calculated and then subtracted from the composite apparent rate constant for that same potential, the difference being k_4. The apparent rate constant k_3 for the mixed bromide-perchlorate supporting electrolyte could have been calculated from the apparent rate constant for the $[Cr(H_2O)_6]^{2+}$ oxidation in a pure perchlorate medium if the change in double layer potentials between the pure perchlorate and mixed bromide-perchlorate solutions were appropriately taken into account. This calculation was used for obtaining k_1 with Eq. (IV-5) for the mixed chloride-perchlorate solutions, but was not possible for the mixed bromide-perchlorate solutions. When the calculation was attempted in the latter case, the values for k_3 generally exceeded the values for the composite apparent rate constants. This indicated that the potentials for the mixed bromide-perchlorate solutions were too large. The omission of not

taking into account the surface concentrations of chromium(II) and chromium(III) when determining the ϕ_2 potentials is more serious with bromide than with chloride. Consequently the double layer corrections applied here must be viewed with extreme caution. A semi-quantitative adjustment to these double layer corrections will be made in Chapter V.

Consequently, a ϕ_2 correction similar to Eq. IV-5 was not applied and k_3 was taken to be identical to the apparent anodic rate constants for the $[Cr(H_2O)_6]^{2+}$ oxidation in a pure perchlorate supporting electrolyte. When k_3 was subtracted from the composite apparent rate constants, the difference was k_4. The inability to make a proper correction is regrettable and reflects one of the serious limitations imposed on electrochemical kinetic studies by the lack of sufficient information, either experimentally or theoretically, concerning the double layer.

The apparent rate constant k_3 was double layer corrected using the ϕ_2 data for a pure perchlorate supporting electrolyte. The true transfer coefficient for this correction was taken as 0.43. The apparent rate constant k_4 was also double layer corrected using the ϕ_2 data for a mixed bromide-perchlorate supporting electrolyte. The true transfer coefficient was calculated for each run from the apparent transfer coefficient and ϕ_2 data, and was used for the double layer corrections.

The second voltammetry peak to be discussed is the new cathodic peak which corresponded to the reduction of $[Cr(H_2O)_5Br]^{2+}$.

$$[Cr(H_2O)_5Br]^{2+} + e^- \xrightarrow{k_{-4}} [Cr(H_2O)_6]^{2+} + Br^-_{ad} \qquad \text{(IV-10)}$$

where $k_{-4} = k'_{-4}\theta_{H_2O} \simeq k'_{-4}$. The apparent rate constant k_{-4} was calculated with the computer program in Appendix II and then double layer corrected with the ϕ_2 potentials for mixed bromide-perchlorate supporting electrolytes. With reaction (IV-10), as with reaction (IV-6), the question arises as to the orientation of the $[Cr(H_2O)_5Br]^{2+}$ cation as it approaches the electrode and the consequences of that orientation. This question will also be discussed in the last chapter.

The last voltammetry peak to be discussed is the original cathodic peak which corresponded to the reduction of $[Cr(H_2O)_6]^{2+}$.

$$[Cr(H_2O)_6]^{3+} + e^- \xrightarrow{k_{-3}} [Cr(H_2O)_6]^{2+} \qquad \text{(IV-11)}$$

where $k_{-3} = k'_{-3}\theta_{H_2O} \simeq k'_{-3}$. For the first cycle voltammetry curves this cathodic peak was slightly more drawn-out in the mixed bromide-perchlorate supporting electrolyte than it was in a pure perchlorate solution. The small change in slope for the log k *vs* E plot for this cathodic peak could change the apparent transfer coefficient from 0.63 (the value in the pure perchlorate supporting electrolyte) to 0.60 (the value in the mixed bromide-perchlorate solution) for supporting electrolytes of high bromide concentrations. The position of this cathodic peak also was 10 mV more positive in the bromide-perchlorate solutions than it was in the pure perchlorate solutions. It can be shown

that this shift in the peak potential means the apparent rate constants in the mixed bromide-perchlorate electrolyte are about a factor of 1.2 on the average higher at any given voltage than what they were in the pure perchlorate supporting electrolyte. As will be discussed further in the last chapter, this increase in rate constants is ascribed to double layer effects, not to a change in the mechanism of the reduction.

The voltammetry curves used for bromide were the "steady-state" curves which showed a more drawn-out $[Cr(H_2O)_6]^{3+}$ reduction peak than did the initial cycle voltammetry curves (see Fig. II-1). A similar, but smaller, difference between the initial and "steady-state" cycle curves for this cathodic peak in mixed chloride-perchlorate solutions can be seen in Fig. IV-4b. Since the initial cycle voltammetry curves in perchlorate and mixed chloride-perchlorate solutions were identical (Fig. IV-5) for this reduction peak, the "steady-state" peak which occurred in the mixed chloride-perchlorate solutions could be analyzed simply by assuming it identical to the corresponding peak which occurred in the pure perchlorate solutions (either "steady-state" or initial cycle sweeps, since the Tafel slopes in each were identical as shown by Fig. II-2), and then double layer correcting it with ϕ_2 data from pure perchlorate solutions. Unfortunately a similar analysis procedure will not work as well for the mixed bromide-perchlorate solutions, since the initial cycle curves in

the bromide-perchlorate solutions were not identical to those in the pure perchlorate solutions. Furthermore, differences in the Tafel slope between initial and "steady-state" cycle sweeps for this reduction peak in the mixed bromide-perchlorate electrolytes existed. At bromide concentrations below 0.1 M the "steady-state" cycle voltammetry curves gave apparent transfer coefficients of about 0.57 as compared to about 0.61 from the initial cycle sweeps. At bromide concentrations of 0.1 M, the "steady-state" apparent transfer coefficients were 0.50 as compared to 0.60 from initial cycle sweeps.

If the double layer corrections could be made precisely, then initial cycle, rather than "steady-state" cycle, data would be needed, particularly at the high bromide concentration. Since these double layer corrections can only be made approximately, and since analysis from the "steady-state" curves instead of from the initial cycle curves caused no serious problem for the evaluation of the $[Cr(H_2O)_6Br]^+/[Cr(H_2O)_5Br]^{2+}$ couple, additional initial cycle curves were not obtained. As far as the mechanism for this reduction process is concerned, the same lack of rate constant dependence on bromide concentration is shown whether initial or "steady-state" cycle data are used. Any analysis based upon the transfer coefficient must be based upon the apparent transfer coefficient from the initial sweep (which ranges from 0.63 to 0.60) and an approximate double layer correction. For the sake of consistency in this section, the experimentally ob-

tained "steady-state" curves for this reduction peak were the ones double layer corrected with ϕ_2 data from pure perchlorate solutions. The resulting slopes must be viewed in light of the above discussion and in light of the fact that this double layer correction is only approximate.

Graphical representations of the rate constants for the voltammetry peaks in mixed bromide-perchlorate solutions which were just discussed will now be presented. The anodic branch of rate constants in Fig. IV-21 represents the composite apparent rate constants ($k_3 + k_4'\theta_{Br}$). Two sets of cathodic branch rate constant lines are present in Fig. IV-21. The set of cathodic branch rate constant lines at less negative potentials corresponds to the apparent rate constants k_{-4}, while the set of cathodic branch rate constant lines at more negative potentials corresponds to the apparent rate constants k_{-3} in the mixed bromide-perchlorate solutions. The computer program calculated apparent rate constants from which Fig. IV-21 was constructed are presented in Figs. IV-22 to IV-24. The apparent rate constants k_3 and k_4 are represented below the anodic branch composite rate constants by the dash-dot and dashed lines, respectively. In Fig. IV-24, the dashed line for k_4 merges with the composite apparent rate constant line at more positive potentials.

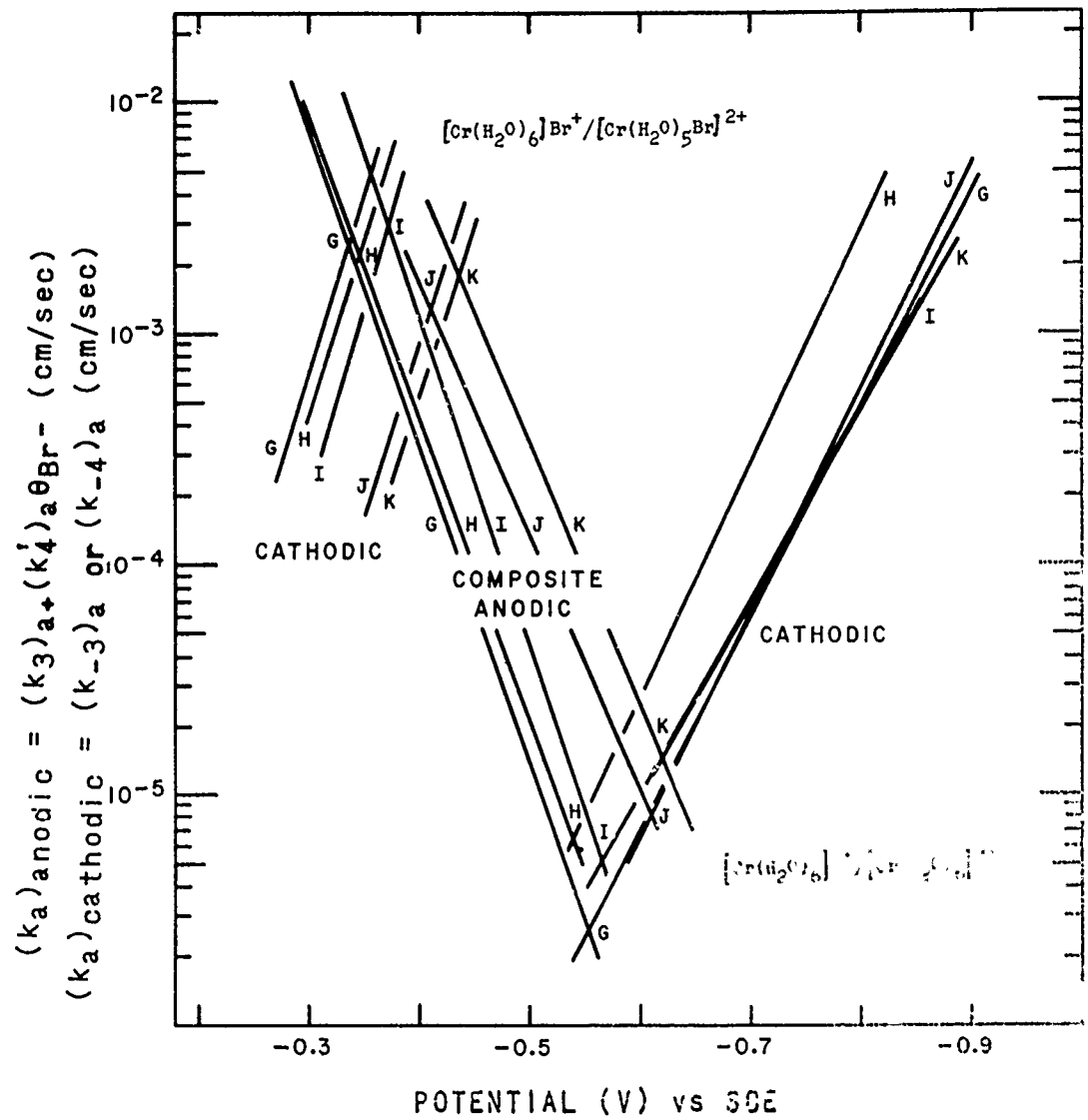

Fig. IV-21. Log of apparent rate constants vs applied potentials in mixed bromide-perchlorate solutions. $[Cr(H_2O)_6]Br^+/[Cr(H_2O)_5Br]^{2+}$ couple (upper set) and $[Cr(H_2O)_6]^{2+}/[Cr(H_2O)_6]^{3+}$ couple (lower set). T=25°C. pH = 2. Bromide concentrations were: G=3.45 mM; H = 5.64 mM; I = 0.0107 M; J = 0.0428 M; K = 0.103 M.

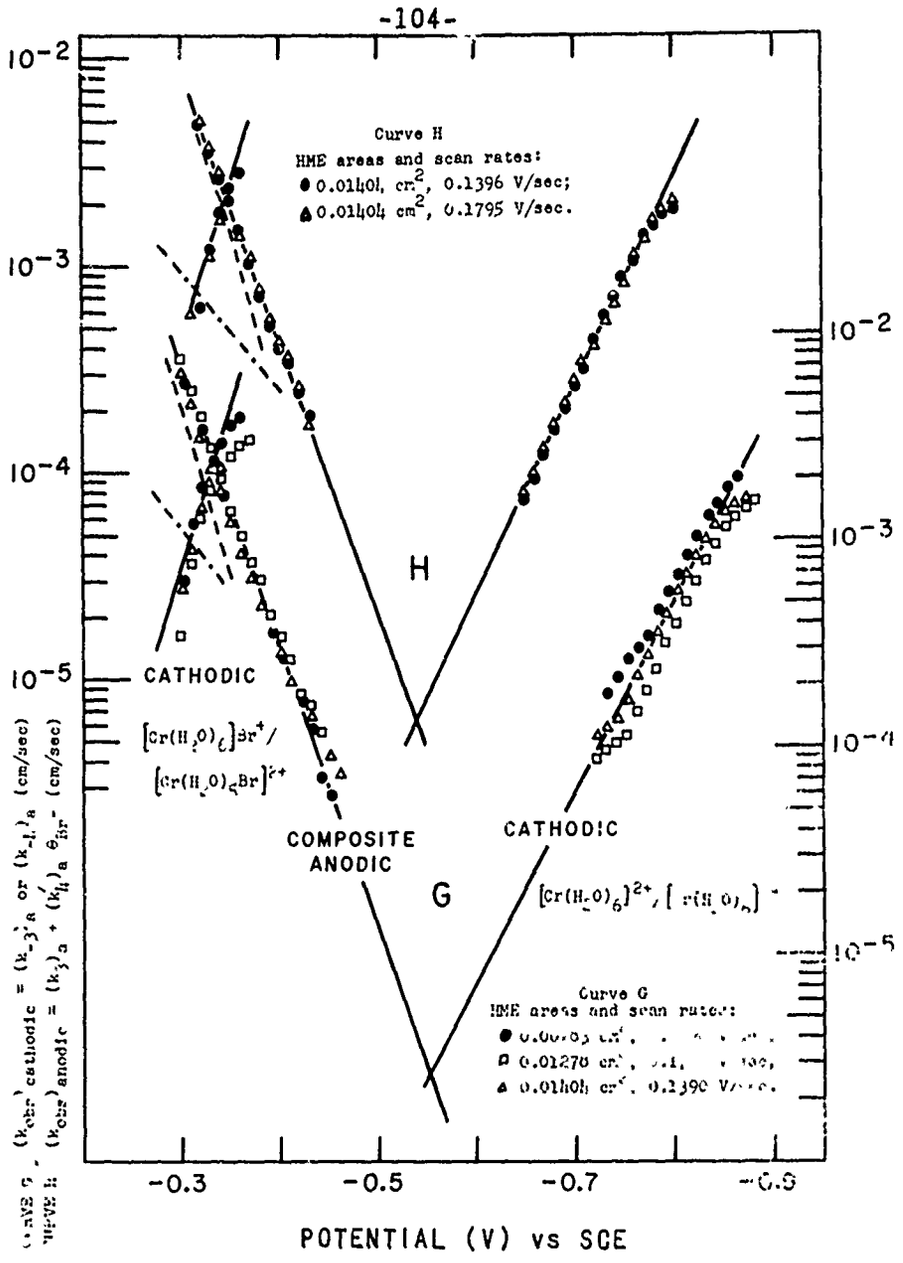

Fig. IV-22. Log of apparent rate constants vs applied potentials in mixed bromide-perchlorate solutions. $[Cr(H_2O)_6]Br^{+}/[Cr(H_2O)_5Br]^{2+}$ couple (left) and $[Cr(H_2O)_6]^{2+}/[Cr(H_2O)_6]^{3+}$ couple (right) in 0.33 M $NaClO_4$, pH = 2.13, T = 25°C, initial $[Cr(H_2O)_6](ClO_4)_3$ concentration = 2.41 mM. Curve G: NaBr = 3.45 mM. Curve H: NaBr = 5.64 mM. $(k_4)_a$ ----- ; $(k_3)_a$ ---- .

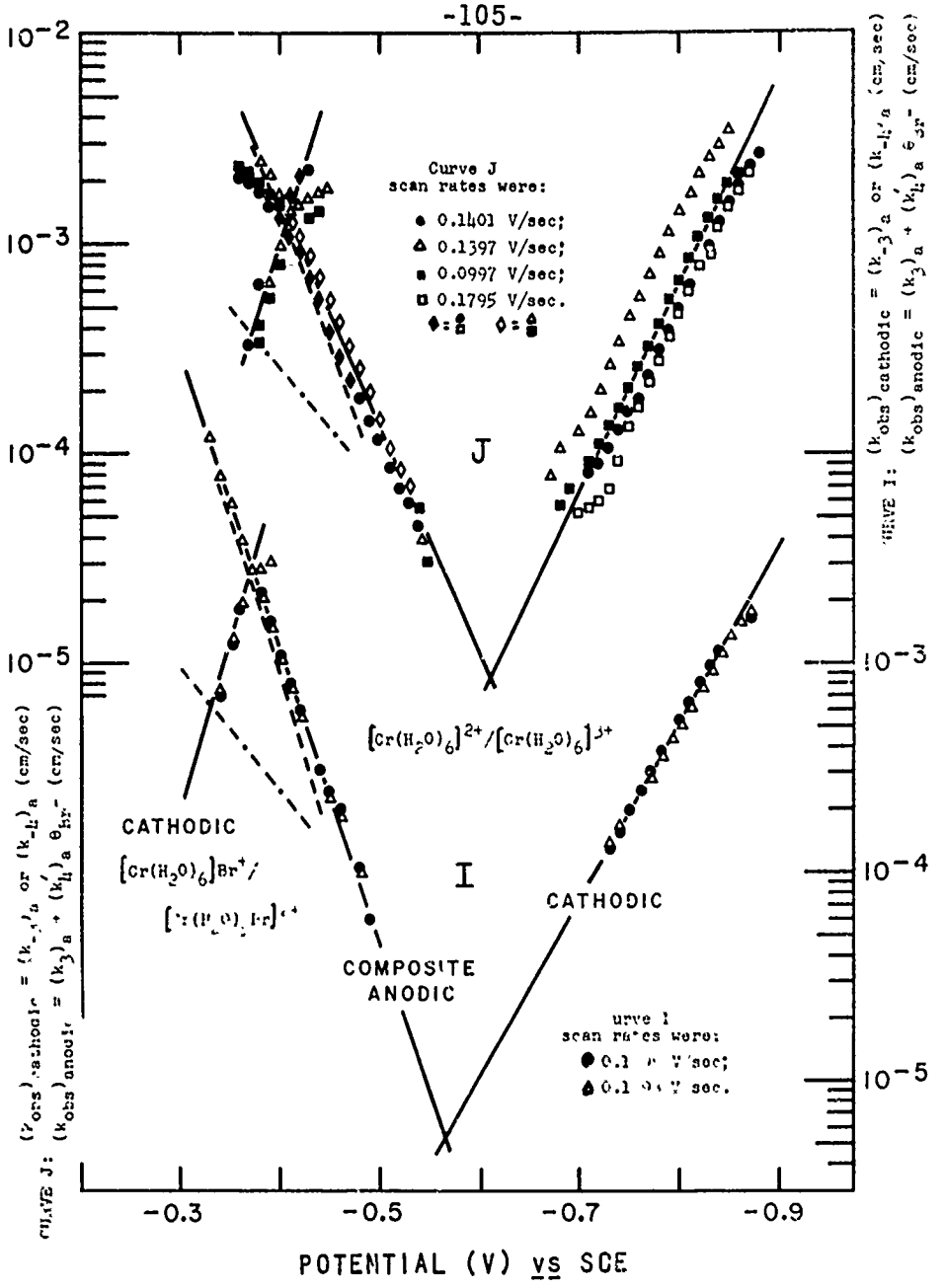

Fig. IV-23. Log of apparent rate constants vs applied potentials in mixed bromide-perchlorate solutions. $[Cr(H_2O)_6]Br^{+}/[Cr(H_2O)_5Br]^{2+}$ couple (left) and $[Cr(H_2O)_6]^{2+}/[Cr(H_2O)_6]^{3+}$ couple (right). Initial $[Cr(H_2O)_6](ClO_4)_3$ concentration = 2.41 mM. T = 25°C. Curve I: 0.316 M $NaClO_4$ and 0.0107 M NaBr, pH = 2.13, HME area = 0.01278 cm^2; Curve J: 0.28 M $NaClO_4$ and 0.0428 M NaBr, pH = 2.30, HME area = 0.0226 cm^2. $(k_4)_a$ ----- $(k_3)_a$ -.-.-.

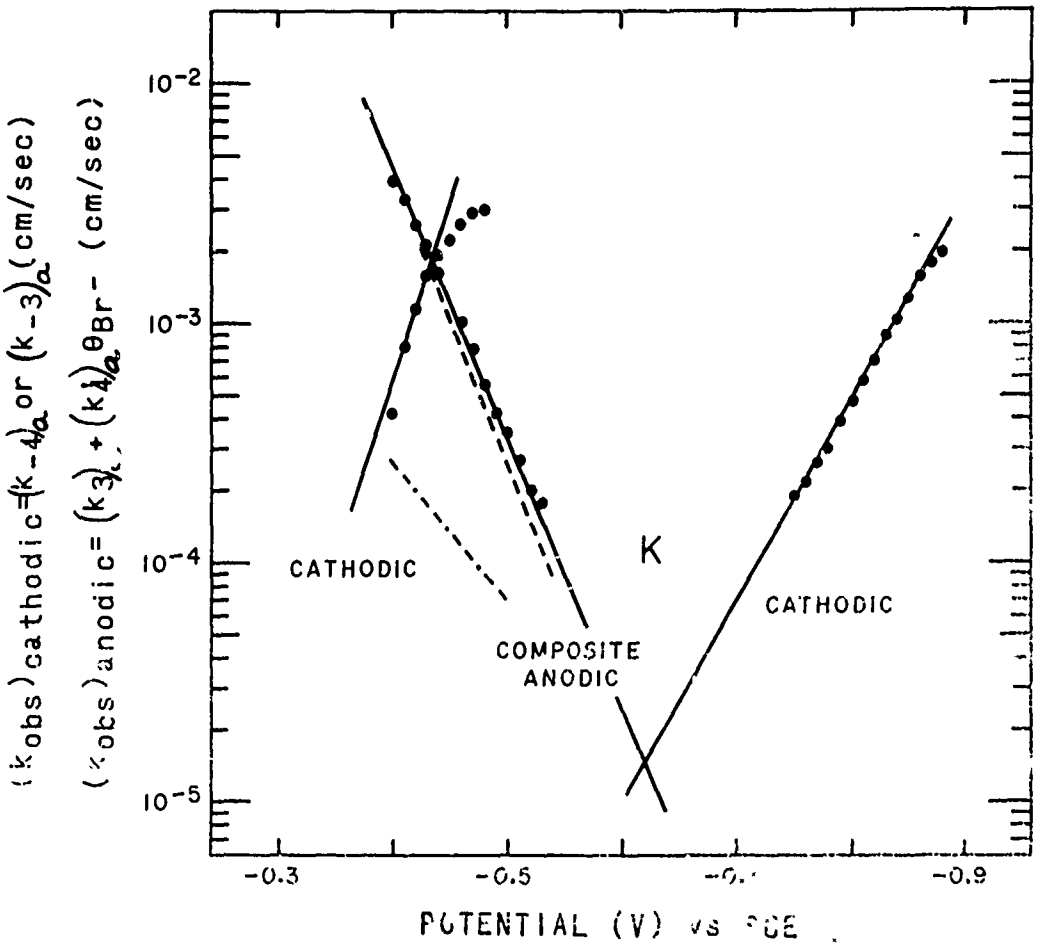

Fig. IV-24. Log of apparent rate constants vs applied potentials in a mixed bromide-perchlorate solution. $[Cr(H_2O)_6]\ Br^{+}/[Cr(H_2O)_5Br]^{2+}$ couple (left) and $[Cr(H_2O)_5Br]^{+}/[Cr(H_2O)_6]^{3+}$ couple (right). Initial $Cr(H_2O)_6(ClO_4)_3$ concentration = 3.41 mM in 0.20 M $NaClO_4$ and 0.103 M NaBr, pH = 2.30, T = 25°C, HME area = 0.01004 cm^2, scan rate = 0.1397 V/sec.
$(k_4)_a$ ---- $(k_3)_a$ -·-·-·.

The intersections of the rate constant lines of the anodic branch in Fig. IV-21 with the corresponding k_{-4} rate constant cathodic lines gave the apparent standard rate constants at the apparent standard potential $(E^o_s)_a$. These apparent standard rate constants still contained the contribution from k_3, but at high bromide concentrations this contribution was so small that these apparent standard rate constants can be interpreted as being those for the $[Cr(H_2O)_6]Br^+/[Cr(H_2O)_5Br]^{2+}$ couple. A log-log plot of the apparent rate constants for this couple vs the corresponding bromide concentrations is given in Fig. IV-25 for all of the bromide concentrations used in this work.

The intersections of the rate constant lines of the anodic branch in Fig. IV-21 with the corresponding k_{-3} rate constant cathodic lines gave the apparent standard rate constants at the apparent standard potential $(E^o_s)_a$ for the $[Cr(H_2O)_6]^{2+}/[Cr(H_2O)_6]^{3+}$ couple in the mixed bromide-perchlorate solutions. A log-log plot of the apparent rate constants for this couple vs the corresponding bromide concentrations is given in Fig. IV-28 for all of the bromide concentrations used in this work.

After k_3 and k_4 were separated from the composite apparent rate constants, and k_3, k_{-3}, k_4, and k_{-4} were each double layer corrected, Fig. IV-30 was constructed. The set of anodic and cathodic rate constant lines at less negative potentials in Fig. IV-30 corresponds to the true rate constants k_4 and k_{-4}, respectively. The one anodic rate constant line and the set of

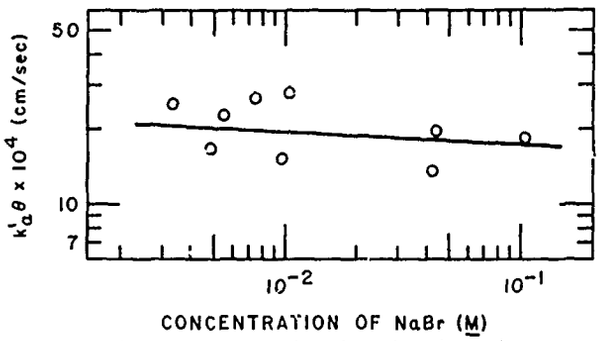

Fig. IV-25. Apparent standard rate constants for $[Cr(H_2O)_5]Br^+/[Cr(H_2O)_5Br]^{2+}$ vs NaBr concentrations in mixed bromide-perchlorate solutions at 25°C.

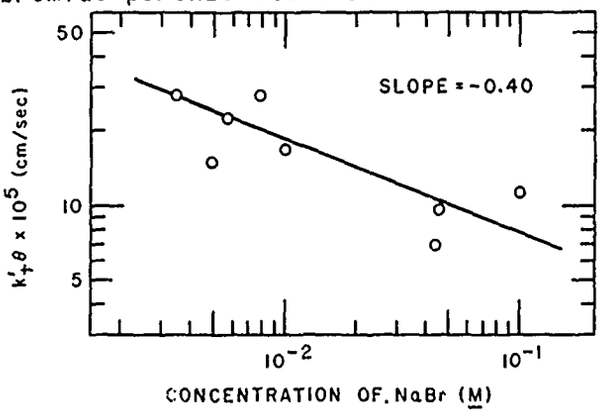

Fig. IV-26. Double layer corrected standard rate constants of Fig. IV-25.

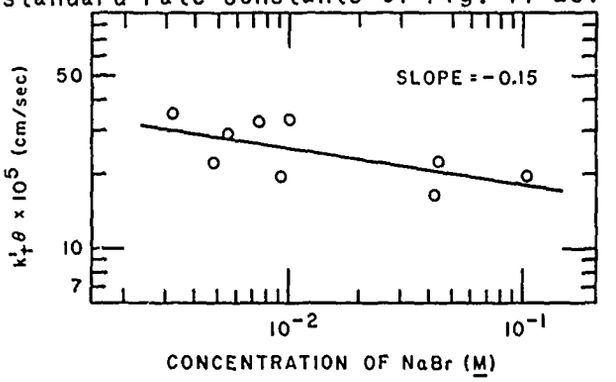

Fig. IV-27. Double layer corrected standard rate constants of Fig. IV-25. AN ADDITIONAL CORRECTION FOR THE CONCENTRATION OF $[Cr(H_2O)_5]^{2+}$ WAS MADE AS WAS DESCRIBED IN THE TEXT.

cathodic rate constant lines occurring at more negative potentials corresponds to the true rate constants k_3 and k_{-3}, respectively.

The intersections of the set of anodic and cathodic rate constant lines occurring at less negative potentials in Fig. IV-30 gave the true standard rate constants for the $[Cr(H_2O)_5]Br^+/[Cr(H_2O)_5Br]^{2+}$ couple at the standard potential $(E^o_s)_t$. A log-log plot of the standard rate constants vs the corresponding bromide concentrations for this couple is given in Fig. IV-26 for all of the bromide concentrations used in this work.

Since it was quite possible that the calculated ϕ_2 values for the mixed bromide-perchlorate solutions, particularly for very low bromide concentrations, were too large, k_4 and k_{-4} for the $[Cr(H_2O)_6]Br^+/[Cr(H_2O)_5Br]^{2+}$ couple were also double layer corrected using the potentials for a pure perchlorate supporting electrolyte. This resulted in standard rate constants that were about a factor of four larger than those obtained with the ϕ_2 data for the mixed bromide-perchlorate solutions. The same relationship between the standard rate constants at different bromide concentrations existed whether they were obtained with the ϕ_2 potentials for a pure perchlorate solution or with the ϕ_2 potentials for the mixed bromide-perchlorate solutions. The true double layer corrected rate constants undoubtedly lie between these two extremes and in all probability are closer to

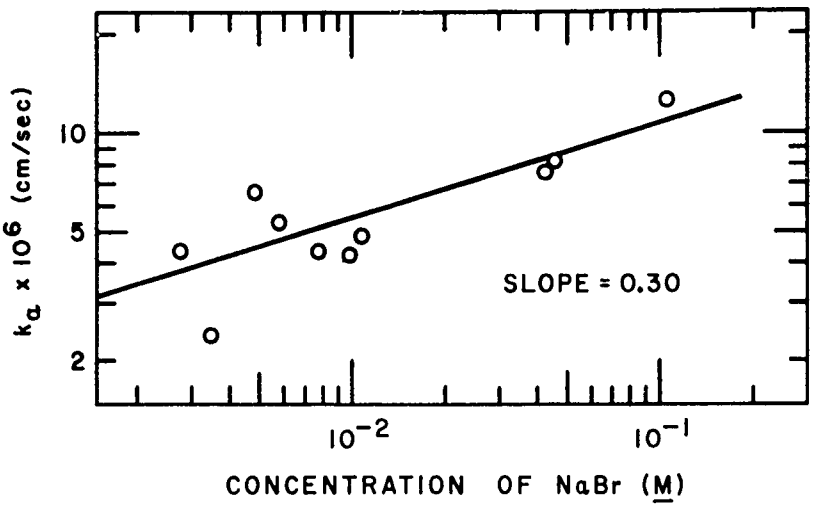

Fig. IV-28. Apparent standard rate constants for $[Cr(H_2O)_6]^{2+}/[Cr(H_2O)_6]^{3+}$ vs NaBr concentrations in mixed bromide-perchlorate solutions at 25°C.

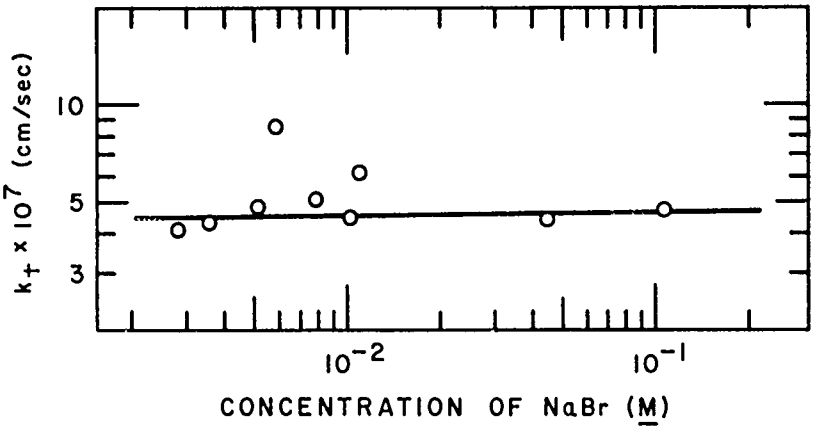

Fig. IV-29. Double layer corrected standard rate constants vs NaBr concentrations for $[Cr(H_2O)_6]^{2+}/[Cr(H_2O)_6]^{3+}$ at 25°C. (The two points far above the line were felt not to be as reliable as the others for drawing this line.)

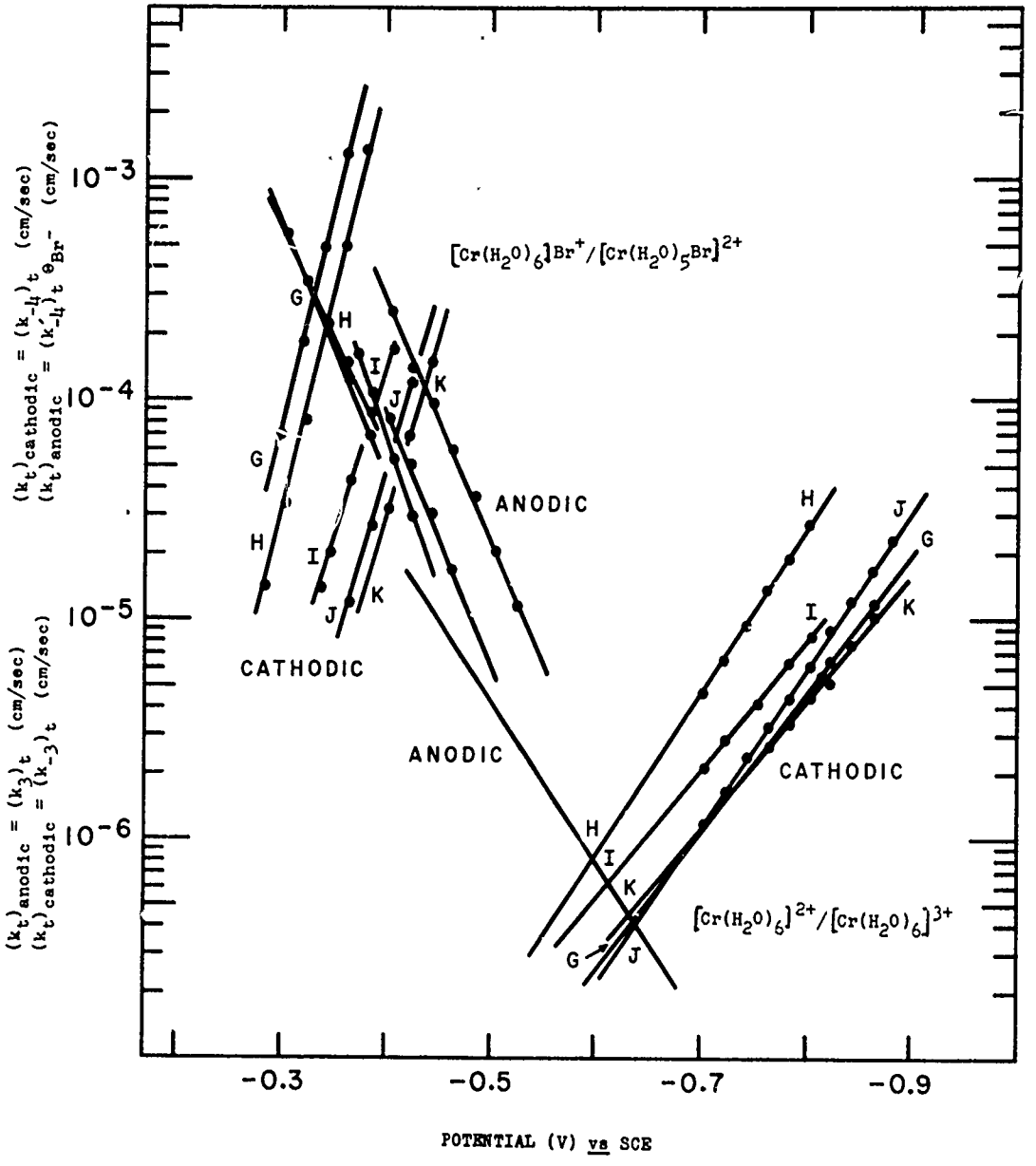

Fig. IV-30. Log of double layer corrected rate constants vs applied potentials for $[Cr(H_2O)_6]Br^+/[Cr(H_2O)_5Br]^{2+}$ (upper set) and $[Cr(H_2O)_6]^{2+}/[Cr(H_2O)_6]^{3+}$ (lower set) in mixed bromide-perchlorate solutions with the other experimental conditions the same as in Fig. IV-21.

the rate constants calculated with the ϕ_2 data for mixed bromide-perchlorate solutions than the rate constants calculated with the ϕ_2 potentials for a pure perchlorate solution.

Returning to the explanation of the figures, the intersections of the one anodic and set of cathodic rate constant lines occurring at more negative potentials in Fig. IV-30 gave the true standard rate constants for the $[Cr(H_2O)_6]^{2+}/[Cr(H_2O)_6]^{3+}$ couple at the standard potential $(E^o_s)_t$. A log-log plot of the standard rate constants vs the corresponding bromide concentrations for this couple is given in Fig. IV-29 for all of the bromide concentrations used in this work.

The decreasing standard rate constants with increasing bromide concentration in Fig. IV-26 is most strange. One of the possible reasons, besides approximate ϕ_2 data, for this unexpected behavior is the fact that in calculating the apparent rate constants k_{-4} the concentration of $[Cr(H_2O)_5Br]^{2+}$ was calculated on the assumption that all of the $[Cr(H_2O)_6]^{2+}$ oxidized in the bromide-perchlorate solutions went to $[Cr(H_2O)_5Br]^{2+}$. This assumption is far more valid at higher bromide concentrations than at lower bromide concentrations as a comparison of k_3 with the composite apparent rate constants in Figs. IV-22 to 24 will show. A correction to the calculated $[Cr(H_2O)_5Br]^{2+}$ concentrations was made by comparing the composite apparent rate constants to the apparent rate constants k_3. The average differ-

ence between these rate constants over the potential range of importance was used as the factor by which to correct the $[Cr(H_2O)_5Br]^{2+}$ concentrations. This corrected concentration was then used with Eqs. (II-5) and (II-6) to calculate new values for the apparent rate constants. These were double layer corrected as before and the results are shown in Fig. IV-27, which is a log-log plot of standard rate constants vs NaBr concentrations.

This corrective procedure could have been refined in the following manner. Once a new set of apparent rate constants was obtained, the net current could be divided into its component contributions and a new average value found by which to correct the $[Cr(H_2O)_5Br]^{2+}$ concentrations. This re-iterative procedure could be repeated until a corrected value was converged upon.

Table IV-2 contains transfer coefficients and standard potentials corresponding to various bromide concentrations for the $[Cr(H_2O)_6]^{2+}/[Cr(H_2O)_6]^{3+}$ couple and the $[Cr(H_2O)_6]Br^{+}/[Cr(H_2O)_5Br]^{2+}$ couple in the mixed bromide-perchlorate solutions. Due to the lack of double layer data, β_t in the mixed bromide-perchlorate solutions was taken to be equal to β_t in the pure perchlorate solution for the $[Cr(H_2O)_6]^{2+}/[Cr(H_2O)_6]^{3+}$ couple. For this couple Table IV-2 shows that the transfer coefficients are not complementary. The major cause of this is probably the inability to calculate α_t and β_t correctly in the mixed electrolyte. For the $[Cr(H_2O)_6]Br^{+}/[Cr(H_2O)_5Br]^{2+}$ couple, the Tafel

TABLE IV-2. Transfer Coefficients and Standard Potentials for $[Cr(H_2O)_6]^{2+}/[Cr(H_2O)_6]^{3+}$ and $[Cr(H_2O)_6]Br^{+}/[Cr(H_2O)_5Br]^{2+}$ Couples in Mixed Bromide-Perchlorate Solution
T = 25°C, pH $\sim$ 2.2

— $[Cr(H_2O)_6]^{2+}/[Cr(H_2O)_6]^{3+}$ —				$[Cr(H_2O)_6]Br^{+}/[Cr(H_2O)_5Br]^{2+}$						Bromide
α_t	β_t	$-(E^o_s)_a$	$-(E^o_s)_t$	$(k_{-4})_a$	$(k_4)_a$	$(k_{-4})_t$	$(k_4)_t$	$-(E^o_s)_a$	$-(E^o_s)_t$	10^{-3} M
	in V vs SCE			in mV/decade				in V vs SCE		
.38	(0.43)	0.552	0.636	63	54	52	88	0.333	0.328	3.45
.38	(0.43)	0.598	0.634	69	8.9	45	.92	0.343	0.336	4.91
.43	(0.43)	0.542	0.598	72	60	51	94	0.347	0.330	5.64
.40	(0.43)	0.564	0.628	72	71	55	109	0.349	0.354	7.73
.41	(0.43)	0.616	0.636	75	70	50	128	0.374	0.368	9.82
.34	(0.43)	0.566	0.609	59	73	64	76	0.371	0.387	10.7
.41	(0.43)	0.573	0.638	.71	67	59	89	0.410	0.403	42.8
-	(0.43)	0.573	--	--	--	--	--	0.389	--	45.0
.31	(0.43)	0.620	0.628	.68	83	63	89	0.434	0.433	103.0

slope/decade for the apparent rate constants showed that the limit of this experimental method with respect to reversibility was approached. The Tafel slope/decade for the double layer corrected rate constants shows that the Tafel slope has decreased for the anodic branch and is not near to the reversible behavior. The discussion which will be presented in Chapter V concerning the limitations of these double layer corrections will show that the double layer corrections in Table IV-2 are more severe than they should be. As with the chloride-perchlorate solutions, the standard potentials are dependent upon the halogen concentration and shift in a direction and with the magnitude predicted by the Nernst equation.

One additional item needs to be considered: the identity of the new cathodic peak. To provide the identity of the new cathodic peak which was believed to be the reduction of $[Cr(H_2O)_5Br]^{2+}$ and which appeared at potentials very positive to the $[Cr(H_2O)_6]^{3+}$ reduction peak, the cyclic voltammetry of $[Cr(H_2O)_5Br]^{2+}$ was studied in an acidic perchlorate supporting electrolyte. The cyclic voltammetry curve of this species is given in Fig. IV-31. The cathodic peak of $[Cr(H_2O)_5Br]^{2+}$ agreed well with the new cathodic peak in the mixed bromide-perchlorate supporting electrolytes. The apparent rate constants for the cyclic voltammetry of $[Cr(H_2O)_5Br]^{2+}$ was obtained with the computer program in Appendix II. A semi-log plot of the

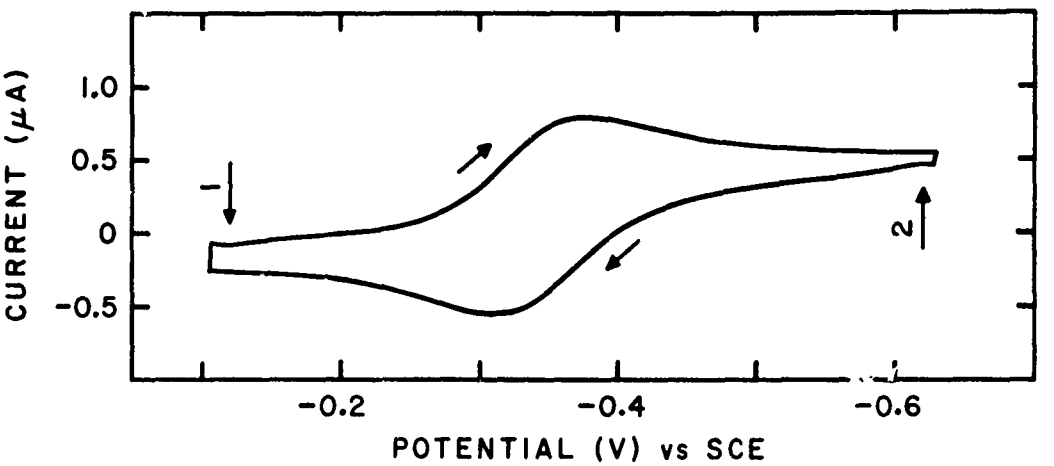

Fig. IV-31. Cyclic voltammetry of $[Cr(H_2O)_5Br]^{2+}$. Initial concentration of $[Cr(H_2O)_5Br]Br_2$ = 1.89 mM in 0.33 M $NaClO_4$, scan rate = 0.0230 V/sec, T = 25°C, pH = 2.13, HME area = 0.01077 cm^2. $\xrightarrow{1}$ = pseudo zero time (1), $\xrightarrow{2}$ = pseudo zero time 2.

apparent rate constants vs applied potential is given in Fig. IV-32. The best straight line through these apparent rate constants was double layer corrected with ϕ_2 potentials for a pure perchlorate solution. A semi-log plot of the true rate constants vs applied potential is given in Fig. IV-33. These figures show that the Tafel slopes/decade from the apparent rate constants are 66 mV for the cathodic branch and 72 mV for the anodic. For the double layer corrected rate constants, the cathodic Tafel slope/decade is 68 mV and for the anodic 80 mV.

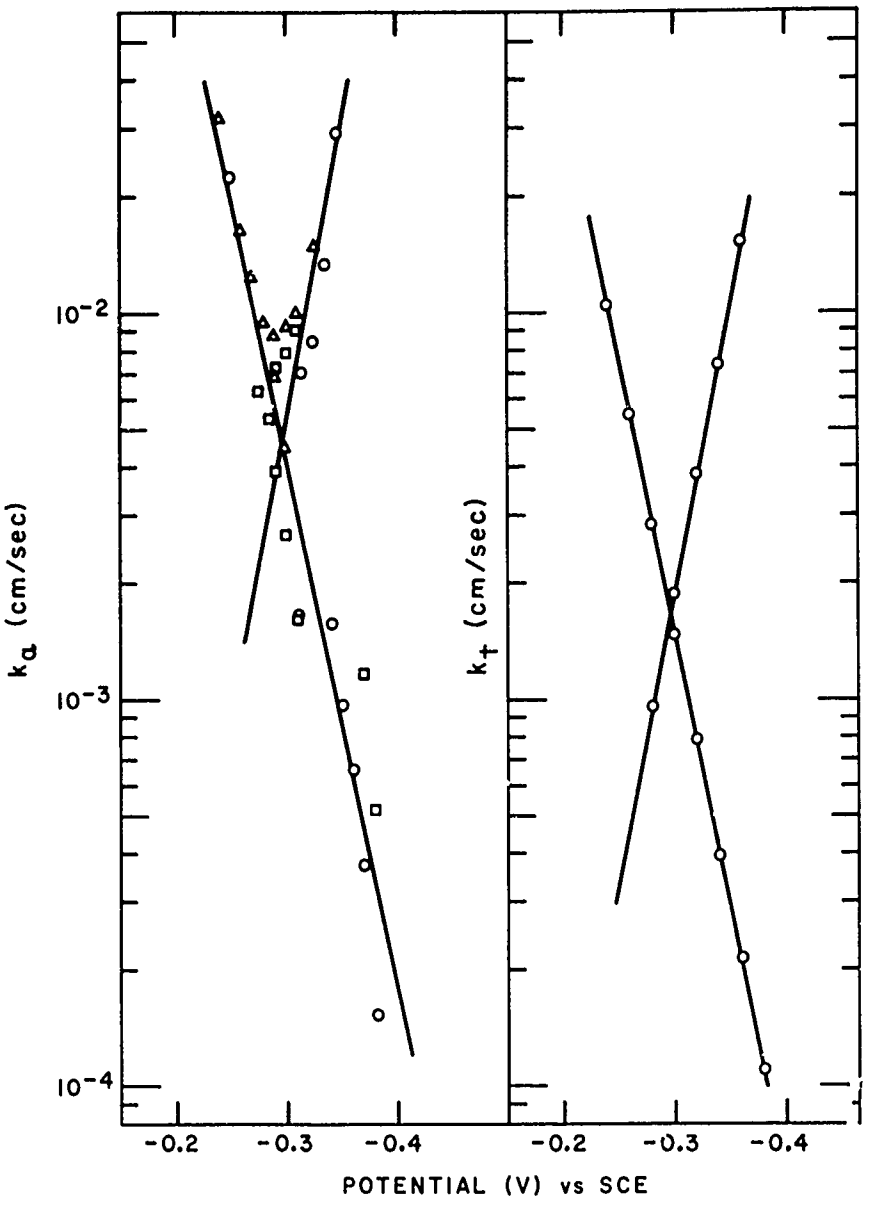

Fig. IV-32. (left) Log of apparent rate constants vs applied potentials for $[Cr(H_2O)_6]Br^{+}/[Cr(H_2O)_5Br]^{2+}$. Initial concentration of $[Cr(H_2O)_5Br]^{2+}$=1.89 mM in 0.33 M $NaClO_4$, pH=2.13, T=25°C. HME area = 0.01077 cm^2 with the following scan rates: o = 0.0944 V/sec; Δ = 0.2622 V/sec; □ = 0.1572 V/sec.

Fig. IV-33. (right) Log of the double layer corrected rate constants shown in Fig. IV-32

CHAPTER V

INTERPRETATION OF EXPERIMENTAL DATA

The $[Cr(H_2O)_6]^{2+}/[Cr(H_2O)_6]^{3+}$ Couple in Pure Perchlorate Solutions

Interaction of Reactants

When mechanisms for reactions are discussed, consideration must be given to the statistical distribution of activation states which exist. Two important aspects for the activation states are their actual structures and the distance of the chromium metal ion from the mercury electrode surface. Each of these aspects will be considered.

Current theories[58-61] of radiationless electron transfer agree that the most probable activation state will have an atomic configuration and solvation which is a compromise between that for the reactant and that for the product. The $[Cr(H_2O)_6]^{3+}$ complex has an octahedral configuration while the $[Cr(H_2O)_6]^{2+}$ complex has a distorted octahedral configuration. The most probable activation state for the $[Cr(H_2O)_6]^{2+}/[Cr(H_2O)_6]^{3+}$ couple will be a distorted octahedral configuration. This configuration will not be as distorted as that for $[Cr(H_2O)_6]^{2+}$. For ease of pictorial representation, the chromium activation states will be drawn with octahedral symmetry.

Both the homogeneous and electrochemical hexaaquochromium (II)/(III) reaction will be discussed in this chapter. For a

homogeneous reaction involving weak interaction between the reactants (< a few hundred cal/mole), Marcus' expression for calculating[58,62] the total free energy of activation ΔF^* is

$$\Delta F^* = \Delta F_c^{\ddagger} + \Delta F_i^{\ddagger} + \Delta F_o^{\ddagger} + \Delta F_e^{\ddagger} \qquad (V\text{-}1)$$

where $\Delta F_c^{\ddagger}$ is the free energy change due to coulombic interaction of reactants at the most probable separation distance R_m in the activated complex, $\Delta F_o^{\ddagger}$ is the rearrangement free energy of the outer-sphere solvent and ion atmosphere, $\Delta F_i^{\ddagger}$ is the rearrangement free energy of the inner-sphere ligands, and $\Delta F_e^{\ddagger}$ is the energy change due to a change of electronic quantum numbers when electron transfer occurs. This general equation can be written more explicitly for a homogeneous weak interaction reaction as

$$\Delta F_H^{\ddagger} = \Delta F_c^{\ddagger} + m^2(\lambda)_H \qquad (V\text{-}2a)$$

where $-(2m+1)(\lambda)_H = \Delta F^o + w^p - w^r = \Delta F^o$; m is a Lagrangian multiplier in the theory and is -0.5 for symmetrical homogeneous reactions when the overall change in free energy ΔF^o is zero; λ_H is the sum of the reorganizational energies for the outer-sphere $(\lambda_o)_H$ and the inner-sphere $(\lambda_i)_H$; and w^r or w^p is the work required to bring the reactant or the products to the most probable charge transfer distance R_m. Furthermore, $\Delta F_o^{\ddagger} = m^2(\lambda_o)_H$ and $\Delta F_i^{\ddagger} = m^2(\lambda_i)_H$.

For a weak interaction electrode process, the free energy of activation is

$$\Delta F_E^* = w^r + m^2(\lambda)_H/2 \qquad \text{(V-2b)}$$

where $-(2m+1)(\lambda)_H/2 = ne(E-E_o) + w^p - w^r$; w^p and w^r are the work terms required to bring the product or the reactant to the most probable interaction distance of R_e, E is the actual electrode potential and E_o is the standard electrode potential. For $(E-E_o) = 0$, $m = -0.5$. As with the homogeneous case, $(\lambda)_H = (\lambda_o)_H + (\lambda_i)_H$.

More explicit functions for obtaining the work and reorganizational functions will be given and used later. An important point to note here is that the reorganizational energies for the electrochemical process are predicted to be half of those for the homogeneous process to a good approximation. This prediction will be examined in detail further on in this discussion. It should be noted that a double layer correction has been built into the free energy expression for the electrochemical process. The derivation for these equations is given elsewhere.[58]

Of particular importance are the values for R_m and R_e which are contained in the reorganizational terms λ. Levich gives[60] an explicit equation for the calculation of the most probable distance R_m for a homogeneous reaction which is a function of the size and charge of the ions and their interaction with the dielectric medium.

$$R_m = [(e^2/2kt)((C/4) - n_1n_2)(bD_{ef}/Z_{ef})]^{1/2} \qquad \text{(V-3)}$$

where e = charge of electron, n_1,n_2 = valence of ions in reaction, k = Boltzmann constant, T = temperature in degrees Kelvin, C = $(1/\varepsilon_0 - 1/D)$ where ε_0 = square of refractive index and D = bulk dielectric constant, b = radius of first Bohr orbit of hydrogen, D_{ef} = effective dielectric constant at the most probable charge transfer distance of R_m, and Z_{ef} = effective atomic number. For homogeneous redox reactions when $n_1 = 2$ and $n_2 = 3$, R_m has a value of about 7 Å.

In contrast to Levich, Marcus[58] sets $R_m = 2a$, where a is the ionic radius of the central metal ion plus the diameter of its inner coordination shell. For R_m, Marcus would obtain a value of about 7.0 Å for the $[Cr(H_2O)_6]^{2+}/[Cr(H_2O)_6]^{3+}$ couple. This is in good agreement with Levich's value, mostly by accident. The value of a was obtained from the average radii of unhydrated Cr^{2+} and Cr^{3+}, 0.74 Å[61] and the diameter of a water molecule, 2.76 Å.[63]

For the most probable distance of closest approach R_e for the electrochemical reaction, neither Marcus nor Levich have solved their own theoretically complicated expressions for R_e. Levich has identified R_e with the outer Helmholtz plane[64] and Marcus represents R_e as (2a+2c)/2 where a is the ionic radius of the central metal ion plus the diameter of its inner coordination shell, and c is the thickness of whatever species is covering the electrode surface. For the present situation, water molecules are covering the electrode surface. If the effective diameter of

a water molecule on the electrode surface is taken as 2.76 Å and (2a) = 7.0 Å, then R_e = 6.3 Å. This is in agreement with the value for R_e obtained by identifying R_e with the outer Helmholtz plane as was suggested by Levich. The fact that neither Marcus nor Levich has obtained theoretical values for R_e is unfortunate, since such values are important in interpreting the behavior of the system. Even if Marcus or Levich had evaluated R_e theoretically, the values would be questionable since the theories of both men employed a dielectric continuum model for the solvent. A discrete particle model for the solvent is necessary when R_m or R_e approach the dimensions of the water molecule.

One approach for determining whether a weak interaction is operative for the hexaaquochromium(II)/(III) couple is to compare the experimentally obtained standard rate constants or free energies of activation with those which would be predicted by theory for a weak interaction process. The theoretical ΔF_H^* value and then the theoretical ΔF_E^* value for the hexaaquochromium(II)/(III) couple will be calculated with Marcus' weak interaction theory for homogeneous and heterogeneous reactions and respectively compared with the experimentally obtained values. The ratio of the experimentally obtained free energies $\Delta F_E^*/\Delta F_H^*$ also will be compared to the ratio of the theoretically obtained outer-sphere rearrangement free energies $(\lambda_o)_E/(\lambda_o)_H$.

First the homogeneous hexaaquochromium(II)-(III) exchange will be considered. The terms in Eq. (V-1) will be calculated.[58,65]

$$\Delta F_c^{\ddagger} = \frac{w_r + w_p}{2} = \frac{Z_1 Z_2 e^2}{DR_m} \exp[-R_m(\frac{8\pi e^2 N_o \mu}{1000DkT})^{1/2}] \qquad (V\text{-}4a)$$

where Z_1 and Z_2 are the valencies of the reacting species, N_o is Avogadro's number, μ is the ionic strength of the electrolyte, and the other terms have been previously defined. When the dielectric constant is taken as 78.5 at 25°C, Eq. (V-4a) may be simplified to

$$\Delta F_c^{\ddagger} = \frac{4.22 Z_1 Z_2}{R_m} 10^{-0.143 R_m \sqrt{\mu}} \text{ kcal/mole} \qquad (V\text{-}4b)$$

when R_m is expressed in Angstroms. For a solution of ionic strength 1.0, $\Delta F_c^{\ddagger}$ is 0.36 kcal/mole when $Z_1 = 2$, $Z_2 = 3$, and $R_m = 7$ Å.

The internal free energy of rearrangement, as expressed by Marcus, is[58,66]

$$F_i^{\ddagger} = \frac{n f_1 f_2 (r_1 - r_2)^2}{2(f_1 + f_2)} \text{ ergs/molecule} \qquad (V\text{-}5)$$

where n = number of ligands = 6, r_1 and r_2 are the equilibrium distances for the M-OH$_2$ bonds of each reactant and f_1 and f_2 are their force constants. This equation considers only the symmetrical vibrational modes. To the best of this author's knowledge, experimental force constants are not available for $[Cr(H_2O)_6]^{2+}$ and $[Cr(H_2O)_6]^{3+}$. Sutin[67] calculated theoretical force constants for the hexaaquoiron(II)/(III) couple with a classical potential

energy function and then used these values in Eq. (V-5) with the proper r values for chromium for determining $\Delta F_i^{\ddagger}$. Sutin's values for f_1 and f_2 were 1.49×10^5 and 4.16×10^5 dynes/cm and the difference between r_1 and r_2 was estimated as 1.8×10^{-9} Å, which is in agreement with those r values reported by Sacher and Laidler.[61] Sutin's value for $\Delta F_i^{\ddagger}$ for the hexaaquochromium(II)/(III) couple was 15.1 kcal/mole, but substitution of the given values into Eq. (V-5) yields $\Delta F_i^{\ddagger}$ = 15.6 kcal/mole. The latter value will be used in this discussion.

The free energy of outer-sphere rearrangement is given by Marcus as[58,68]

$$\Delta F_o^{\ddagger} = m^2\lambda_o = m^2(\Delta Z)^2e^2\left[\frac{1}{2r_1^{\ddagger}} + \frac{1}{2r_2^{\ddagger}} - \frac{1}{R_m}\right]\left[\frac{1}{D_o} - \frac{1}{D}\right] \qquad \text{(V-6a)}$$

where D_o is the optical dielectric constant or square of the refractive index. If $r_1^{\ddagger}$ and $r_2^{\ddagger}$, which are the radii of the reactants in the activated complex, are assumed to sum to R_m, and if D is taken as 78.5, D_o as 1.8, and m = -0.5, the Eq. (V-6a) can be simplified to

$$\Delta F_o^{\ddagger} = \frac{22.7(\Delta Z)^2}{r_1^{\ddagger}} \text{ kcal/mole} \qquad \text{(V-6b)}$$

where r_1 is again expressed in Angstroms. For a (ΔZ) of 1 and an $r_1^{\ddagger}$ of 3.5 Å, $\Delta F_o^{\ddagger}$ = 6.48 kcal/mole.

The quantity $\Delta F_e^{\ddagger}$ in Eq. (V-1) can be approximated as zero since the equation is being applied to an exchange process. Thus

for the homogeneous electron transfer reaction of hexaaquochromium(II)-(III), the total free energy of activation ΔF_H^* at 25°C and in a solution of ionic strength 1.0 is (0.36) + (15.6) + (6.48) = 22.4 kcal/mole.

Experimentally, the rate constant[11] for this homogeneous reaction in a 1.0 $\underline{M}$ $HClO_4$ solution at 24.5°C is 1.22×10^{-4} $\underline{M}^{-1}sec^{-1}$ with an activation energy of 22 ± 2 kcal/mole. From the data in reference 11, Sacher and Laidler[61] calculated a ΔF_H^* of > 24.3 kcal/mole and Reynolds and Lumry[69] calculated a ΔF_H^* of 24.4 kcal/mole. The accuracy of these ΔF_H^* values must be considered to be not better than ± 2 kcal/mole. The experimental free energy of activation is in good agreement with the theoretical ΔF_H^* of 22.4 kcal/mole.

Sacher and Laidler (S&L)[61] have proposed a somewhat modified model for calculating the ΔF_H^* of a weak interaction homogeneous reaction. The (S&L) approach will not be discussed here in detail, but a comparison between the (S&L) and Marcus approach will be given, since these approaches differ in their view of the weak interaction charge transfer for homogeneous reactions. Whereas Marcus says little about the actual charge transfer and takes the transmission coefficient κ to be of the order of unity, the (S&L) treatment assumes the charge transfer to occur by tunnelling with κ being small compared to unity.

In the (S&L) model, the total ΔF_H^* is comprised of three terms: a free energy of electrostatic interaction, a free energy of inner- and outer-sphere rearrangement, and a free energy of tunnelling. Each term will be discussed and compared with the corresponding Marcus term. The electrostatic free energy term was calculated in much the same way as was Marcus' with two differences: the effect of the ionic strength of the supporting electrolyte was not considered, but the change in dielectric constant with distance from the central metal ion was. Marcus did not consider the change in dielectric constant with distance, but did consider the attenuation of the electrostatic interaction by the presence of a supporting electrolyte. At a separation distance of 7 Å and in a supporting electrolyte of ionic strength 0.35, Marcus' electrostatic free energy term was 0.92 kcal/mole, while (S&L) gave a value of 2.6 kcal/mole.

For calculating the inner- and outer-sphere reorganizational energies, Marcus assumed that each process was independent of the other. This assumption was also made by (S&L). They calculated a total reorganizational energy using equations similar in principle to Marcus' equations. For a separation distance R_m of 7 Å, the (S&L) value for the total reorganizational free energy was 13.6 kcal/mole, while Marcus' value was 22.1 kcal/mole.

The question of tunnelling is the significant difference between the Marcus and the (S&L) approach. One consequence of (S&L) assuming tunneling is that the most probable interaction dis-

tance for electron transfer is made smaller than 7 Å and is about 4 to 4.5 Å. Such short interaction distances do have precedence with the reactions of some transition metal oxides. At a separation distance of 7 Å, the tunnelling free energy, ΔF^{*}_{tun}, with a rectangular barrier was 11 kcal/mole for the hexaaquoiron(II)/(III) system.

At a separation distance R_m of 7 Å, the (S&L) treatment gave an electrostatic free energy of 2.6 kcal/mole, a total reorganizational free energy of 13.6 kcal/mole and a tunnelling free energy (assuming a rectangular barrier) of 11 kcal/mole. Thus ΔF^{*}_{H} according to (S&L) is 27.2 kcal/mole. At the separation distance R_m of about 4.5 Å, (S&L) calculated a $\Delta F^{\ddagger}_{c}$ = 4.8, a $\Delta F^{\ddagger}_{reorg}$ = 13.6 and a $\Delta F^{\ddagger}_{tun}$ = 4.8, giving a ΔF^{*}_{H} of 23.2 kcal/mole. Here also the $\Delta F^{\ddagger}_{tun}$ is for the hexaaquoiron(II)/(III) system. The experimentally observed ΔF^{*}_{H} was about 24 kcal/mole for hexaaquochromium (II)-(III).

A theoretical ΔF^{*}_{E} of activation for the electrochemical hexaaquochromium(II)/(III) couple will now be calculated from Marcus' weak interaction theory and compared to an experimental ΔF^{*}_{E} value. When $(neE-neE_o) = 0$, Marcus represents the relationship between ΔF^{*}_{E} and the electrostatic and reorganizational parameters as[58]

$$\Delta F^{*}_{E} = \frac{w^{r}+w^{p}}{2} + \frac{(\lambda_i)_E+(\lambda_o)_E}{4} + \frac{(w^{p}-w^{r})^2}{4[(\lambda_1)_E+(\lambda_o)_E]} \qquad (V\text{-}7)$$

For an electrochemical process, w^r and w^p can be obtained as follows. Let w^r be the work required to bring $[Cr(H_2O)_6]^{2+}$ to the

electrode surface and w^p be the work required to bring $[Cr(H_2O)_6]^{3+}$ to the electrode surface. Each of these work terms[70] is equal to $Z_i e\emptyset_2$, the energy difference between the bulk of the solution and the outer Helmholtz plane where the reaction has been assumed to occur. At this couple's standard potential of -0.65 V vs SCE, $\emptyset_2$+ -38 mV for a 0.33 M $NaClO_4$ supporting electrolyte. Thus w^r = -1.8 kcal/mole and w^p = -2.6 kcal/mole.

In accord with Marcus, the reorganizational terms, $(\lambda_i)_E$ and $(\lambda_o)_E$, will be assumed half of what they were for the homogeneous process. This is true when R_m is large or when R_m is small with no specific interactions.[58] The calculations of the reorganizational terms for the electrode process are as follows.

For the homogeneous inner-sphere reorganization,

$$\Delta F_i^{\ddagger} = m^2(\lambda_i)_H = 15.6 \text{ kcal/mole} \qquad \text{(V-8)}$$

With m = -0.5, $(\lambda_i)_H$ = 62.4 kcal/mole. Thus $(\lambda_i)_E$ for the electrochemical process is equal to 31.2 kcal/mole. For the homogeneous outer-sphere reorganization,

$$\Delta F_o^{\ddagger} = m^2(\lambda_o)_H = 6.48 \text{ kcal/mole} \qquad \text{(V-9)}$$

With m = -0.5, $(\lambda_o)_H$ = 25.92 kcal/mole. Thus $(\lambda_D)_E$ for the electrochemical process is equal to 12.96 kcal/mole. Substituting these values and the ones for w^r and w^p into Eq. (V-7), ΔF_E^* = 8.8 kcal/mole.

This theoretical ΔF_E^* must now be compared to an experimental ΔF_E^*. The following simple equation which Marcus[58] uses for converting ΔF^* to rate constants can be used in reverse for calculating a ΔF_E^* from the experimentally observed apparent rate constant in this work at 25°C.

$$k = \kappa Z \exp(-\Delta F^*/RT) \qquad \text{(V-10)}$$

where k is the rate constant, κ is a transmission coefficient, and Z is a frequency factor. Here κ is taken as unity. For a homogeneous process, $Z \sim 2.5 \times 10^{11}$ $\underline{M}^{-1}sec^{-1}$ and for an electrochemical process, $Z \sim 5 \times 10^4$ cm/sec. The experimentally observed apparent standard heterogeneous rate constant is 1.1×10^{-5} cm/sec, which at 25°C yields a ΔF_E^* of 13.2 kcal/mole. Parsons and Passeron[24] calculated an experimental ΔF_E^* of about 12 kcal/mole for this reaction at 25°C in 0.5 $\underline{M}$ $NaClO_4$ at a pH of 3.4 by assuming no entropy effects. These experimental ΔF_E^* values are to be compared with the theoretical value of 8.8 kcal/mole.

Alternatively an experimental ΔF_E^* calculated from the experimental double layer corrected standard rate constant can be compared with a corresponding theoretical value[24]

$$\Delta F_E^* = \frac{(\lambda_i)_E + (\lambda_o)_E}{4} \text{ kcal/mole} \qquad \text{(V-11)}$$

The experimental value is 15.1 kcal/mole from a double layer corrected standard rate constant of 4.0×10^{-7} cm/sec, while the theoretical ΔF_E^* value is 11.0 kcal/mole. The discrepancy between

the theoretical ΔF_E^* calculated with Eq. (V-7) and the appropriate ΔF_E^* experimentally determined is the same as the discrepancy between the theoretical ΔF_E^* calculated with Eq. (V-11) and the appropriate ΔF_E^* experimentally determined. The comparison between theory and experiment is considerably less favorable for the electrode process than for the homogeneous process.

A further interesting comparison between experiment and theory can be made for the relationship between the experimentally obtained ratio of $\Delta F_E^*/\Delta F_H^*$ and the theoretically predicted ratio of $(\lambda_o)_E/(\lambda_o)_H$ which is proportional to the theoretically predicted $\Delta F_E^*/\Delta F_H^*$ ratio. The last part of this statement is contingent on the work terms being small compared to the reorganizational terms, which they are, and the $(\lambda_i)_E$ and $(\lambda_i)_H$ terms having the same relationship to each other as do the $(\lambda_o)_E$ and $(\lambda_o)_H$ terms. Marcus states that such a relationship does exist.[58]

The theoretically predicted $(\lambda_o)_E/(\lambda_o)_H$ will be compared to the experimentally observed $\Delta F_E^*/\Delta F_H^*$. For the calculation of the theoretical $(\lambda_o)_E/(\lambda_o)_H$ the following equations are presented.

$$m^2(\lambda_o)_H = m^2(ne)^2\left[\frac{1}{2r_1^{\ddagger}} + \frac{1}{2r_2^{\ddagger}} - \frac{1}{R_m}\right]\left[\frac{1}{D_o} - \frac{1}{D}\right] \qquad \text{(V-6a)}$$

$$m^2(\lambda_o)_E = \frac{m^2(ne)^2}{2}\left[\frac{1}{r_1^{\ddagger}} - \frac{1}{R_e}\right]\left[\frac{1}{D_o} - \frac{1}{D}\right] \qquad \text{(V-12)}$$

where $r_i^{\ddagger}$ are the radii of the reactants in the activated complex and R_m and R_e are the most probable distances of interaction.

From these two equations,

$$\frac{(\lambda_o)_E}{(\lambda_o)_H} = \frac{\frac{1}{2}\left(\frac{1}{r_1^{\ddagger}} - \frac{1}{R_e}\right)}{\left(\frac{1}{r_1^{\ddagger}} + \frac{1}{r_2^{\ddagger}} - \frac{1}{R_m}\right)} \qquad \text{(V-13a)}$$

is obtained which can be simplified to

$$\frac{(\lambda_o)_E}{(\lambda_o)_H} = \frac{R_e - r_1^{\ddagger}}{R_e} \qquad \text{(V-13b)}$$

when $r_1^{\ddagger} = r_2^{\ddagger}$ and $R_m = 2r_1^{\ddagger}$. Equation (V-13b) says that the ratio $(\lambda_o)_E/(\lambda_o)_H$ is 0.5 when $R_e = 2r_1^{\ddagger}$. This was the assumption which has been used throughout this chapter when R_m was set equal to 7 Å and R_e was set equal to the distance from the outer Helmholtz plane to the electrode, which is approximately 7 Å also and twice the value of $r_1^{\ddagger}$. If $R_e > a$, Eq. (V-13b) predicts that $(\lambda_o)_E/(\lambda_o)_H = 1$. If $R_e = a$, Eq. (V-13b) breaks down, since a dielectric continuum model was used to derive Eqs. (V-6a and 12). However, if $R_e = a$, $(\lambda_o)_E/(\lambda_o)_H$ could be expected to be much smaller than 0.5.

What remains to be done now is to compute $\Delta F_E^*/\Delta F_H^*$ from experimental data. From the double layer corrected standard rate constant of 4.0×10^{-7} cm/sec, $\Delta F_E^* = 15.1$ kcal/mole. The experimentally obtained ΔF_H^* of about 24.4 kcal/mole should be corrected for the electrostatic interaction between $[Cr(H_2O)_6]^{2+}$ and $[Cr(H_2O)_6]^{3+}$. The ΔF_H^* for this reaction was obtained in a 1.0 M $HClO_4$ solution. According to Eq. (V-4b), $\Delta F_c^{\ddagger}$ for a solu-

tion of ionic strength 1.0 is 0.36 kcal/mole. The experimental ΔF_H^* which should be used for the comparison with the experimental ΔF_E^* is (24.4-0.36) kcal/mole = 24.0 kcal/mole. Therefore, experimentally, $\Delta F_E^*/\Delta F_H^*$ - 15.1/24.0 = 0.63. This value is in reasonable agreement with 0.5. The slight deviation might be due to the fact that R_e is not exactly equal to (2a), but equal to $\simeq$ (2.5a). However, considering that the experimental ΔF^* values are not exact, the slight deviation from 0.5 is probably not significant.

An attempt to measure ΔH^* more precisely by measuring the rate constants at various temperatures was not attempted in this work for the following reasons. To obtain such preciseness with cyclic voltammetry techniques is extremely difficult, and the resulting data could not be double layer corrected at the various temperatures, since the temperature dependence of the double layer data is unavailable.

With such good agreement between the theoretical and experimental ΔF_H^* values, and fair agreement between the theoretical ΔF_E^* and experimental ΔF_E^*, and reasonable agreement between the theoretical $(\lambda_o)_E/(\lambda_o)_H$ ratio and the experimental $\Delta F_E^*/\Delta F_H^*$ ratio, a safe statement is that Marcus' model for homogeneous and electrode reactions is functionally as well as semi-quantitatively correct.

Models for the Redox Kinetics of $[Cr(H_2O)_6]^{2+}/[Cr(H_2O)_6]^{3+}$

The probable mechanisms for $[Cr(H_2O)_6]^{3+}$ reduction and $[Cr(H_2O)_6]^{2+}$ oxidation in a perchlorate supporting electrolyte will now be discussed. The reduction of $[Cr(H_2O)_6]^{3+}$ will be considered first.

Four possible positions for the $[Cr(H_2O)_6]^{3+}$ cation in the activation state for reduction are pictured in Fig. V-1. Since this reduction occurs at potentials from -0.72 to -0.90 V vs SCE, the water molecules along the mercury surface would be oriented with their hydrogens facing the electrode. Perchlorate does not specifically adsorb in this potential range. The in-set picture in the upper left hand corner of Fig. V-1 shows the orientation of water on the mercury surface. Pauling[69] gives the radius of the O^{2-} ion as 1.4 ± 0.02 Å. If this is assumed to be applicable to water, the distance from the electrode to the center of the oxygen is about 1.9 Å. The distance from the electrode to the center of the oxygen in the water molecule could be slightly reduced from 1.9 Å due to d-orbital overlap between the mercury surface and the water molecules. The lower in-set picture in Fig. V-1 gives a functional representation of the central chromium ion and its six inner-sphere water ligands. In this complex the water ligands are oriented with oxygen facing the chromium. Water molecules along the mercury surface, with their oxygen atoms facing away from the electrode, would not hinder the approach of the $[Cr(H_2O)_6]^{3+}$ complex for electrostatic reasons,

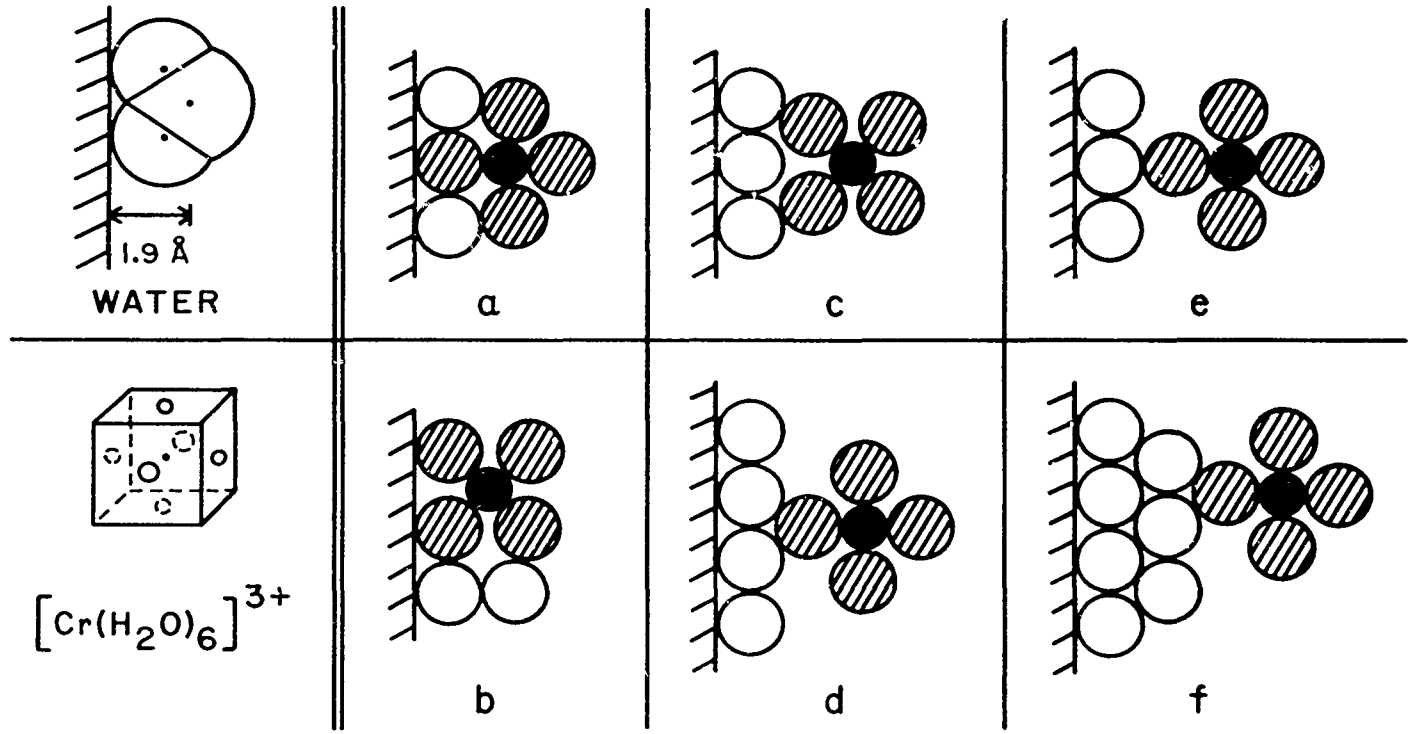

Fig. V-1. Possible configurations for the activated state for the reduction of $[Cr(H_2O)_6]^{3+}$ in $NaClO_4$.

since the approaching complex has the hydrogens of its ligand water pointing outward from the chromium.

In the diagrams of Fig. V-1, chromium is represented by the solid circles. Inner-coordination sphere water ligands which can be shown in a two-dimensional diagram are the cross-hatched circles, and other water molecules are the open circles.

In configuration a of Fig. V-1, the chromium shares its inner-coordination sphere water ligand with the mercury surface. Configuration b shows a different orientation of the same situation. In c, the chromium shares its outer-coordination sphere water ligand with the electrode surface. Configuration d shows the chromium placed slightly further from the electrode. In e, the chromium is separated from the electrode surface by two water molecules. In f, the chromium is more than two water molecule diameters from the electrode.

Both Marcus and Levich identify R_e with the outer Helmholtz plane of about 7 Å from the electrode surface. The outer Helmholtz plane is defined here as the distance of closest approach of the cation to the electrode. Configurations c, d, and e correspond to outer Helmholtz planes of about 7 Å from the mercury surface. This distance can be estimated in the following manner. The distance between the mercury electrode and the center of the oxygen in a water molecule adjacent to the surface is about 1.9 Å. The distance from the center of this oxygen to the center of an oxygen belonging to an inner-sphere ligand water is not greater than

the diameter of the water molecule, or 2.76 Å.[72] The variation in distance between these two oxygens depends upon the relative orientation of the water molecules to each other. The distance from the center of the oxygen in the ligand water to the center of the chromium(II) is 2.2 Å.[61] Thus the distance from the electrode to the center of the chromium(II) in configurations c, d, and e is between 6 and 7 Å.

For each of the possible chromium positions for the activated state shown in Fig. V-1, the inner-coordination sphere has been pictured as remaining intact. Chromium(III) is non-labile. Any exchange of inner-sphere ligands would have to occur after the chromium was in the labile chromium(II) state.

For the oxidation of $[Cr(H_2O)_6]^{2+}$ in a perchlorate solution, the orientation of water molecules on the electrode surface is important. At least 90% of the electrode surface is covered by water, with the remainder covered by the weakly adsorbed perchlorate ions. In the potential range 100 to 300 mV positive to the point of zero charge where the oxidation of $[Cr(H_2O)_6]^{2+}$ occurred, the water molecules would ordinarily be expected to be oriented with their hydrogens facing away from the electrode. Information is lacking as to the energy to re-orient a water molecule at the surface, but it is probably not greater than a few kcal/mole. The energy of a $[Cr(H_2O)_6]^{2+}$ cation at the outer Helmholtz plane relative to the bulk of the solution is also typically a few kcal/mole. For example, for a ϕ_2 potential of -33 mV, which is the average ϕ_2 potential in a 0.33 M $NaClO_4$

solution for the potential range over which the $[Cr(H_2O)_6]^{2+}$ oxidation occurs, the energy of the $[Cr(H_2O)_6]^{2+}$ cation is $Z_i e\phi_2$ or -1.5 kcal/mole. Since the energy of the $[Cr(H_2O)_6]^{2+}$ cation is close to the energy needed to turn the water molecule, the configurations a, b, and d of Fig. V-3 for the activated state for the oxidation of $[Cr(H_2O)_6]^{2+}$ are possible.

In addition to considering the orientation of water molecules along the mercury surface, the water molecules in the second layer away from the electrode and the presence of perchlorate ions must be taken into account. The water molecules in the second layer away from the electrode surface would probably have orientations ranging from random to those similar to the first layer water molecules. Since this oxidation occurs from -0.2 to -0.5 V vs SCE, the perchlorate ions will be weakly adsorbed on the mercury surface. These perchlorate ions on the electrode surface and elsewhere in the double layer, even in the outer-coordination sphere of $[Cr(H_2O)_6]^{2+}$, will serve to stabilize the presence of the $[Cr(H_2O)_6]^{2+}$ cation near the electrode.

The $[Cr(H_2O)_6]^{2+}$ cation could approach to the plane of the second layer waters, since the repulsion (on a relative basis) between the ligand water hydrogens and first layer water hydrogens would be effectively reduced by the more unstructured second layer water molecules and perchlorate anions. With a cation that is labile to inner-sphere ligand substitution, several different mechanisms can be proposed for the electron transfer.

Three possible mechanisms are depicted in Fig. V-2. Mechanism A shows $[Cr(H_2O)_6]^{2+}$ adsorbing onto the mercury electrode prior to oxidation. Mechanism B, which is less probable than the others, shows the chromium metal specifically adsorbing onto the mercury surface after its own inner-sphere ligand water moves from between it and the electrode. Another manner in which the chromium metal could become specifically adsorbed is as follows. The $[Cr(H_2O)_6]^{2+}$ cation adjacent to the electrode could lose a water ligand that is remote to the electrode, causing the remaining water ligands to rearrange such that the chromium metal is then specifically adsorbed. Mechanism C depicts the perchlorate ion bridging to the $[Cr(H_2O)_6]^{2+}$ cation.

Still four more possible configurations for the activation state in the oxidation of $[Cr(H_2O)_6]^{2+}$ are shown in Fig. V-3. Configurations a and c show the chromium outer-sphere water ligand and perchlorate ions shared also by the electrode. Configuration b shows chromium separated from the electrode by two water molecules. Configuration d shows the chromium-electrode separation to be more than two water molecule diameters. Since the most probable chromium-electrode separation is about 7 Å, the most probable mechanisms or configurations for the activated state are mechanism C in Fig. V-2 and configurations a, b, and c of Fig. V-3.

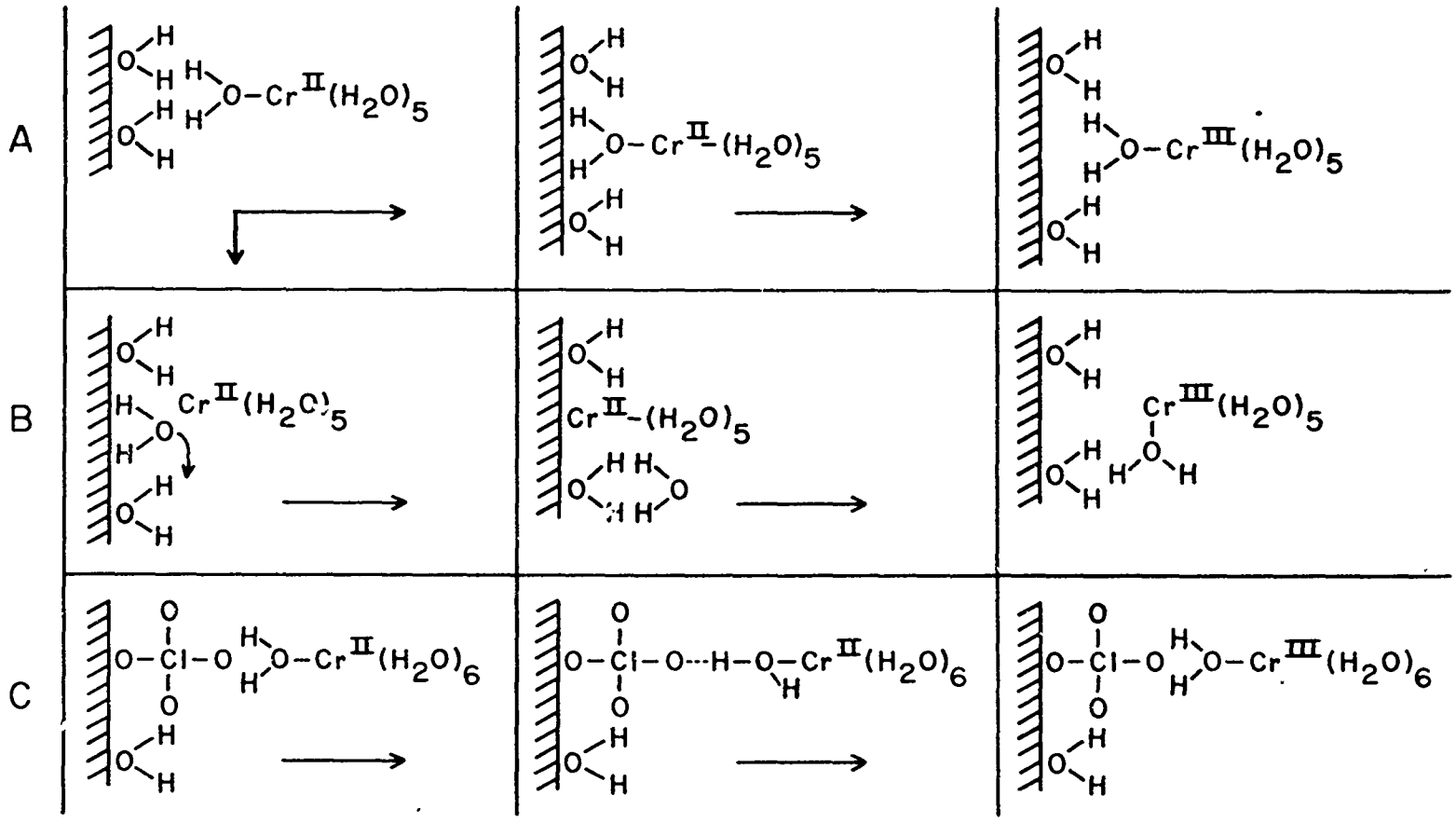

Fig. V-2. Possible mechanisms for the oxidation of $[Cr(H_2O)_6]^{2+}$ in pure $NaClO_4$.

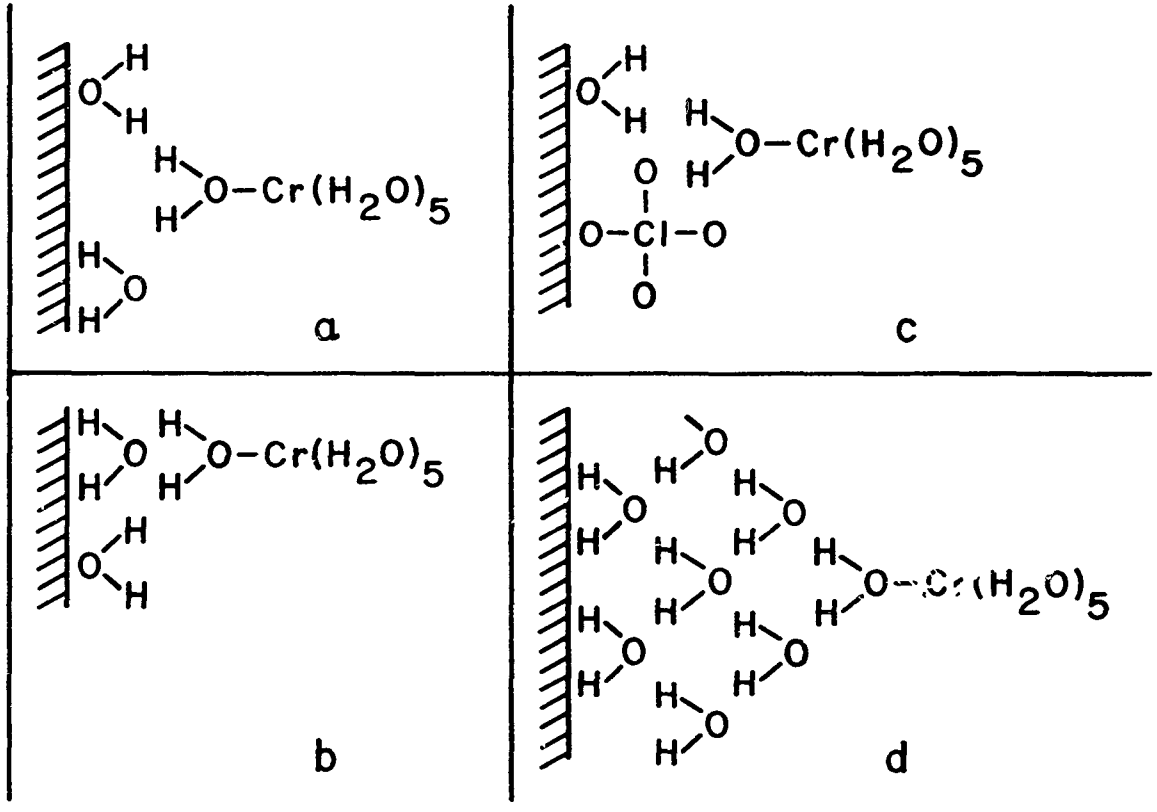

Fig. V-3. Additional possible configurations of the activated state for the oxidation of $\left[Cr(H_2O)_6\right]^{2+}$ in pure $NaClO_4$.

Corrections to the Double Layer

In calculating the true rate constant, the correction $\exp[(\alpha n-Z)F\emptyset_2/RT]$ was applied. This correction is only valid[50] if the pre-reaction state is the outer Helmholtz plane with the outer Helmholtz plane defined in terms of the supporting electrolyte, that is, the distance of closest approach of the cations or anions to the electrode with a layer of water interposed. The definition of the outer Helmholtz plane is contingent upon the ions involved. Even in an electrolyte with no specifically adsorbed ions such as NaF, the distance of the outer Helmholtz plane from the electrode will differ depending upon whether the outer Helmholtz plane is defined in terms of cations or anions. The situation is even more confusing when more than one type of cation and anion are present in solution. Under such circumstances, the equivalent of several outer Helmholtz planes may exist. Fortunately the errors arising because of the existence of more than one outer Helmholtz plane are partially compensating and hence not as serious as they might otherwise be, but they can lead to values for α_t and β_t which are still not fully characteristic of the charge transfer in an elementary step.

The use of Payne's double layer data for $HClO_4$ in lieu of unavailable double layer data for $NaClO_4$ was not expected to cause any serious error. To ascertain what the possible error might be, the double layer differential capacities at 25°C for 0.1 and 1 M HCl solutions[73] were compared to those for 0.1 and 1 M

KCl solutions at the same potentials from -0.1 to -1.0 V vs NCE. The K^+ would be expected to behave the same as Na^+. For the 0.1 M solutions, the different capacities are virtually identical. For the 1 M solutions, the capacities are about 4% higher for the salt than for the acid at potentials positive to the point of zero charge and about 2% higher for the acid than for the salt at potentials negative to the point of zero charge. Since the solutions used in this present work were 0.33 M in $NaClO_4$, the difference between hydronium and sodium ions is probably closer to that for the 0.1 M than for the 1.0 HCl and KCl solutions. Even in the more concentrated solutions the difference between the hydronium and sodium ions is small. The closeness of the differential capacities implies that the ϕ_2 data of KCl and HCl solutions also are similar. This is evident from the following equation[74] if no specific adsorption occurs.

$$\int_{E=E_{pzc}}^{E} C dE = q = \pm \left[\frac{RTD}{2\pi} \sum_i C_i^* \left(\exp - \frac{z_i F \phi_2}{RT} - 1\right)\right]^{1/2} \qquad \text{(V-14)}$$

The capacity C integrated from the point of zero charge to a particular potential is equal to the charge q on the metal. The summation of the right-hand side of Eq. (V-14) must be over all of the ions in solution, which would include the chromium ions. The bulk concentration of each ion is C_i^*, the charge on the ion, with sign, is Z_i, the dielectric constant is D, and the other symbols have their usual significance.

An important problem with the ϕ_2 data is the effect that chromium ions present in the solutions had on the ϕ_2 values. Pure perchlorate solutions containing chromium ions will be considered. To determine the chromium effect on the ϕ_2 potentials, Eq. (V-14) was used, assuming no specific adsorption for sodium, perchlorate or chromium ions in the potential range of interest. At potentials positive to -0.5 V vs SCE, weak specific adsorption of perchlorate does occur. The ϕ_2 values calculated in the pure $HClO_4$ solutions only considered the H_3O^+ and ClO_4^- ions. If chromium ions are also present in the solution and the assumption is made that the q on the metal will not be significantly changed by the inclusion of the chromium ions, then ϕ_2 can be calculated for each potential and q of interest with terms included for the chromium ions as well as the hydronium (or sodium) and perchlorate ions. The assumption of the constancy of q is made on the basis that ϕ_2 is believed to be more sensitive to the chromium concentration than to the charge q on the metal.

For the approximately 2.5 mM $[Cr(H_2O)_6](ClO_4)_3$ concentration used in 0.33 M $NaClO_4$ the chromium influence on ϕ_2 only became noticeable for $[Cr(H_2O)_6]^{3+}$ in the potential range where it is reduced. In the anodic range (-0.2 to -0.5 V vs SCE) the concentrations of chromium(II) and chromium(III) were not sufficient to modify ϕ_2 values provided the assumptions that q is not a function of chromium concentration and that perchlorate is not specifically adsorbed are still valid. Actually there is weak

perchlorate specific adsorption in this potential region which would make the use of Eq. (V-14) only approximate. Other arguments to be presented shortly show that the transfer coefficient β will be changed by a small amount. For the present, perchlorate will be assumed not to be specifically adsorbed in the potential region of -0.2 to -0.5 V vs SCE.

Near the peak potential for the $[Cr(H_2O)_6]^{3+}$ reduction in 0.33 M $NaClO_4$, the ϕ_2 value obtained from the pure perchlorate solutions was -52 mV at -0.86 V vs SCE. By assuming q in Eq. (V-14) constant and by knowing the ϕ_2 value for a pure perchlorate solution, a new ϕ_2 value could be calculated with Eq. (V-14) which reflected the influence of the presence of chromium. The new ϕ_2 value at -0.86 V vs SCE was -46 mV. Near the foot of the $[Cr(H_2O)_6]^{3+}$ reduction peak, the ϕ_2 value obtained from a pure perchlorate solution was -45.1 mV at -0.76 V vs SCE and when corrected with Eq. (V-14), -41 mV was obtained. The double layer corrected curve for the $[Cr(H_2O)_6]^{2+}/[Cr(H_2O)_6]^{3+}$ couple in a pure perchlorate solution shown in Fig. IV-2 was corrected with the ϕ_2 data from a pure perchlorate solution. To ascertain how much these double layer corrected rate constants would differ, had the presence of chromium ions been considered, the apparent rate constants were double layer corrected with the ϕ_2 values obtained with the aid of Eq. (V-14) and a transfer coefficient α of 0.48. The result was an increase in the double layer corrected rate constants over those values shown in Fig. IV-2

and a change in the true transfer coefficient. The newly obtained transfer coefficient of 0.52 was then used to repeat the double layer correction to the apparent rate constants for the purpose of converging on the true transfer coefficient. The transfer coefficient converged upon was $\alpha = 0.51$. At -0.86 V vs SCE the double layer corrected rate constant increased by a factor of about 1.1 over what it was in Fig. IV-2 and at -0.76 V vs SCE the increase was by a factor of about 1.8. With a transfer coefficient α of 0.51, the standard rate constant for the $[Cr(H_2O)_6]^{2+}/[Cr(H_2O)_6]^{3+}$ couple changed from 3.6×10^{-7} to 4.0×10^{-7} cm/sec, and the standard potential shifted from -0.650 to -0.642 V vs SCE. Since the double layer potentials in the perchlorate solutions are not large, the effect of correcting them for the presence of chromium ions was quite small as evidenced by the small changes in transfer coefficient and standard rate constant.

An additional comment must be made here concerning the earlier implicit assumption that θ_{H_2O} in the potential range for the oxidation of $[Cr(H_2O)_6]^{2+}$ was unity. The fractional surface coverage for H_2O could not be exactly unity as there was weak perchlorate specific adsorption. Even though the fractional surface coverage of perchlorate might change as much as four-fold over the potential range (-0.2 to -0.5 V vs SCE) for this oxidation, the change in θ_{H_2O} would be much less, perhaps 5% at most. Over one decade of current with a 120 mV slope, this

5% change in θ_{H_2O} would result in only a 2% change in the transfer coefficient. The exact implications of θ_{H_2O} are contingent on the model used for the oxidation.

If the reaction occurs at a water covered electrode site, then the anodic transfer coefficient ß would increase slightly. The following reasoning may be employed for predicting this change in ß. As the potential becomes more negative, θ_{H_2O} increases. The rate constant k can be expressed as $k = k'\theta_{H_2O}$. As θ_{H_2O} increases, k' will have a smaller absolute numerical Tafel slope than k. Thus ß' will be larger than ß. If the reaction occurs at a perchlorate covered site, then ß would decrease slightly, since the perchlorate coverage decreases as the potential becomes more negative. Reasoning similar to the above may be used to explain this change in ß. The effect is well below the level of experimental error in the present study.

Reactions in Chloride and Bromide Containing Solutions

Mechanisms of Redox Couples

The mechanisms of the following additional situations need to be considered: the oxidation of $[Cr(H_2O)_6]Cl^{+}$ and $[Cr(H_2O)_6]^{2+}$ in chloride-perchlorate solutions; the oxidation of $[Cr(H_2O)_6]Br^{+}$ and $[Cr(H_2O)_6]^{2+}$ in bromide-perchlorate solutions; the reduction of $[Cr(H_2O)_5Cl]^{2+}$ and $[Cr(H_2O)_6]^{3+}$ in chloride-perchlorate solutions; and the reduction of $[Cr(H_2O)_5Br]^{2+}$ and $[Cr(H_2O)_6]^{3+}$ in bromide-perchlorate solutions.

The discussion of mechanism will begin with the reduction of $[Cr(H_2O)_6]^{3+}$ in both the perchlorate-chloride and perchlorate-bromide solutions. For both of these reductions, the reduction mechanism would be expected to be identical to that for the $[Cr(H_2O)_6]^{3+}$ cation in pure perchlorate solutions, since the inner coordination sphere of $[Cr(H_2O)_6]^{3+}$ is not labile. The apparent rate constants are the same for this reduction in both the pure perchlorate and perchlorate-chloride solutions. In the bromide-perchlorate solutions, a small increase in apparent rate constants was noted. This small increase can be explained by double layer effects.

For the oxidation of $[Cr(H_2O)_6]^{2+}$ in either chloride-perchlorate or bromide-perchlorate solutions, the mechanisms of oxidation would be expected to be similar to the same oxidation occurring in a pure perchlorate electrolyte. In the halogen-containing solutions, the additional possibility exists for the

chromium complex to approach a halogen-covered site and undergo charge transfer there, with the halogen never entering the inner-coordination sphere of chromium. The change in potential distribution in the compact double layer due to the presence of specifically adsorbed ions is theoretically correctible with a double layer correction.

For the $[Cr(H_2O)_6]^{2+}/[Cr(H_2O)_6]^{3+}$ couple in either bromide-perchlorate or chloride-perchlorate solutions, the standard double layer corrected rate constants showed no dependence on halogen concentration (see Figs. IV-13 and 29) and had standard rate constants within 12% of those for the couple in pure perchlorate solutions. The agreement in standard potentials obtained in pure perchlorate or perchlorate-chloride solutions for this couple was within a few mV. For this couple in bromide-perchlorate solutions, the standard potential deviated as much as 50 mV from that for a pure perchlorate solution. This deviation is probably due to the error associated with "steady-state" curves being used. For the initial cycle curves, the agreement in standard potentials for this couple in bromide-perchlorate solutions and pure perchlorate solutions is within 10 mV.

For the oxidation of $[Cr(H_2O)_6]Cl^+$ to $[Cr(H_2O)_5Cl]^{2+}$ or the oxidation of $[Cr(H_2O)_6]Br^+$ to $[Cr(H_2O)_5Br]^{2+}$, the mechanisms are quite similar. One plausible manner in which to explain these oxidations is to postulate that the chromium(II) cation bonds directly to either chloride or bromide which is specifically ad-

sorbed on the mercury electrode, incorporates the halogen into its inner-coordination sphere and undergoes charge transfer. The bonding of the chromium(II) cation to the specifically adsorbed halogen could occur either through a step involving a seven or a five-coordinated chromium activated complex. A diagram of this oxidation mechanism showing it occurring through a seven-coordinated chromium complex is given in mechanism A of Fig. V-4. A second plausible mechanism for this oxidation is for a specifically adsorbed halogen which is also located in the outer-coordination sphere of chromium to exchange positions with an inner-sphere coordinated water ligand. The possibility of the halogen reacting homogeneously in a slow rate determining step with the chromium(II) cation and then approaching the electrode for charge transfer has been ruled out as the most probable mechanism because the standard first order rate constants for these reactions show only a small dependence on the bulk halogen concentration (see Figs. IV-11 and 27). For the chromium(II) oxidation occurring in a mixed chloride-perchlorate solution, the second order rate constant will be shown to have an even smaller dependence on the bulk chloride concentration than did the first order rate constant. This will be discussed in the following section.

The reductions of $[Cr(H_2O)_5Cl]^{2+}$ and $[Cr(H_2O)_5Br]^{2+}$ will be discussed together. The possibility exists for these cations to approach the electrode with two distinct orientations: the halogen ligand oriented toward the electrode or away from the electrode.

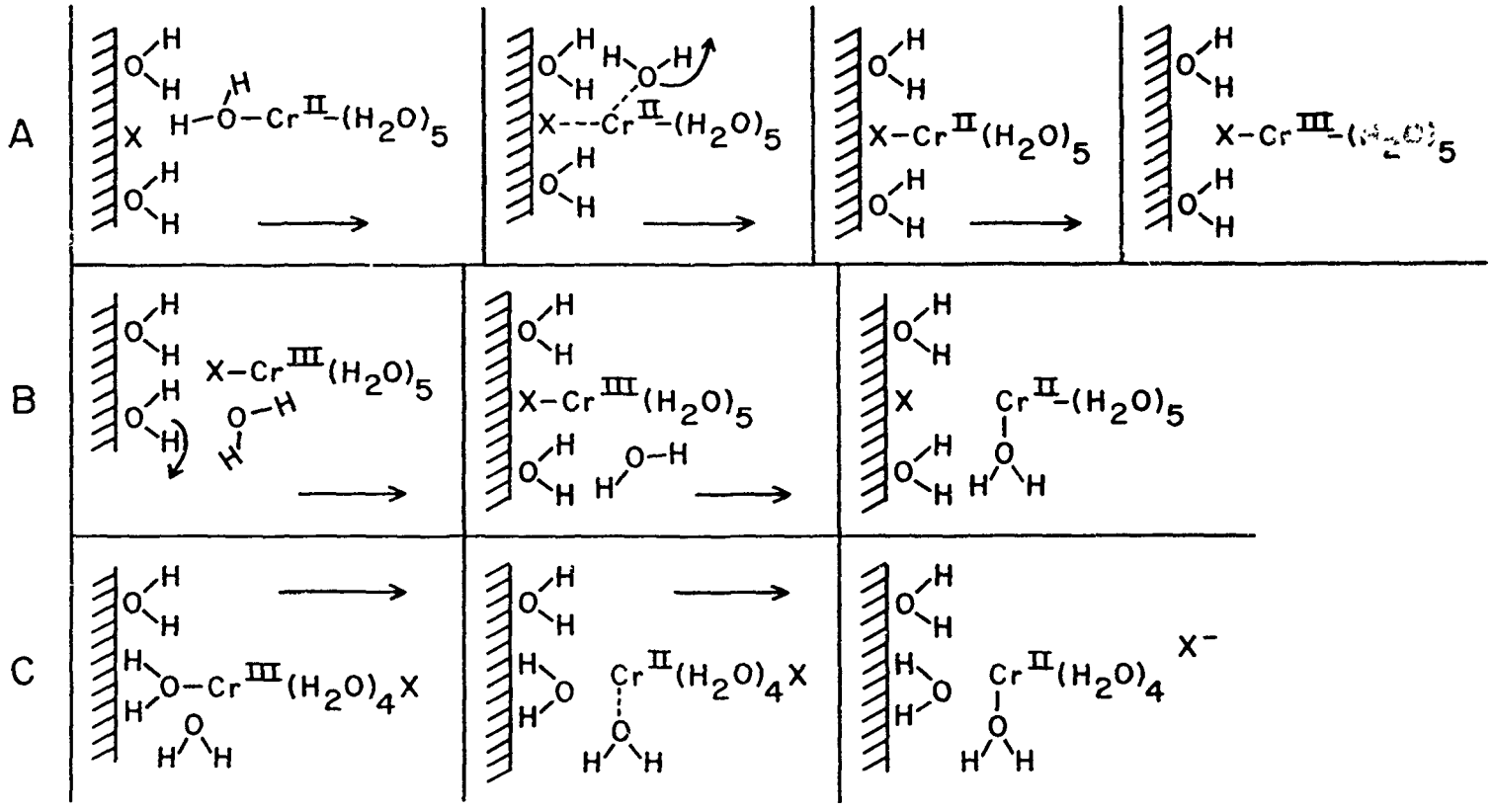

Fig. V-4. Possible redox mechanisms. A = oxidation of $[Cr(H_2O)_6]^{2+}$ at a halogen covered site; B and C = reduction of $[Cr(H_2O)_5X]^{2+}$ where X = Cl^- or Br^-:

In Fig. V-4, mechanism B depicts the complex approaching the electrode with the ligand halogen oriented toward the electrode. Mechanism C depicts the complex with the ligand halogen oriented away from the electrode. Besides approaching the electrode with a distinct orientation, the complex is quite capable of rotating while it approaches the mercury surface. In Fig. V-5, four more possible configurations for the activated complex are shown. Configuration a of Fig. V-5 shows the central metal chromium ion to be two water molecule diameters away from the electrode surface. Configuration b shows the outer-sphere water ligand of chromium to be shared by the electrode. Configuration c depicts the central metal chromium ion as being farther than two water molecule diameters from the electrode. Configuration d shows the central metal chromium ion to be the same distance from the electrode surface as was shown in configuration b. However, in configuration d the complex is oriented 180° different from the orientation in configuration b.

Since both chloride and bromide are specifically adsorbed on mercury in the potential range over which the $[Cr(H_2O)_5Cl]^{2+}$ and $[Cr(H_2O)_5Br]^{2+}$ reductions occur, and since the $[Cr(H_2O)_5Br]^{2+}$ reduction occurs positive to the point of zero charge and the $[Cr(H_2O)_5Cl]^{2+}$ reduction occurs near the point of zero charge, the pre-reaction state for both complexes in all probability has the halogen directly interacting with the electrode and adsorbed on it. Of course, the possibility exists for some fraction of either reduction to occur by a different mechanism. The consequences of

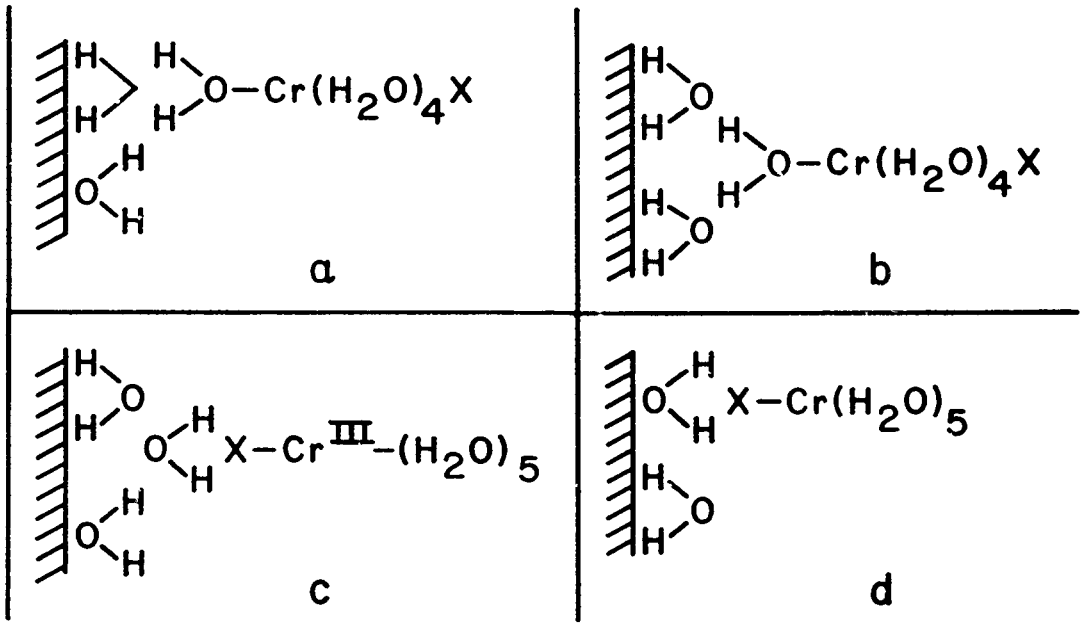

Fig. V-5. Additional possible orientations for the activated state for the $\left[Cr(H_2O)_5X\right]^{2+}$ ($X = Cl^-$, Br^-) reductions.

different mechanisms occurring and of the halogen ligand specifically adsorbing for these reductions with respect to the double layer corrections will be discussed in the next section.

Since both the $[Cr(H_2O)_6]Cl^+/[Cr(H_2O)_5Cl]^{2+}$ and $[Cr(H_2O)_6]Br^+/[Cr(H_2O)_5Br]^{2+}$ couples proceed with a change of inner-sphere ligands, neither couple can be described by weak interaction processes. Thus Eq. (V-7) is not applicable to these couples.

Both of these couples can be viewed either as an example of ligand bridging or atom transfer. Atom transfer implies that all of the charge to be transferred resides on the halogen ligand and that the halogen ligand becomes essentially neutral during some stage as it physically enters or leaves the inner-coordination sphere of the chromium. Ligand bridging implies that the charge to be transferred is spread out over the electrode-ligand-chromium system in the activated state. The atom transfer mechanism could involve high activation energy approaching that corresponding to the production of the halogen atom from the ion adsorption here and seems very unlikely. The orbital overlap between the halogen ion orbitals and the 3d orbitals of the two chromiums should be quite substantial in the activated state and hence the ligand bridge mechanism would be expected to have a lower energy of activation.

Corrections to the Double Layer

To correct the ϕ_2 data for the presence of chromium ions in the mixed chloride-perchlorate or bromide-perchlorate solutions,

Eq. (IV-14, probably could be used as a first approximation in potential ranges where specific adsorption is low. This condition applies to the double layer corrections for the reduction of $[Cr(H_2O)_6]^{3+}$ in each of the mixed electrolytes, and the reduction of $[Cr(H_2O)_5Cl]^{2+}$ in the mixed chloride-perchlorate solution. Each will be discussed.

For the reduction of $[Cr(H_2O)_6]^{3+}$ in the mixed chloride-perchlorate supporting electrolyte, the $\emptyset_2$ modification would be the same as in the case of the pure perchlorate supporting electrolyte. This follows from the fact that the $[Cr(H_2O)_6]^{3+}$ reduction curves in the mixed chloride-perchlorate electrolyte were identical to those in the pure perchlorate supporting electrolyte (Fig. IV-5) and were analyzed as such. (Apparent rate constants from the initial cycle curve in the mixed chloride-perchlorate solution given in Fig. IV-4c can be compared to apparent rate constants from both the initial and "steady-state" cycle curves in Fig. II-2 or to the apparent rate constants in Fig. IV-2 obtained from "steady-state" curves in pure perchlorate solutions.) Thus the transfer coefficient changed from 0.48 to 0.51 due to the chromium influence in the mixed chloride-perchlorate solution just as it did in the pure perchlorate solution.

For the reduction of $[Cr(H_2O)_6]^{3+}$ in a mixed bromide-perchlorate supporting electrolyte, the apparent rate constants given in Chapter IV were double layer corrected with $\emptyset_2$ data from a pure perchlorate solution, since more precise data were not available.

The following digression will elucidate the frustrations encountered in attempting to obtain precise $\emptyset_2$ data for mixed bromide-perchlorate solutions over the potential range for the $[Cr(H_2O)_6]^{3+}$ reduction. Solutions of low and high bromide concentration will be considered in turn.

For perchlorate solutions containing less than 4% bromide, the $\emptyset_2$ values at potentials more negative than -0.76 V vs SCE would be expected to behave very much like those for pure perchlorate solutions. The $\emptyset_2$ values given for the potential range between -0.76 and -0.86 V vs SCE by the method of Dutkiewicz and Parsons[54] which was described in Chapter II were between -82 and -106 mV for a bromide concentration of 5 mM in 0.33 M $NaClO_4$ as compared with -45.2 and -52 mV for a pure 0.33 M $NaClO_4$ solution. These extremely high calculated $\emptyset_2$ values indicate that the Dutkiewicz and Parsons method cannot be applied to mixed bromide-perchlorate solutions of low bromide concentrations. This limitation of the Dutkiewicz and Parsons method for solutions containing extremely low concentrations of specifically adsorbed species in a weakly or non-adsorbing electrolyte has already been mentioned. The one occasion in the present study that this method could be used in a situation of this kind was for the double layer corrections of the oxidation of $[Cr(H_2O)_6]^{2+}$ or $[Cr(H_2O)_6]Cl^{+}$ in chloride-perchlorate solutions of low chloride concentrations. The reason why such a calculation did not cause any apparent complications when applied to the chloride-perchlorate solutions for low chloride concentrations was

that the difference between the ϕ_2 values for pure perchlorate and the calculated values for the mixed chlorate-perchlorate solutions was small. Consequently the absolute magnitude of the error was small although its relative magnitude was probably large.

In mixed bromide-perchlorate solutions of high bromide concentration, the method of Dutkiewicz and Parsons would be expected to be more reliable and the ϕ_2 values so obtained can be approximately corrected for the effect of the chromium ions. For solutions of high (0.1 M) bromide concentration, the ϕ_2 value at a potential near the foot of the curve was -63.5 mV (at -0.76 V vs SCE), and near the peak of the curve, the ϕ_2 value was -68 mV (at -0.86 V vs SCE). When these values were corrected by Eq. (V-14) for the presence of chromium ions, a ϕ_2 value of -53 mV was obtained for the potential near the foot of the curve and -55.7 mV was obtained for the potential near the peak of the curve.

An independent estimate of the ϕ_2 values in the mixed bromide-perchlorate solutions of high bromide concentration, taking into account the chromium ions, can be made from the apparent rate constants for the reduction of $[Cr(H_2O)_6]^{3+}$ in bromide-perchlorate solutions of high bromide concentration. This independent estimate is extremely desirable since it will give some measure of the reliability of the Dutkiewicz and Parsons method and the equation being used to correct for the influence of the chromium ions. An estimate of the ϕ_2 values in the mixed bromide-perchlorate solutions can be made from a knowledge of the difference in apparent

rate constants for the reduction of $[Cr(H_2O)_6]^{3+}$ in pure perchlorate solutions and in mixed bromide-perchlorate solutions. Since the apparent rate constants for this reduction in the mixed bromide-perchlorate solutions of high bromide concentrations were only a factor of 1.2 on the average higher than those in the pure perchlorate solutions, the ϕ_2 values for the mixed bromide-perchlorate solutions of high bromide concentrations would be expected to be, on the average, 2 mV higher than those for the perchlorate solution. This estimate was based on Eq. (II-11). The ϕ_2 values from a pure perchlorate solution, after correction for the presence of the chromium ions, were -45 and -42 mV at -0.86 and -0.76 V vs SCE, respectively. At these same potentials, the ϕ_2 values in the mixed bromide-perchlorate solutions at high bromide concentrations, according to the above reasoning, would be -47 and -43 mV. The ϕ_2 values calculated at these same potentials by the Dutkiewicz and Parsons method and corrected for the presence of the chromium ions were -55.7 and -53 mV, as stated previously. These latter ϕ_2 values are about 9 mV larger than those estimated directly from the apparent rate constants. This 9 mV difference can be considered the result of inadequacies in both the Dutkiewicz and Parsons method and in the use of Eq. (V-14). For small absolute values of ϕ_2, the Dutkiewicz and Parsons method is more reliable, since absolute errors would be small, although relative errors could be larger.

While the ϕ_2 values for bromide-perchlorate solutions of

high bromide concentrations could be estimated from the apparent rate constants, nevertheless the apparent rate constants for this reduction in mixed bromide-perchlorate solutions of both high and low bromide concentrations were made with the $\emptyset_2$ data from pure perchlorate solutions. The use of pure perchlorate $\emptyset_2$ data for solutions of low bromide concentration in this negative potential region is quite reasonable, but could be questioned for solutions of high bromide concentration. Possibly the $\emptyset_2$ data from pure bromide solutions should have been used. This idea was considered and rejected, since the $\emptyset_2$ values thus obtained were unrealistically high, causing the double layer corrected rate constants to be extraordinarily low. For example, the $\emptyset_2$ values in a 0.1 M pure KBr[53] solution are -82 and -62 mV at -0.86 and -0.76 V vs SCE, respectively. In conclusion, the pure perchlorate $\emptyset_2$ values used to correct the apparent rate constants for the $[Cr(H_2O)_6]^{3+}$ reduction in mixed bromide-perchlorate solutions were quite valid for solutions of low bromide concentration, and were the only $\emptyset_2$ data which gave reasonable results for solutions of high bromide concentrations.

The double layer corrected rate constants for the $[Cr(H_2O)_6]^{2+}/[Cr(H_2O)_6]^{3+}$ couple in the mixed bromide-perchlorate solutions should be viewed as very approximate. Any correction to the $\emptyset_2$ values used for this double layer correction because of the presence of chromium ions would be small since the $\emptyset_2$ data from pure perchlorate solutions were used for the initial double layer

correction. Since the $\emptyset_2$ data even without chromium taken into account is highly questionable, it would make little sense to make small corrections for the presence of chromium.

Before the discussion of double layer effects on the $[Cr(H_2O)_6]^{3+}$ reduction is terminated, an experimental observation should be mentioned and commented upon. After careful study of the linear portions in the semi-log plots of apparent rate constants for this reduction vs applied potential, the conclusion was reached that a difference in the apparent transfer coefficient α for this reduction in a solution of high or low bromide concentration does exist. For solutions of low bromide concentrations, the apparent transfer coefficient α for this reduction was 0.63, the same as for this reduction in a pure perchlorate solution. For solutions of high bromide concentration, the apparent transfer coefficient α was 0.60. This difference in the transfer coefficients is small, but real, and in all probability can be explained by double layer effdcts.

The last electrochemical reaction to be considered for which Eq.(V-14) was used to correct approximately the $\emptyset_2$ values due to the presence of chromium is the reduction of $[Cr(H_2O)_5Cl]^{2+}$ in mixed chloride-perchlorate solutions. For a solution 0.47 M in chloride, at -0.523 and -0.60 V vs SCE, the $\emptyset_2$ values obtained for the mixed chloride-perchlorate solutions were -41 and -55.7 mV, respectively. With Eq.(V-14) these values became -40.8 and -45 mV, respectively. For a solution 0.09 M in chloride, the $\emptyset_2$

values obtained from mixed chloride-perchlorate solutions at -0.523 and -0.70 V vs SCE were -42 and -61 mV, respectively. When these ϕ_2 values were corrected with Eq. (V-14) they became -41.5 and -51 mV, respectively. Using these newly obtained ϕ_2 values to correct the apparent rate constants, a transfer coefficient α of 0.30 was obtained for each chloride solution just described. This transfer coefficient is different than those obtained with the original ϕ_2 data (see Fig. IV-1). One of those transfer coefficients was extremely low, 0.13, but it corrected to 0.30. Furthermore, the transfer coefficient α of 0.30 agrees with the transfer coefficient obtained from the reduction of $[Cr(H_2O)_5Cl]^{2+}$ when this complex was the initial form of chromium(III) in the supporting electrolyte (Fig. IV-17). Since double layer corrections for this reduction (chromium initially in the $[Cr(H_2O)_5Cl]^{2+}$ form) were done with pure perchlorate ϕ_2 data, corrections to these ϕ_2 values due to the presence of chromium ions were extremely small. The transfer coefficient increased from 0.30 to 0.31. For solutions of low chloride concentrations, the ϕ_2 values from pure perchlorate solutions were used to double layer correct the apparent rate constants. These ϕ_2 values are influenced very little by the presence of chromium ions. Thus the curves in Fig. IV-14 corresponding to low chloride concentrations remain as given.

The above discussion concerning corrections to ϕ_2 for the $[Cr(H_2O)_5Cl]^{2+}$ reduction is contingent upon the model used for this

reduction. As has already been stated, this reduction is believed to proceed in such a manner that the chloride ligand is oriented toward the electrode in the pre-reaction state and in the activated complex. Thus the chromium cation could be positioned at a plane of closest approach that is closer to the electrode than the plane of closest approach for the potassium cation from which the double layer ϕ_2 values were obtained. Since potential varies as a function of distance from the electrode, and since this variance is often abnormal when specific adsorption is involved, the ϕ_2 values used for the double layer corrections could be in error by a large amount. The fact that α is only 0.30 would seem to suggest that the potentials corresponding to the pre-reaction state are much different than the ϕ_2 values used. The possibility also exists for the reduction to occur a certain fraction of the time in an orientation such that the chloride ligand is oriented away from the mercury electrode. Therefore the above correction to ϕ_2 for this reduction should be viewed with caution.

All of the corrections to ϕ_2 and the consequences of them which have been discussed so far in this chapter are summarized in Table V-1.

TABLE V-1. Transfer Coefficients and ϕ_2 Data Used in Correcting Them

Electrochemical Reaction	Supporting Electrolyte*	Original $-\phi_2$(mV)	Corrected $-\phi_2$(mV) with Eq. (V-14)	(α_t) Original	(α_t) Corrected
$[Cr(H_2O)_6]^{3+} + e^-$	0.33 M $NaClO_4$	52 at -0.86V‡ 45.2 at -0.76 V	45 41	0.48	0.51
$[Cr(H_2O)_6]^{3+} + e^-$	mixed Cl^--ClO_4^- and Br^--ClO_4^- solutions of total salt concentrations of 0.33 M	52 at -0.86 V 45.2 at -0.76 V	45 41	0.48	0.51
$[Cr(H_2O)_5Cl]^{2+} + e^-$	0.33 M $NaClO_4$ 2-8 mM NaCl	34.2 at -0.60V 30 at -0.52V	no change	0.21 to 0.35	no change
$[Cr(H_2O)_5Cl]^{2+} + e^-$	0.28 M $NaClO_4$ 0.047M NaCl	55.7 at -0.60V 41 at -0.52V	45 40.8	0.33	0.30
$[Cr(H_2O)_5Cl]^{2+} + e^-$	0.24 M $NaClO_4$ 0.09 M NaCl	61 at -0.70V 42 at -0.52V	51 41.5	0.13	0.30

* All solutions at pH ≈ 2.2

‡ All electrode potentials are against SCE.

For the electrochemical reactions which occur in potential ranges which have substantial specific adsorption, Eq. (V-14) cannot be used to correct the $\emptyset_2$ values for the presence of the chromium ion even as an approximation. These reactions include the oxidation of $[Cr(H_2O)_6]^{2+}$ or $[Cr(H_2O)_6]Cl^+$ in mixed solutions of chloride-perchlorate, the oxidation of $[Cr(H_2O)_6]^{2+}$ or $[Cr(H_2O)_6]Br^+$ in mixed bromide-perchlorate solutions, and the reduction of $[Cr(H_2O)_5Br]^{2+}$ in mixed bromide-perchlorate solutions.

Only qualitative insight can be given concerning the correction to $\emptyset_2$ for these reactions. The true $\emptyset_2$ values will be numerically smaller than the ones used in Chapter IV. If the $\emptyset_2$ values which were used for the double layer corrections in Chapter IV are termed the apparent $\emptyset_2$ values and those $\emptyset_2$ values which should have been used because of the presence of the chromium ions are termed the true $\emptyset_2$ values, then the true $\emptyset_2$ values are not only numerically smaller than the apparent $\emptyset_2$ values at any given potential, but the difference between the apparent and the true $\emptyset_2$ values becomes increasingly larger as the potentials become more remote from the point of zero charge. Both of these statements can be deduced from experimental evidence. A good example was provided by Timmer et al.[74] The double layer differential capacity of a solution containing 0.4 mM In^{3+} and 1 M KCNS was lower than the differential capacity of a pure 1 M KCNS solution. At the following potentials positive to the point of zero charge in these solutions, the double layer differential

capacity data in $\mu F/cm^2$ for solutions with and without In^{3+} present were: at 50 mV, 35.9, 36.9; at 100 mV, 34.0, 37.7; at 150 mV, 33.5, 38.5; at 200 mV, 34.0, 39.4; at 250 mV, 34.5, 40.7. These values were read from Fig. 3 in reference 74. Although the electrocapillary curves with or without In^{3+} present in the KCNS solutions were unchanged, Timmer et al. stated that In^{3+} is specifically adsorbed.

The $\emptyset_2$ values can be calculated from differential capacity[75] data as follows. From differential capacity data measured at various chemical potentials, the change in capacity with respect to chemical potential at a given electrode potential can be calculated. Integration of this value over electrode potential yields the integral capacity of the cation. Integration of the integral capacity over electrode potential gives the cationic surface excess which in turn is proportional to $\emptyset_2$. Since the differential capacity of an In^{3+} containing solution is less than the differential capacity of the supporting electrolyte alone, the integral capacity away from the point of zero charge will become increasingly less than for the In^{3+} containing solution than for the supporting electrolyte solution. Hence the $\emptyset_2$ values for the In^{3+} containing solution will become increasingly less from the point of zero charge than the $\emptyset_2$ values for the supporting electrolyte solution.

For each of the above mentioned reactions, except the $[Cr(H_2O)_5Br]^{2+}$ reduction, this change in the $\emptyset_2$ values will pro-

duce numerically larger transfer coefficients. For the $[Cr(H_2O)_5Br]^{2+}$ reduction, the transfer coefficient α will decrease. For the reactions occurring in the solutions containing chloride, the absolute change in ϕ_2 values and transfer coefficients would be expected to be smaller than the same changes in the solutions containing bromide. This follows from the fact that the ϕ_2 values in bromide containing solutions are much larger than those for chloride containing solutions. Each of the above reactions will be discussed.

For the oxidation of $[Cr(H_2O)_6]^{2+}$ in the mixed chloride-perchlorate solutions, Table IV-1 shows that the true transfer coefficient β varied from 0.41 to 0.44 with most of the values being 0.42. Since the change in integral capacity between chloride-perchlorate solution with and without chromium ions would probably differ by not more than 10% (estimate based on reference 74) at potentials remote to the point of zero charge, the ϕ_2 values at the same potentials remote to the point of zero charge would probably decrease only by 1 or 2 mV. Such a change in ϕ_2 values would increase the transfer coefficient β to 0.43 from 0.42.

The ϕ_2 values applicable for the oxidation of $[Cr(H_2O)_6]Cl^+$ to $[Cr(H_2O)_5Cl]^{2+}$ in the mixed chloride-perchlorate solutions were the same ones used for the oxidation of $[Cr(H_2O)_6]^{2+}$ in the mixed chloride-perchlorate solutions. Therefore the previous discussion applies here also. The effect a change in ϕ_2 will have on the transfer coefficient for this oxidation (Table IV-1) is dependent

upon the model used for the oxidation. As previously discussed, one plausible model for this oxidation is for the $[Cr(H_2O)_6]^{2+}$ cation to bond directly to a specifically adsorbed chloride ion. Consequently the reacting chromium(II) cation could be located at a plane of closest approach which is closer to the electrode than the plane of closest approach for the potassium cation from which the ϕ_2 values were obtained. Thus the ϕ_2 values used in Chapter IV for the double layer corrections were not completely correct because they corresponded to potentials at the plane of closest approach for potassium ions. Whatever transfer coefficient the ϕ_2 values for the position occupied by the chromium(II) cation during oxidation would have given, that transfer coefficient should be corrected for the presence of the chromium ions. As shown in the last paragraph, this correction is probably small.

To discuss the oxidations of $[Cr(H_2O)_6]^{2+}$ or $[Cr(H_2O)_6]Br^{+}$ or the reduction of $[Cr(H_2O)_5Br]^{2+}$ in the mixed bromide-perchlorate solutions with respect to the ϕ_2 changes is more difficult than the same for the counterpart of these reactions in the mixed chloride-perchlorate solutions. The difference in integral capacity for bromide solutions with and without chromium present would be larger than the same difference for the chloride-perchlorate solutions, since bromide is specifically adsorbed more strongly. Furthermore, as has already been mentioned, the ϕ_2 values originally obtained by the Dutkiewicz and Parsons method are not completely correct. When relatively large corrections must be

made to a value which is initially in some doubt, the problem is virtually impossible. Whatever the change in $\emptyset_2$ is, the transfer coefficients will be affected.

Since the oxidation of $[Cr(H_2O)_6]^{2+}$ in the bromide-perchlorate solutions was double layer corrected with pure perchlorate $\emptyset_2$ data as previously discussed in Chapter IV, only a negligible change in $\emptyset_2$ would result from the presence of chromium.

For the $[Cr(H_2O)_6]Br^+$ oxidation, the true $\emptyset_2$ values which become progressively smaller than the apparent $\emptyset_2$ values the more positive the potential is to the point of zero charge because of the presence of the chromium ions, would cause the numerical value of the Tafel slopes in mV/decade to be smaller than they already are in Table IV-2. Of course, this statement is contingent on the model used for the oxidation, just as a similar statement for the oxidation of $[Cr(H_2O)_6]Cl^+$ was contingent on the model used for that oxidation. As has been discussed earlier, one plausible model for the oxidation of $[Cr(H_2O)_6]Br^+$ to $[Cr(H_2O)_5Br]^{2+}$ is for the chromium(II) cation to bond directly to the specifically adsorbed bromide ion. Thus the chromium(II) ion could be at a plane of closest approach that is closer to the electrode than the plane of closest approach for the potassium cations from which the $\emptyset_2$ values were calculated. Although no serious error seemed to result from this situation with the $[Cr(H_2O)_6]Cl^+$ oxidation, the results could be far more serious for the $[Cr(H_2O)_6]Br^+$ oxidation, since the potentials in the com-

pact double layer for the bromide containing solution would be expected to change far more as a function of distance from the electrode, than would be the case for chloride containing solutions.

For the $[Cr(H_2O)_5Br]^{2+}$ reduction, the change in ϕ_2 would cause the numerical value of the Tafel slope in mV/decade to be larger than those reported in Table IV-2. This statement, too, is contingent upon the model used for this reduction and all that has been said concerning the reduction of $[Cr(H_2O)_5Cl]^{2+}$ and ϕ_2 is applicable here. Since bromide adsorbs more strongly on mercury than does chloride, and since this reduction occurs at potentials more positive than the $[Cr(H_2O)_5Cl]^{2+}$ reduction, the potential drop in the compact double layer for bromide-perchlorate solutions will vary far more than that for chloride-perchlorate solutions. Any abnormal behavior in the potential drop across the compact double layer also will be more pronounced in the bromide containing solutions than in the chloride containing solutions.

Effects of Fractional Surface Coverage for Chloride and Bromide on the Rate Constants

For the oxidation of both $[Cr(H_2O)_6]Cl^+$ to $[Cr(H_2O)_5Cl]^{2+}$ and $[Cr(H_2O)_6]Br^+$ to $[Cr(H_2O)_5Br]^{2+}$ the surface concentration of the halogen has been assumed large and incorporated into the first order rate constants. An attempt will be made to separate the halogen concentration from the first order

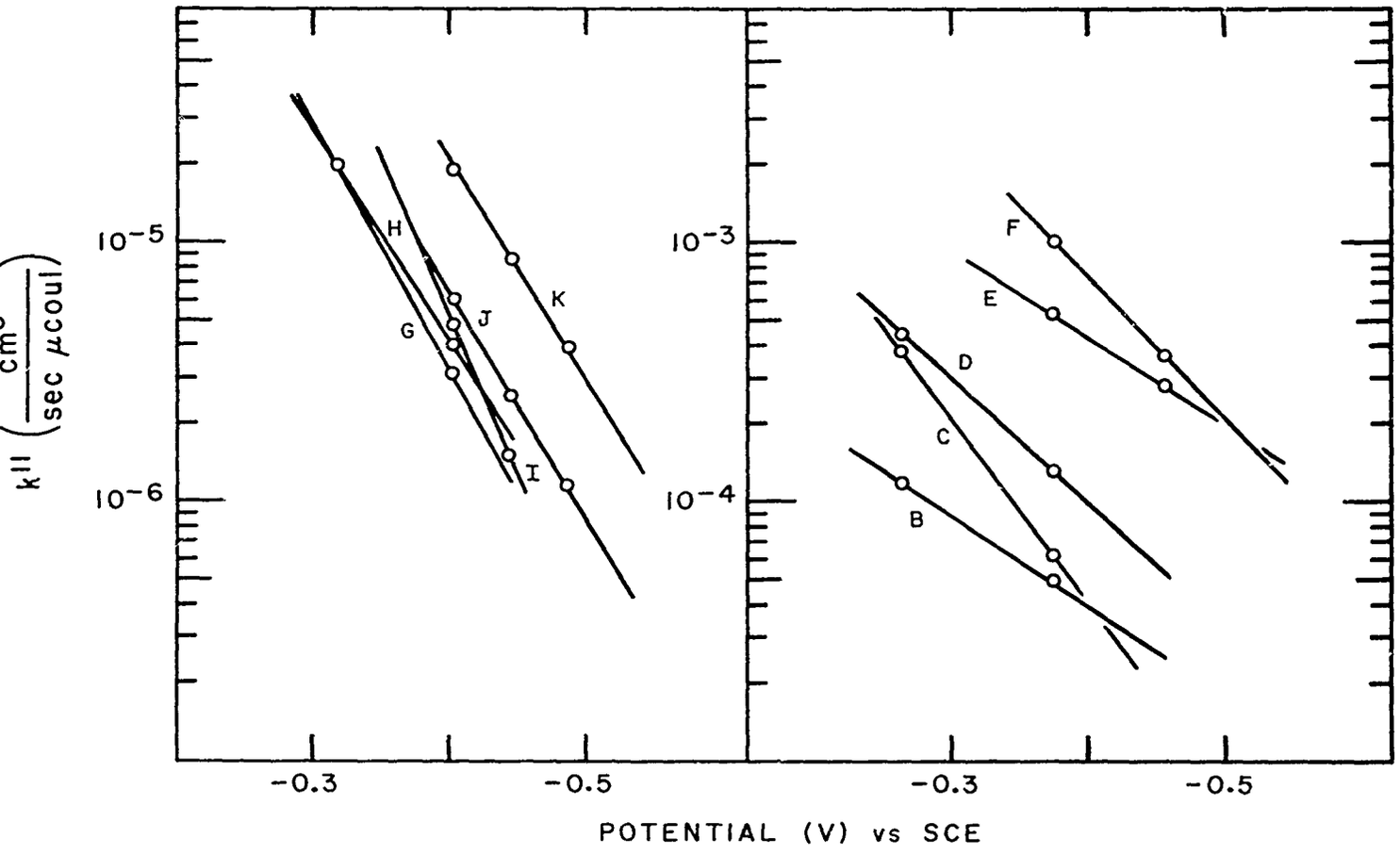

Fig. V-6. Second order rate constants vs applied potentials for the oxidation of $[Cr(H_2O)_6]Br^{+}$(left) and $[Cr(H_2O)_6]Cl^{+}$(right).

rate constant on a relative basis. For either oxidation, the first order rate constant can be rewritten as

$$k = k'\theta_{X^-} = k'(n_{X^-}/n_T) = k''n_{X^-} \qquad \text{(V-15)}$$

where θ_{X^-} is the fractional surface coverage for the halogen at any given potential, n_{X^-} is the surface coverage in charge/cm^2 (which is directly proportional to moles/cm^2) at any given potential and n_T is the total number of electrode sites. Since the total number of sites is a constant, it can be incorporated into k' yielding a new rate constant k''. Values for n_{X^-} at different potentials are available for both chloride[52] and bromide[53] solutions. Values for n_{X^-} at different potentials are given in Table V-2. Using these values a correction was made on the double layer corrected rate constants k for each oxidation. Dividing k by n_{X^-} yielded k'. Fig. (V-15) shows how the transfer coefficients for each oxidation were decreased over those values listed in Tables IV-1 and 2. For n_{Cl^-}, the values in 0.02 M KCl were used for calculating k' from k. For n_{Br^-}, the values in 0.1 M KBr were used for calculating k' from k. The n_{Br^-} values for 0.01 M KBr go to zero, making their use difficult. The fact that the n_{Br^-} values reach zero and even go to a positive 1.4 μcoul/cm^2 throws suspicion on the use of this adsorption data as an estimate of relative θ_{X^-} values. Actually, the calculation of k'' for a solution containing a certain halogen bulk concentration should be performed with n_{X^-}

data for that same halogen bulk concentration. However, only relative changes with electrode potential were calculated here and approximately the same relative changes are evident whether the n_{X^-} value at the higher or lower concentrations given in Table V-2 are used.

For the oxidation of $[Cr(H_2O)_6]Br^+$, the numerical increase in the Tafel slope in mV/decade caused by the effect of the bromide surface coverage will be off-set by the numerical decrease of the Tafel slope in mV/decade caused by the correction to ϕ_2 due to the presence of the chromium ions. Which of the two effects -- the change due to ϕ_2 or θ_{Br^-} -- will dominate and thus determine whether the numerical value of the Tafel slope in mV/decade will increase or decrease, is a moot question.

For the oxidation of $[Cr(H_2O)_6]Cl^+$, the transfer coefficient β decreases due to the effect of θ_{Cl^-}. This decrease will be off-set only slightly by the small increase in β due to the correction of ϕ_2. The resultant β will be significantly lower than 0.5. Although a significant amount of strong interaction reactions have been reported with transfer coefficients of about 0.5, there is no reason to expect such to be true for the present case. The fact that β is not 0.5 may mean that the pre-reaction plane does not correspond to the plane of closest approach or outer Helmholtz plane for which the ϕ_2 values were evaluated, or the ϕ_2 values are in error.

TABLE V-2. Values of n_{Cl^-} and n_{Br^-}

-Potential vs SCE	$-n_{Cl^-}$ (μcoul/cm^2) in 0.02 M KCl	-Potential vs SCE	$-n_{Br^-}$ (μcoul/cm^2) in 0.01 M KBr
0.2082	8.96		
0.2614	6.82	0.236	11.5
0.3150	4.73	0.279	9.0
0.3741	2.75	0.325	6.6
0.4523	1.15	0.371	4.1
		0.420	1.8
		0.480	0.0
	in 0.1 M KCl		in 0.1 M KBr
0.1996	12.49	0.319	17.3
0.2517	10.12	0.360	14.8
0.3026	7.80	0.402	12.2
0.3531	5.59	0.444	9.8
0.4069	3.56	0.486	7.4
0.4668	1.87		

In view of the preceding discussions, any very small correction to the first order rate constants become insignificant for those reactions which occur at a water covered site and for which the assumption was made that θ_{H_2O} equalled unity.

Of interest also is how θ_{X^-} changes with respect to bulk halogen concentrations so that the dependence of k', the second order rate constant, on bulk halogen concentration can be obtained. For the oxidation of $[Cr(H_2O)_6]Cl^+$ to $[Cr(H_2O)_5Cl]^{2+}$ in a mixed chloride-perchlorate solution, Fig. (IV-11) shows that the dependence of k, the first order double layer corrected rate constant, on bulk chloride concentration is low. The slope of the line for k vs chloride concentration is 0.22. As the bulk halogen concentration increases, so also does n_{Cl^-} (see Table V-3), which is proportional to θ_{Cl^-}. For the more positive potentials, n_{Cl^-} in 0.1 M KCl is about a factor of 1.5 larger than the n_{Cl^-} values in 0.02 M KCl. If the n_{Cl^-} values in 0.02 M KCl are also about a factor of 1.5 larger than the n_{Cl^-} values in a 0.002 M KCl solution, then the slope of a plot of k' vs chloride concentration would be close to zero. Thus, with the reasonable assumption of how surface coverage changes with bulk chloride concentration, the second order rate constant is independent of bulk chloride concentration.

For the oxidation of $[Cr(H_2O)_6]Br^+$ to $[Cr(H_2O)_5Br]^{2+}$ in mixed bromide-perchlorate solutions, Fig. IV-27 shows that the slope of the first order double layer corrected rate constant vs

bulk bromide concentration is -0.15. This negative slope is contrary to expectations and may be viewed as a product of the uncertain double layer corrections for bromide-perchlorate solutions. In this case, a plot of the second order rate constant k' vs bulk bromide concentration would have an even greater negative slope than the similar plot for the first order rate constants.

A partial summary of kinetic data from the cyclic voltammetry curves with chromium initially present in solution as $[Cr(H_2O)_6]^{3+}$ is presented in Table V-3. In different supporting electrolytes, different redox couples are observed. In the pure perchlorate solution, the simple $[Cr(H_2O)_6]^{2+}/[Cr(H_2O)_6]^{3+}$ couple was present. In mixed chloride-perchlorate solutions, two different couples were present: $[Cr(H_2O)_6]^{2+}/[Cr(H_2O)_6]^{3+}$, which has rate constants that are essentially the same as those for this couple in the pure perchlorate solution, and $[Cr(H_2O)_6]Cl^{+}/[Cr(H_2O)_5Cl]^{2+}$, which was significantly different from the $[Cr(H_2O)_6]^{2+}/[Cr(H_2O)_6]^{3+}$ couple. In mixed bromide-perchlorate solution, two different couples were also present: $[Cr(H_2O)_6]^{2+}/[Cr(H_2O)_6]^{3+}$, which has rate constants that are essentially the same as those for this couple in the pure perchlorate solution, and $[Cr(H_2O)_6]Br^{+}/[Cr(H_2O)_5Br]^{2+}$, which is significantly different from either $[Cr(H_2O)_6]^{2+}/[Cr(H_2O)_6]^{3+}$ or $[Cr(H_2O)_6]Cl^{+}/[Cr(H_2O)_5Cl]^{2+}$. The standard rate constants increased in the

order $[Cr(H_2O)_6]^{2+}/[Cr(H_2O)_6]^{3+}$. < $[Cr(H_2O)_6]Cl^{+}/[Cr(H_2O)_5Cl]^{2+}$ < $[Cr(H_2O)_6]Br^{+}/[Cr(H_2O)_5Br]^{2+}$. This increase in standard rate constants is quite explanable as the following section will show, and quite in accord with the homogeneous counterparts of these electrode reactions.

A comparison of the results in this work with available literature data is favorable. For the hexaaquochromium(II)/(III) couple in an acidic perchlorate supporting electrolyte, the apparent rate constant obtained in this work at -0.65 V vs SCE was 1.1×10^{-5} cm/sec. The values obtained by other workers (see Table I-1) varied from 0.69 to 1.8×10^{-5} cm/sec. The double layer corrected standard rate constant obtained in this work was 4.0×10^{-7} cm/sec at -0.65 V vs SCE. At the same potential Slotter[26] et al. obtained 5.0×10^{-7} cm/sec. For the $[Cr(H_2O)_6]^{3+}$ reduction, Jones[25] obtained an apparent transfer coefficient α of 0.63, as was obtained in this work. Slotter[26] obtained a double layer corrected transfer coefficient α of 0.50, while 0.51 was found for this present work. For the apparent transfer coefficient β for the oxidation of $[Cr(H_2O)_6]^{2+}$ in a perchlorate medium (see Table I-4), both Jones[25] and Aikens and Ross[14] found $\beta_a = 0.37$. In the present work $\beta_a = 0.35$, which double layer corrected to $\beta_t = 0.43$.

For the oxidation of $[Cr(H_2O)_6]^{2+}$ in 0.95 M $NaClO_4$ + 0.005 M NaCl, Aikens and Ross[14] obtained an apparent rate constant at -0.5 V vs SCE of 9.5×10^{-5} cm/sec. From the present work, the

apparent rate constant of $\sim 1 \times 10^{-4}$ cm/sec at -0.5 V vs SCE can be seen from Fig. IV-7. The experimental conditions were 0.33 M $NaClO_4$ + 0.005 M NaCl.

For the oxidation of $[Cr(H_2O)_6]^{2+}$ in 0.91 M NaBr + 0.066 M $HClO_4$, Jones[25] obtained an apparent rate constant of 1.82×10^{-3} cm/sec at -0.5 V vs SCE. In the same solution, Jones obtained an apparent rate constant of 1.88×10^{-3} cm/sec for the reduction of $[Cr(H_2O)_5Br]^{2+}$ at -0.5 V vs SCE. In the present work, the apparent standard rate constant for the $[Cr(H_2O)_6]Br^{+}/[Cr(H_2O)_5Br]^{2+}$ couple at -0.43 V vs SCE in a 0.23 M $NaClO_4$ + 0.103 M NaBr solution was 1.8×10^{-3} cm/sec.

TABLE V-3. Kinetic Data at 25°C from Cyclic Voltammetry Curves with Chromium Present Initially $[Cr(H_2O)_6]^{3+}$

Couple	Supporting Electrolyte	k_a at V vs SCE	k_t	α_t	β_i	Tafel slope in mV/decade anodic	Tafel slope in mV/decade cathodic
$[Cr(H_2O)_6]^{2+}$/ $[Cr(H_2O)_6]^{3+}$	0.33 M $NaClO_4$ pH = 2.20	1.1×10^{-5} at -0.637	4.0×10^{-7}* at -0.65	0.51*	0.43*	137*	116*
$[Cr(H_2O)_6]Cl^{+}$/ $[Cr(H_2O)_5Cl]^{2+}$	0.24 M $NaClO_4$ 0.0899 M NaCl	6.0×10^{-4} at -0.525	6.2×10^{-5} at -0.513	0.30*	0,56	106	192*
$[Cr(H_2O)_6]Br^{+}$/ $[Cr(H_2O)_5Br]^{2+}$	0.23 M $NaClO_4$ 0.103 M NaBr	1.8×10^{-3} at -0.434	1.1×10^{-4} at -0.433	0.94	0.66	89	63

* These numbers contain the corrections to ϕ_2 which have been discussed in this chapter.

Orbital Overlap for the Electrochemical Reactions

The initial electrostatic attraction between reactants of the bridging type will in itself not produce an electrochemical reaction. Sufficient orbital overlap must exist between the reactants. For the oxidations or reductions in which bromide, chloride, perchlorate or water is between the electrode and the chromium complex, the orbitals involved in the electron transfer for the activation state can be described by molecular orbitals. Primarily[76] the sigma molecular orbital between localized mercury d orbitals, p orbitals in bromide, chloride, perchlorate, or water and d orbitals on the chromium complex, will be involved in the electron transfer.

The difference between the relative effects of bromide, chloride, perchlorate and water can be understood simply when couched in crystal field theory terms. A transition group complex can be characterized by two sets of parameters. The first is the orbital energy difference in the partly filled d shells (Δ) and the second a parameter of interelectronic repulsion.[77] Each of these sets of parameters will be considered.

The ability of different ligands about the same central metal ion to increase Δ is qualitatively represented by the spectrochemical series. The right-hand members of the series split the d orbitals of the metal the most and tend to produce low spin complexes. A partial listing of the series is given below.[78]

$I^- < Br^- < Cl^- < F^- \sim$ urea $\sim OH^- < H_2O < SCN^- < NO_2^- << CN^-$

When chromium contains five water ligands and one halogen ligand in its inner coordination sphere, the value of Δ can be estimated by Jorgenson's "rule of average environment"[79]. Briefly this rule states that for a central metal ion surrounded by different ligands, provided these ligands are not separated too far in the spectrochemical series, the value of Δ can be found by a linear interpolation of the Δ values for the same metal ion surrounded solely by each of the ligands. The value for $[Cr(H_2O)_6]^{3+}$ is 49.6 kcal and that for $CrCl_6^{3+}$ is 30.8 kcal[80]. Thus the Δ value for $[Cr(H_2O)_5Cl]^{2+}$ can be estimated at 47.7 kcal. For the $[Cr(H_2O)_5]Br^{2+}$ complex the Δ value would be smaller than 47.7 kcal, since the Δ value for $CrBr_6$ is smaller than that for $CrCl_6$. In either case, not a great variance exists between the Δ value for the hexaaquo complex and either $[Cr(H_2O)_5Cl]^{2+}$ or $[Cr(H_2O)_5Br]^{2+}$.

The second parameter which can be used to characterize a transition complex will prove more fruitful in yielding a difference between bromide, chloride, perchlorate and water. The nephelauxetic series has been constructed according to inter-electronic repulsion parameters. In part, the series is listed below.[81]

$F^- < H_2O <$ urea $< NH_3 <$ en $< ox^{2-} < NCS^- < Cl^- \sim CN^- < Br^- < I^-$

Those ligands toward the right have a greater tendency to form covalent compounds and to lose electrons than do those ligands on

the left-hand side. The term covalency implies a sharing of electrons between the various elements in a complex and thus a significant amount of orbital overlap. A greater degree of variance[82] exists between the members of the nephelauxetic series than does between the members of the spectrochemical series for the same central metal ion. Since the nephelauxetic series parallels the ligands' tendencies to form covalent bonds, while the spectrochemical series parallels the ligands' ability to split the metal's d orbitals, the nephelauxetic series rather than the spectrochemical series will give an indication of orbital overlap. The nephelauxetic series clearly shows that bromide has a greater tendency toward covalency than does chloride or water. Perchlorate would be expected to be near NH_3. This tendency for increased covalency and hence for increased orbital overlap from water to bromide is reflected in the increase of apparent and standard rate constants for the redox couples from $[Cr(H_2O)_6]^{3+}/[Cr(H_2O)_6]^{2+}$ to $[Cr(H_2O)_6]Cl^{+}/[Cr(H_2O)_5Cl]^{2+}$ to $[Cr(H_2O)_6]Br^{+}/[Cr(H_2O)_5Br]^{2+}$.

Conclusions

The following is a summary of the thesis research.

1. The experimentally easy-to-use cyclic voltammetry technique was used for obtaining rate constants.
2. Analysis of the experimental cyclic voltammetry curves was accomplished by computer integration of current-time data according to the convolution theorem in order to obtain concentrations of the reactants at the electrode surface. These concentrations were then used to calculate apparent rate constants both with and without appreciable back reactions.
3. Although the use of initial cycle voltammetry curves was preferable, the use of the "steady-state" curves was found acceptable under the conditions of the present study.
4. In a pure perchlorate supporting electrolyte with chromium initially present as $[Cr(H_2O)_6]^{3+}$, only the hexaaquochromium(II)/(III) couple was observed.
5. In mixed chloride-perchlorate or bromide-perchlorate supporting electrolytes with chromium initially present only as $[Cr(H_2O)_6]^{3+}$, two different redox couples were observed for each solution. In the chloride-

perchlorate electrolyte, the $[Cr(H_2O)_6]^{2+}/[Cr(H_2O)_6]^{3+}$ and the $[Cr(H_2O)_6]Cl^{+}/[Cr(H_2O)_5Cl]^{2+}$ couples were present. In the bromide-perchlorate electrolytes, the $[Cr(H_2O)_6]^{2+}/[Cr(H_2O)_6]^{3+}$ and $[Cr(H_2O)_6]Br^{+}/[Cr(H_2O)_5Br]^{2+}$ couples were present.

6. Double layer corrections were applied to each system. For the pure perchlorate solutions, the double layer corrections worked well. For the chloride-perchlorate solutions, the double layer corrections worked fairly well. For the bromide-perchlorate solutions, the double layer corrections are questionable.

7. For the hexaaquochromium(II)/(III) couple in pure perchlorate solutions, the transfer coefficients α_t and β_t evaluated from the cathodic and anodic branches, respectively, are such that $(\alpha_t + \beta_t) = 0.94$. This is reasonably close to unity, considering the difference in the structural organization of the interface over the potential ranges in which the reduction and oxidation occurred. For the $[Cr(H_2O)_6]Cl^{+}/[Cr(H_2O)_5Cl]^{2+}$ couple in a perchlorate solution with chromium initially in the $[Cr(H_2O)_5Cl]Cl_2$ form, the transfer coefficients evaluated from each branch of the curve give $(\alpha_t + \beta_t) = 0.85$. This is significantly different from unity, but not surprising in view of the specific adsorption in-

volved and the limitations imposed on the use of Eq. (II-11).

8. The standard rate constants increased in the order $[Cr(H_2O)_6]^{2+}/[Cr(H_2O)_6]^{3+} < [Cr(H_2O)_6]Cl^{+}/[Cr(H_2O)_5Cl]^{2+} < [Cr(H_2O)_6]Br^{+}/[Cr(H_2O)_5Br]^{2+}$. The ligand bridge model may be used to explain this increase in rate constants.

9. The hexaaquochromium(II)/(III) couple showed no dependence on bulk halogen concentrations. For both of the halogen containing couples, the first order standard rate constants showed a weak dependence on bulk halogen concentration. In the case of the $[Cr(H_2O)_6]Cl^{+}/[Cr(H_2O)_5Cl]^{2+}$ couple, the second order rate constants were shown to have virtually no dependence on bulk halogen concentrations.

10. The experimental free energies of activation for the hexaaquochromium(II)/(III) electrode and homogeneous reactions were compared to those free energies of activation predicted by a weak interaction theory. The agreement between experiment and theory was good for the homogeneous case and only fair for the electrode case. The weak interaction theory does seem appropriate for describing charge transfer in the absence of bridging ligands. The lack of complete quantitative agree-

ment between experiment and theory is probably due to inadequate description of the structural aspects of the interface.

Final Remarks

Effective experimental methods are available for studies of redox couples. Cyclic voltammetry used in the present work is suitable for supplying data from which apparent rate constants can be calculated, but probably with less certainty than other methods. The advantage of this method is that in a single experiment different reacting couples can be identified and apparent rate constants obtained.

The principal complication in the interpretation of the apparent rate constants is that relatively complete double layer corrections can be applied only when specific adsorption is not involved and the reacting species have spherical charge symmetry. When specific adsorption of either the reacting species or the supporting electrolyte occurs, at the best only a semi-quantitative analysis of the apparent rate constants can be made. The situation has been further complicated in the present study by a lack of double layer data for mixed electrolytes. Future work should concentrate on gathering adequate experimental double layer data for the actual electrolytes in which the redox experiments are performed and on a theoretical understanding of the double layer to aid in interpretation of the reacting systems.

APPENDIX I

COMPUTER PROGRAM MAINLINE WHEN BACK REACTION CAN BE NEGLECTED

```
   DIMENSION CURR(500),TIME(500),X(500),Y(500),SUM(500),J(500),
  1CURO(500),CURD(500),NAME(10)
   READ 41,ICOUNT
41 FORMAT(13)
   DO 34 IJK=1,ICOUNT
   READ 42,(NAME(I),I=1,10)
42 FORMAT(13A6,A2)
   PRINT 43,(NAME(I),I=1,10)
43 FORMAT(1H ,13A6,A2)
   READ 1,N
 1 FORMAT (I3)
   PRINT8,N
 8 FORMAT(1H,21HNUMBER OF LAST POINT=,I3)
   READ 99,LX,LY
99 FORMAT(2I3)
   READ 2, (CURO(I), I=LX,N)
 2 FORMAT(10F8.3)
   READ3,A,CHROM,CURC
 3 FORMAT (3F10.5)
   PRINT 11,A,CHROM,CURC
11 FORMAT(1H,2HA=,F10.5,5X,6HCHROM=,F10.5,5X,5HCURC=,F10.5,5X)
   READ40, FARCON,RATCON
40 FORMAT(2F20.10)
   PRINT 111,FARCON,RATCON
111 FORMAT(1H ,7HFARCON=,F20.10,5X,7HRATCON=,F20.10)
   READ4 TINCR,TIME(1)
 4 FORMAT(2F10.4)
   PRINT12,TINCR,TIME(1)
12 FORMAT(1H,6HTINCR=,F10.5,5X,8HTIME(1),F10.5)
   PRINT9
 9 FORMAT(1H,26HOBSERVED VALUES OF CURRENT)
   PRINT 10,(I,CURO(I),I=LX,N)
10 FORMAT(7(1H ,I3,2X,F8.5,5X))
   READ 5,M
 5 FORMAT(1I3)
   PRINT13,M
13 FORMAT(1H,2HM=,I3)
   READ6 (J(K),K=1,M)
 6 FORMAT(20I4)
   CURCN=-CURC
   DO7 I=LY,N
   IF(I.GT.100)CURC=CURCN
 7 CURR(I) = CURO(I) - CURC
```

```
      PRINT 55
   55 FORMAT(1H,26HCORRECTD VALUES OF CURRENT)
      PRINT 56,(I,CURR(I),I=LY,N)
   56 FORMAT(7(1H,I3,2X,F8.5,5X))
      DO34 K=1,M
      JK=J(K)
      JM = JK - (LY-1)
      DO 24 L = 1,JM
      JKE = L + (LY-1)
      Z = L - 1
      X(L)=TIME(1)+Z*TINCR
      CURD(L) = CURR(JKE)
   24 CONTINUL
      PRINT25,JK
   25 FORMAT(1H ,3HJK=,I3)
      JKB = JM - 1
      DO 27 I = 1,JKB
   27 Y(I) = CURD(I)/SQRT (ABS(X(JM) - X(I)))
      AREA=0.0
      JKC = JM - 2
      DO29I=1,JKC
      SUM(I)=0.5*(Y(I)+Y(I+1))*(X(I+1)-X(I))
   29 AREA=AREA+SUM(I)
      AREAT = AREA+SUM(JM-2)
      IF(JK.GT.120)GO TO 31
      CONC = CHROM - (AREAT*FARCON/A)
      GO TO 32
   31 CONC=AREAT*FARCON/A
      CONC=-CONC
   32 RCONST = CURD(JM)/(RATCON*A*CONC)
      PRINT33,JM,AREAT,CONC
   33 FORMAT(1H,6HINDEX=,I3,5X,6HAREA=,E20.10,5X,5HCONC=,E20.10,5X)
      PRINT 35,CURD(1),RCONST
   35 FORMAT(1H ,8HCURD(1)=,E20.10,5X,11HRATE CONST=,E20.10)
   34 CONTINUE
      STOP
      END
```

Definition of Symbols

CURO = Observed current

CURR = Faradaic current

ICOUNT = Total number of runs for which rate constants will be calculated

NAME = Name of run

N = Number of last point

A = HME Area

M = Number of rate constants

J(K) = Time index where rate constants will be determined

CHROM = Initial concentration of chromium(III)

CURC = Non-Faradaic correction

FARCON = $(\pi D)^{-\frac{1}{2}}F^{-1}$ where D = diffusion coefficient and F = Faraday

RATCON = F

TINCR = Time increment between current points

TIME(1) = Initial time

RCONST = Rate constant

APPENDIX II

COMPUTER PROGRAM MAINLINE WHEN BACK REACTION IS CONSIDERED

```
   DIMENSION CONC(100)
   DIMENSION CURD(500)
   DIMENSION X(500)
   DIMENSION CURR(500),TIME(500),J(500),CURO(500)
   DIMENSION NAME(10)
   DIMENSION LA(100)
   DIMENSION AREAT(100)
   READ 41,ICOUNT
41 FORMAT(I3)
   DO 34 IJK=1,ICOUNT
   READ 42,(NAME(I),I=1,10)
42 FORMAT(13A6,A2)
   PRINT 43,(NAME(I),I=1,10)
43 FORMAT(1H ,13A6,A2)
   READ 1,N
 1 FORMAT (I3)
   PRINT8,N
 8 FORMAT(1H,21HNUMBER OF LAST POINT=,I3)
   READ 2, (CURO(I), I=1,N)
 2 FORMAT(10F8.3)
   READ3,A,CHROM,CURC
 3 FORMAT (4F10.5)
   PRINT 11,A,CHROM,CURC
11 FORMAT(1H,2HA=,F10.5,5X,6HCHROM=,F10.5,5X,5HCURC=,F10.5,5X)
   READ40, FARCON,RATCON
40 FORMAT(2F20.10)
   PRINT 111,FARCON,RATCON
111 FORMAT(1H ,7HFARCON=,F20.10,5X,7HRATCON=,F20.10)
   READ4 TINCR,TIME(1)
 4 FORMAT(2F10.4)
   PRINT12,TINCR,TIME(1)
12 FORMAT(1H,6HTINCR=,F10.5,5X,8HTIME(1),F10.5)
   PRINT9
 9 FORMAT(1H,26HOBSERVED VALUES OF CURRENT)
   PRINT 10, (I,CURO(I), I=1,N)
10 FORMAT(7(1H ,I3,2X,F8.5,5X))
   CURCN=-CURC
   DO7 I=1,N
   IF(I.GT.101)CURC=CURCN
 7 CURR(I) = CURO(I) - CURC
   PRINT 55
```

```
55 FORMAT(1H,26HCORRECTD VALUES OF CURRENT)
   PRINT 56,(I,CURR(I),I=1,N)
56 FORMAT(7(1H ,I3,2X,F8.5,5X))
   READ 58, KOUNT
58 FORMAT(I4)
   DO 59 KJK = 1,KOUNT
   READ 60, KSUBED
60 FORMAT (I4)
   READ 61, (J(I), K=1,KSUBED)
61 FORMAT (2I4)
   READ 63, ITOTAL
63 FORMAT (I4)
   READ 64, (LA(IT), IT=1,ITOTAL)
64 FORMAT (2I4)
   DO 62 K = 1,KSUBED
   DO 13 IT = 1,ITOTAL
   CALL TRAPZ(CURR,CURD,IT,K,AREAT,JM,TIME,TINCR,J,LA,I,L,N)
   IF(K.EQ.1)JA=J(K)
   CONC(IT)=AREAT(IT)*FARCON/A
   IF((K.EQ.1) .AND. (IT.EQ.1))  CONUS = CONC(1)
   IF((K.EQ.1) .AND. (IT.EQ.2)) CRBRA = CONC(2)
   IF(K.EQ.2) GO TO 47
65 PRINT66
66 FORMAT(1H,15HCONC OF CHROMUS,8X,24HCONC OF CHROMICBR ANODIC)
   PRINT 67,CONUS,CRBRA
67 FORMAT(1H,E20.10,5X,E20.10)
   GO TO 46
47 IF(K.EQ.2)JB=J(K)
   IF((K.EQ.2) .AND. (IT.EQ.1)) CONUSC = CONC(1)
   IF((K.EQ.2) .AND. (IT.EQ.2)) CRBR = CONC(2)
68 PRINT69
69 FORMAT(1H,17HCONC OF CHROMICBR,8X,25HCONC OF CHROMOUS CATHODIC)
   PRINT70,CRBR,CONUSC
70 FORMAT(1H,E20.10,5X,E20.10)
46 CONTINUE
13 CONTINUE
62 CONTINUE
   RCONBR = (((CONUSC*CURR(JA))/(RATCON*A))
  1-((CONUS*CURR(JB))/(RATCON*A)))/(-(CONUS*CRBR)+(CONUSC*CRBRA))
   PRINT71,RCONBR
71 FORMAT(1H,7HRCONBR=,E20.10)
   RPARAL = ((CRBRA*RCONBR) - (CURR(JA))/(RATCON*A))/CONUS
   PRINT 72,RPARAL
72 FORMAT(1H,7HRPARAL=,E20.10)
59 CONTINUE
   READ 80,LC,M
```

```
80 FORMAT (2I4)
   IT=1
   LA(IT)=LC
   READ 81, (J(K), K=1,M)
81 FORMAT (20I4)
   DO 82 K=1,M
   CALL TRAPZ(CURR,CURD,IT,K,AREAT,JM,TIME,TINCR,J,LA,I,L,N)
   COMC = CHROM - (AREAT(IT)*FARCON/A)
   JC=J(K)
   RCONST = CURR(JC)/(RATCON*A*COMC)
   PRINT 5, JM, AREAT(IT), COMC
 5 FORMAT(1H,6HINDEX=,I3,5X,6HAREA=,E20.10,5X,5HCOMC=,E20.10,
  15X)
   PRINT 35,CURR(JC),RCONST
35 FORMAT(1H ,8HCURD(1)=,E20.10,5X,11HRATE CONST=,E20.10)
82 CONTINUE
34 CONTINUE
   STOP
   SUBROUTINE TRAPZ(CURR,CURD,IT,K,AREAT,JM,TIME,TINCR,J,
  1LA,I,L,N)
   DIMENSION J(100),LA(100),TIME(500),K(500),Y(500),SUM(500),
  1CURR(500),CURD(500)
   DIMENSION AREAT(100)
   JK=J(K)
   IF(JK.GT.LA(IT)) JM = JK-(LA(IT)-1)
   IF(JK.LT.LA(IT)) JM = N-(LA(IT)-1)+JK
   IF(JM.LE.2) GO TO 28
   DO 24 L = 1,JM
   IF(J(K).GT.LA(IT))JKE = L+LA(IT)-1
   IF((J(K).LT.LA(IT)).AND.(N.GE.(L+LA(IT))))JKE=L+LA(IT)-1
   IF((J(K).LT.LA(IT)).AND.(N.LT.(L+LA(IT))))JKE=(L+LA(IT)
  1-1)-N
   Z = L - 1
   X(L)=TIME(1)+Z*TINCR
   CURD(L) = CURR(JKE)
24 CONTINUE
   GO TO 26
28 LSTART = LA(IT)
   CURD(1) = CURR(LSTART)
   CURD(2) = (CURR(LSTART+1) + CURR(LSTART))/2.0
   CURD(3) = CURR(LSTART+1)
   X(1) = 0.0
   X(2) = TINCR/2.0
   X(3) = TINCR
   JM = 3
26 CONTINUE
   PRINT25,JK
```

```
 25 FORMAT(1H ,3HJK=,I3)
    JKB = JM - 1
    DO 27 I = 1,JKB
 27 Y(I) = CURD(I)/SQRT (ABS(X(JM) - X(I)))
    AREA=0.0
    JKC = JM - 2
    DO29I=1,JKC
    SUM(I)=0.5*(Y(I)+Y(I+1))*(X(I+1)-X(I))
 29 AREA=AREA+SUM(I)
    AREAT(TT) = AREA + SUM(JM-2)
    PRINT 86 ,(I,X(I),Y(I),I=1,JKB)
 86 FORMAT(1H,4(I3,2F10.5))
    PRINT 31,(I,SUM(I),I=1,JKC)
 31 FORMAT(1H,10(I3,F8.5))
    PRINT 33, JM,AREAT(IT),SUM(JM-2)
 33 FORMAT(1H,3HJM=,I3,5X,10HAREAT(IT)=,E20.10,5X,10HSUM(JM-2)=,
   1E20.10)
    RETURN
    END
```

Definition of Additional Symbols

KOUNT = Number of pairs of rate constants to be determined from each run

KSUBED = Number of integration limits

ITOTAL = Number of pseudo zeroes

RCONBR = Apparent rate constant k_{-4}

RPARAL = Apparent composite anodic rate constant

RCONST = Apparent rate constant k_{-3}

CONUS = $C'_{Cr(H_2O)_6^{2+}}$ (cf. p. 24)

CRBRA = $C'_{Cr(H_2O)_5Br^{2+}}$

CONUSC = $C_{Cr(H_2O)_6^{2+}}$

CRBR = $C_{Cr(H_2O)_5Br^{2+}}$

In the above computer program, two different points are given at which the integration of the current over time was begun. These two different points correspond to pseudo time zero (1) and pseudo time zero (2) which are indicated on Fig. II-1. When working with a "steady-state" curve, integration begun from pseudo zero (1) and stopped at the appropriate limit, will give $C'_{Cr(H_2O)_6^{2+}}$ or $C_{Cr(H_2O)_6^{2+}}$ (cf. p. 24); integration begun from pseudo zero (2) and stopped at the appropriate limit, will give $C'_{Cr(H_2O)_5Br^{2+}}$ or $C_{Cr(H_2O)_5Br^{2+}}$. When working with an initial cycle curve, integration begun from true time zero and stopped at the appropriate limit, will give $C'_{Cr(H_2O)_6^{2+}}$ or $C_{Cr(H_2O)_6^{2+}}$; integration begun from pseudo zero (2) and stopped at the appropriate limit, will give $C'_{Cr(H_2O)_5Br^{2+}}$ or $C_{Cr(H_2O)_5Br^{2+}}$.

For the program in Appendix I which can be used for the voltammetry curves in perchlorate or mixed chloride-perchlorate solutions, two different initial points for integration were necessary only for the voltammetry curves in the mixed chloride-perchlorate supporting electrolytes. Integration begun from true time zero (for an initial cycle curve) or from pseudo time zero (1)(for a "steady-state" curve) and stopped at the appropriate limit, gave the interface concentration of $[Cr(H_2O)_6]^{2+}$ or $[Cr(H_2O)_6]^{3+}$. Integration begun at pseudo zero (2) (for both initial and "steady-state" cycle curves) and stopped at the appropriate limit gave the interface concentra-

tion of $[Cr(H_2O)_5Cl]^{2+}$.

In the mixed bromide-perchlorate solutions, the apparent rate constants for the reduction of $[Cr(H_2O)_6]^{3+}$ were obtained with the integration begun at pseudo time zero (3).

APPENDIX III. DOUBLE LAYER DATA OF RICHARD PAYNE FOR $HClO_4$ IN WATER AT 25°C

TABLE (AIII-1). Potential, EM, Corresponding to Different Electrode Charges, Q, and $HClO_4$ Molarities, M.

The potential EM was measured against a hydrogen electrode in the same solution

Q	-EM (Volt)								
$\mu C/cm^2$)	0.01085 M $HClO_4$	0.02713 M $HClO_4$	0.05426 M $HClO_4$	0.1085 M $HClO_4$	0.2170 M $HClO_4$	0.5426 M $HClO_4$	0.9307 M $HClO_4$	1.861 M $HClO_4$	3.723 M $HClO_4$
0	0.0850	0.1150	0.1396	0.1644	0.1928	0.2367	0.2672	0.3204	0.4070
-1	0.1437	0.1616	0.1803	0.2015	0.2279	0.2708	0.3015	0.3557	0.4446
-2	0.2028	0.2118	0.2243	0.2411	0.2645	0.3055	0.3358	0.3907	0.4812
-3	0.2588	0.2656	0.2716	0.2837	0.3034	0.3413	0.3708	0.4255	0.5172
-4	0.3136	0.3165	0.3216	0.3299	0.3455	0.3789	0.4068	0.4608	0.5528
-5	0.3689	0.3708	0.3742	0.3798	0.3913	0.4193	0.4445	0.4968	0.5883
-6	0.4259	0.4271	0.4293	0.4333	0.4414	0.4643	0.4848	0.5342	0.6242
-7	0.4850	0.4855	0.4870	0.4899	0.4954	0.5110	0.5282	0.5734	0.6607
-8	0.5462	0.5461	0.5471	0.5493	0.5530	0.5634	0.5756	0.6152	0.6982
-9	0.6094	0.6088	0.6092	0.6111	0.6138	0.6199	0.6272	0.6600	
-10	0.6742	0.6732	0.6732	0.6749	0.6768	0.6797		0.7083	
-11	0.7401	0.7389	0.7383	0.7399		0.7423			
-12	0.8066	0.8052							
-13	0.8731	0.8715							

Q	-EM (Volt)								
($\mu C/cm^2$)	0.01085 M $HClO_4$	0.02713 M $HClO_4$	0.05426 M $HClO_4$	0.1085 M $HClO_4$	0.2170 M $HClO_4$	0.5428 M $HClO_4$	0.9307 M $HClO_4$	1.861 M $HClO_4$	3.723 M $HClO_4$
0	0.0850	0.1150	0.1396	0.1644	0.1928	0.2367	0.2672	0.3204	0.4070
1	0.0356	0.0760	0.1016	0.1288	0.1585	0.2026	0.2326	0.2843	0.3683
2	-0.0059	0.0348	0.0653	0.0940	0.1243	0.1681	0.1973	0.2473	0.3282
3	-0.0446	-0.0028	0.0296	0.0592	0.0898	0.1319	0.1610	0.2090	0.2867
4	-0.0823	-0.0395	-0.0061	0.0239	0.0545	0.0965	0.1236	0.1694	0.2437
5	-0.1202	-0.0767	-0.0426	-0.0123	0.0180	0.0589	0.0848	0.1284	0.1992
6	-0.1590	-0.1149	-0.0803	-0.0499	-0.0198	0.0199	0.0447	0.0861	0.1536
7	-0.1991	-0.1548	-0.1194	-0.0890	-0.0590	-0.0204	0.0053	0.0428	0.1070
8	-0.2405	-0.1958	-0.1600	-0.1295	-0.0996	-0.0619	-0.0389	-0.0012	0.0598
9	-0.2833	-0.2785	-0.2020	-0.1714	-0.1414	-0.1012	-0.0818	-0.0456	0.0125
10	-0.3270	-0.2818	-0.2450	-0.2143	-0.1840	-0.1471	-0.1250	-0.0900	-0.0347
11	-0.3711	-0.3258	-0.2886	-0.2577	-0.2271	-0.1901	-0.1680	-0.1340	-0.0813
12	-0.4152	-0.3698	-0.3322	-0.3012	-0.2702	-0.2329	-0.2107	-0.1774	-0.1272
13	-0.4586	-0.4133	-0.3755	-0.3442	-0.3129	-0.2752	-0.2528	-0.2201	-0.1721
14	-0.5011	-0.4560	-0.4179	-0.3866	-0.3549	-0.3168	-0.2941	-0.2620	-0.2159
15	-0.5424	-0.4975	-0.4593	-0.4279	-0.3959	-0.3574	-0.3345	-0.3029	-0.2584
16	-0.5824	-0.5377	-0.4995	-0.4680	-0.4358	-0.3971	-0.3740	-0.3427	-0.2995
17	-0.6209	-0.5766	-0.5385	-0.5069	-0.4747	-0.4358	-0.4126	-0.3815	-0.3391

	-EM (Volt)								
Q ($\mu C/cm^2$)	0.01085 M $HClO_4$	0.02713 M $HClO_4$	0.05426 M $HClO_4$	0.1085 M $HClO_4$	0.2170 M $HClO_4$	0.5428 M $HClO_4$	0.9307 M $HClO_4$	1.861 M $HClO_4$	3.723 M $HClO_4$
18	-0.6577	-0.6140	-0.5761	-0.5446	-0.5123	-0.4734	-0.4501	-0.4191	-0.3771
19	-0.6924	-0.6499	-0.6124	-0.5810	-0.5487	-0.5099	-0.4865	-0.4555	-0.4133
20	-0.7252	-0.6841	-0.6472	-0.6160	-0.5838	-0.5451	-0.5217	-0.4905	-0.4472
				-0.6494	-0.6174	-0.5791	-0.5555	-0.5238	-0.4792
						-0.6116	-0.5877	-0.5555	-0.5098
								-0.5860	-0.5399
									-0.5689
									-0.5989
									-0.6288

TABLE (AIII-2). $-\phi_2$ Values Corresponding to Different Electrode Charges and $HClO_4$ Molarities

$HClO_4$ in M	$-\phi_2$ (Volt)								
	Q = -8	Q = -6	Q = -4	Q = -2	Q = 0	Q = 2	Q = 4	Q = 6	Q = 8
0.01085	0.1359	0.1178	0.0932	0.0620	0.0196	-0.0184	-0.0087	-0.0712	-0.0644
0.02713	0.1104	0.0947	0.0752	0.0541	0.0328	0.0206	0.0203	0.0080	0.0049
0.05426	0.0919	0.0782	0.0627	0.0476	0.0344	0.0278	0.0259	0.0196	0.0161
0.10890	0.0744	0.0631	0.0513	0.0409	0.0328	0.0290	0.0266	0.0230	0.0195
0.21700	0.0583	0.0495	0.0413	0.0348	0.0302	0.0281	0.0255	0.0235	0.0202
0.54260	0.0399	0.0344	0.0302	0.0272	0.0255	0.0247	0.0222	0.0213	0.0184
0.93070	0.0305	0.0269	0.0247	0.0235	0.0230	0.0226	0.0202	0.0198	0.0172
1.86100	0.0201	0.0188	0.0190	0.0195	0.0202	0.0203	0.0180	0.0180	0.0156
3.72300	0.0105	0.0120	0.0146	0.0168	0.0186	0.0191	0.0169	0.0173	0.0150

	Q = 10	Q = 12	Q = 14	Q = 15	Q = 16	Q = 17	Q = 18
0.01085	-0.0397	-0.0167	0.0058	0.0195	0.0253	0.0340	0.0386
0.02713	0.0045	0.0052	-0.1479	0.0135	0.0145	0.0179	0.0191
0.05426	0.0134	0.0105	-0.0311	0.0100	0.0089	0.0093	0.0085
0.10890	0.0161	0.0120	-0.0099	0.0074	0.0052	0.0037	0.0017
0.21700	0.0166	0.0121	-0.0007	0.0055	0.0027	0.0001	-0.0025
0.54260	0.0150	0.0107	0.0041	0.0036	0.0008	-0.0021	-0.0048
0.93070	0.0139	0.0098	0.0054	0.0028	0.0002	-0.0027	-0.0054
1.86100	0.0127	0.0088	0.0064	0.0021	-0.0004	-0.0032	-0.0057
3.72300	0.0121	0.0084	0.0075	0.0015	-0.0009	-0.0038	-0.0063

BIBLIOGRAPHY

1. J. Halpern, Quart. Rev., 15, 207 (1961).

2. M. Pourbaix, "Atlas of Electrochemical Equilibria in Aqueous Solutions," 1st English ed., Pergamon Press Ltd., London, 1966, p. 256.

3. J. P. Candlin, J. Halpern, and D. L. Trimm, J. Am. Chem. Soc., 86, 1019 (1964).

4. J. F. Endicott and H. Taube, J. Am. Chem. Soc., 86, 686 (1964).

5. R. T. M. Fraser, Inorg. Chem., 3, 1561 (1964).

6. J. P. Candlin, J. Halpern, and S. Nakamura, J. Am. Chem. Soc., 85, 2517 (1963).

7. T. J. Conocchioli, G. H. Nancollas, and N. Sutin, Inorg. Chem., 5, 1 (1965).

8. J. H. Espenson and E. L. King, J. Am. Chem. Soc., 85, 3328 (1963).

9. H. Taube and H. Myers, J. Am. Chem. Soc., 76, 2103 (1954).

10. D. L. Ball and E. L. King, J. Am. Chem. Soc., 80, 1091 (1958).

11. A. Anderson and N. A. Bonner, J. Am. Chem. Soc., 76, 3826 (1954).

12. R. A. Marcus, J. Chem. Phys., 43, 679 (1965).

13. R. A. Marcus, J. Phys. Chem., 72, 891 (1968).

14. D. A. Aikens and J. W. Ross Jr., J. Phys. Chem., 65, 1213 (1961).

15. T. W. Swadle and E. L. King, Inorg. Chem., 4, 532 (1965).

16. G.W. Haupt, J. Research Natl. Bur. Standards, 48, 414 (1952).

17. P. Elving and B. Zemel, J. Am. Chem. Soc., 79, 1281 (1957).

18. R. W. Kolaczkowski and R. Plane, Inorg. Chem., 3, 322 (1964).

19. M. Ardon and R. Plane, J. Am. Chem. Soc., 81, 3197 (1959).

20. R. C. Thompson and G. Gordon, Inorg. Chem., 4, 557 (1966).

21. M. Ardon and G. Stein, J. Chem. Soc., 1956, 2095 (1956)

22. G. Grube and G. Breitinger, Z. Elecktrochem., 33, 112 (1927).

23. W. M. Latimer, "The Oxidation States of the Elements and Tehir Potentials in Aqueous Solutions," 2nd ed., Prentice-Hall Inc., Englewood Cliffs, New Jersey, 1952, p. 248.

24. R. Parsons and E. Passeron, J. Electroanal. Chem., 12, 524 (1966).

25. J. G. Jones, Ph.D. Dissertation, California Institute of Technology (1967).

26. R. A. Slotter, J. R. Weaver, and R. W. Parry, J. Phys. Chem., 71, 2619 (1967).

27. W. Kemula and E. Rakowska, Roczniki Chemii Ann. Soc. Chim. Polonorum, 36, 203 (1962).

28. R. L. Pecsok and J. J. Lingane, J. Am. Chem. Soc., 72, 189 (1950).

29. P. J. Elving and B. Zemel, Can. J. Chem., 37, 247 (1959).

30. K. M. Abubacker and W. U. Malik, J. Indian Chem. Soc., 36, 459 (1959).

31. Ibid., 36, 463 (1959).

32. V. S. Srinivasan, G. Torsi, and P. Delahay, J. Electroanal. Chem., 10, 165 (1965).

33. J. E. B. Randles and K. W. Somerton, Trans. Faraday Soc., 48, 937 (1952).

34. D. A. Aikens and J. W. Ross Jr., unpublished data, see Reference 25.

35. J. G. Jones and F. C. Anson, Anal. Chem., 36, 1137 (1964).

36. J. G. Jones Urlich and F. C. Anson, Inorg. Chem., 8, 195 (1968).

37. P. Delahay, "New Instrumental Methods in Electrochemistry," Interscience Publishers, Inc., New York, 1966, p. 199.

38. G. Geier, Bunsenges. Physik. Chem., 69, 617 (1965), in F. Basolo and R. G. Pearson, "Mechanisms of Inorganic Reactions," 2nd ed., John Wiley and Sons, Inc., New York, 1958, p. 155.

39. R. L. Connick, "Symposium on Relaxation Techniques," Buffalo, New York, June 1965, reported in F. Basolo and R. G. Pearson, "Mechanisms of Inorganic Reactions," 2nd ed., John Wiley and Sons., Inc., New York, 1958, p. 152.

40. P. Debye, Trans. Electrochem. Soc., 82, 265 (1942).

41. M. Eigen, Z. Physik. Chem. (Frankfurt), 1, 176 (1954).

42. R. Fuoss, J. Am. Chem. Soc., 80, 5059 (1958).

43. R. L. Pecsok and J. Bjerrum, Acta Chem. Scand., 11, 1419 (1957).

44. Reference 62, p. 71.

45. R. A. Marcus, Electrochim. Acta, 13, 995 (1968).

46. R. S. Nicholson and I. Shain, Anal. Chem., 36, 706 (1964).

47. Reference 37, p. 46.

48. J. J. Lingane and R. L. Pecsok, J. Am. Chem. Soc., 71, 425 (1949).

49. J. Heyrovsky and J. Kuta, "Principles of Polarography," Academic Press, New York, 1966, p. 77.

50. P. Delahay, "Double Layer and Electrode Kinetics," Interscience Publishers, John Wiley and Sons, Inc., New York, 1965, p. 164.

51. Reference 50, p. 201.

52. D. C. Graham and R. Parsons, J. Am. Chem. Soc., 83, 1291 (1961).

53. J. Lawrence, R. Parsons, and R. Payne, J. Electroanal. Chem., 16, 193 (1968).

54. E. Dutkiewicz and R. Parsons, J. Electroanal. Chem., 11, 100 (1966).

55. (a) P. Teppema, M. Sluyters-Rehbach, J. H. Sluyters, J. Electroanal. Chem., 16, 165 (1968); (b) D. C. Yohe, Ph.D. Dissertation, Western Reserve University, 1967, p. 98.

56. U. Klanning and M. C. R. Symonds, J. Chem. Soc., 1961, 3205 (1961).

57. Reference 2, p. 452.

58. R. A. Marcus, J. Chem. Phys., 43, 679 (1965).

59. V. G. Levich and R. R. Dogonadze, Coll. Czech. Chem. Comm., 26, 193 (1961).

60. V. G. Levich, "Present State of the Theory of Oxidation-Reduction in Solution," in Advances in Electrochemistry and Electrochemical Engineering, Vol. 4, Edited by P. Delahay and C. W. Tobias, John Wiley and Sons, Inc., New York, 1966, p. 306.

61. E. Sacher and J. Laidler, "Theories of Elementary Homogeneous Electron-Transfer Reactions," in Modern Aspects of Electrochemistry, No. 3, Edited by J. O. M. Bockris and B. E. Conway, Butterworths, Washington, 1964, p. 1.

62. W. L. Reynolds and R. W. Lumry, "Mechanisms of Electron Transfer," The Ronald Press Company, New York, 1966, p. 122.

63. L. Pauling, "The Nature of the Chemical Bond," Cornell University Press, Ithaca, New York, 1948, p. 304.

64. Reference 60, p. 334.

65. Reference 62, p. 123.

66. Reference 62, p. 125.

67. N. Sutin, Ann. Rev. Nucl. Sci., 12, 285 (1962).

68. Reference 62, p. 128.

69. Reference 62, p. 70.

70. R. A. Marcus, Can. J. Chem., 37, 155 (1959).

71. Reference 63, p. 189.

72. D. G. Conning, Ph.D. Dissertation, University of Southampton, England.

73. Reference 50, p. 35.

74. B. Timmer, M. Sluyters-Rehbach, and J. H. Sluyters, J. Electroanal. Chem., 15, 343 (1967).

75. D. G. Grahame, J. Am. Chem. Soc., 80, 4201 (1958).

76. H. S. Hush, Progr. Inorg. Chem., 8, 391 (1967).

77. C. K. Jørgensen, "Absorption Spectra and Chemical Bonding in Complexes," Pergamon Press, Oxford, 1962, p. 134.

78. Reference 77, p. 109.

79. J. Lewis and R. G. Wilkins, "Modern Coordination Chemistry," John Wiley and Sons, Inc., New York, 1960, p. 253.

80. Reference 77, p. 110.

81. Reference 77. p. 138.

82. Reference 77, p. 139.